

Middle East Respiratory Syndrome Coronavirus: Another Zoonotic Betacoronavirus Causing SARS-Like Disease

Jasper F. W. Chan,^{a,b} Susanna K. P. Lau,^{a,b} Kelvin K. W. To,^{a,b} Vincent C. C. Cheng,^b Patrick C. Y. Woo,^{a,b} Kwok-Yung Yuen^{a,b}

State Key Laboratory of Emerging Infectious Diseases and Research Centre of Infection and Immunology, The University of Hong Kong, Hong Kong Special Administrative Region, China^a; Carol Yu Centre for Infection, Department of Microbiology, The University of Hong Kong, Hong Kong Special Administrative Region, China^b

SUMMARY	465
INTRODUCTION	466
TAXONOMY, NOMENCLATURE, AND GENERAL VIROLOGY	466
VIRAL REPLICATION CYCLE	467
SEQUENCE OF EVENTS IN THE MERS EPIDEMIC	471
EPIDEMIOLOGY	475
Risk Factors for Severe Disease	475
Seroepidemiology	475
Animal Surveillance	479
Molecular Epidemiology	483
Mathematical Modeling	487
CLINICAL MANIFESTATIONS	490
HISTOPATHOLOGY AND PATHOGENESIS	491
Histological Changes	491
Innate Immune Response	491
Adaptive Immune Response	492
Organ-Specific Pathology and Systemic Virus Dissemination	493
LABORATORY DIAGNOSIS	493
Specimen Collection	493
Nucleic Acid Amplification Assays	495
Antibody Detection Assays	495
Antigen Detection Assays	495
Viral Culture	497
CLINICAL MANAGEMENT AND ANTIVIRALS	497
INFECTION CONTROL AND LABORATORY SAFETY	505
VACCINATION	506
Active Immunization	506
Passive Immunization	506
ANIMAL MODELS AND ANIMALS SUSCEPTIBLE TO MERS-CoV	506
CONCLUSIONS	509
ACKNOWLEDGMENTS	510
REFERENCES	510
AUTHOR BIOS	521

SUMMARY

The source of the severe acute respiratory syndrome (SARS) epidemic was traced to wildlife market civets and ultimately to bats. Subsequent hunting for novel coronaviruses (CoVs) led to the discovery of two additional human and over 40 animal CoVs, including the prototype lineage C betacoronaviruses, *Tylonycteris* bat CoV HKU4 and *Pipistrellus* bat CoV HKU5; these are phylogenetically closely related to the Middle East respiratory syndrome (MERS) CoV, which has affected more than 1,000 patients with over 35% fatality since its emergence in 2012. All primary cases of MERS are epidemiologically linked to the Middle East. Some of these patients had contacted camels which shed virus and/or had positive serology. Most secondary cases are related to health care-associated clusters. The disease is especially severe in elderly men with comorbidities. Clinical severity may be related to MERS-CoV's ability to infect a broad range of cells with DPP4 expression, evade the host innate immune response, and induce cytokine dysregulation. Reverse transcription-PCR on respiratory and/or ex-

trapulmonary specimens rapidly establishes diagnosis. Supportive treatment with extracorporeal membrane oxygenation and dialysis is often required in patients with organ failure. Antivirals with potent *in vitro* activities include neutralizing monoclonal antibodies, antiviral peptides, interferons, mycophenolic acid, and lopinavir. They should be evaluated in suitable animal models before clinical trials. Developing an effective camel MERS-CoV vaccine and implementing appropriate infection control measures may control the continuing epidemic.

Published 25 March 2015

Citation Chan JFW, Lau SKP, To KKW, Cheng VCC, Woo PCY, Yuen K-Y. 25 March 2015. Middle East respiratory syndrome coronavirus: another zoonotic betacoronavirus causing SARS-like disease. Clin Microbiol Rev doi:10.1128/CMR.00102-14.

Address correspondence to Kwok-Yung Yuen, kyyuen@hku.hk.

Copyright © 2015, American Society for Microbiology. All Rights Reserved.

doi:10.1128/CMR.00102-14

INTRODUCTION

Frequent mixing of different animal species in markets in densely populated areas and human intrusions into the natural habitats of animals have facilitated the emergence of novel viruses. Examples with specific geographical origins include severe acute respiratory syndrome coronavirus (SARS-CoV) and avian influenza A/H7N9 and H5N1 viruses in China, Nipah virus in Malaysia and Bangladesh, and Ebola and Marburg viruses in Africa (1–8, 329). The Middle East is a region encompassing most of western Asia and Egypt and contains 18 countries with various ethnic groups. It is one of the busiest politico-economic centers in the world, with many unique religious and cultural practices such as the annual Hajj along with a reliance on camels for food, medicine, business, and travel in both rural and urban areas. These distinct regional characteristics have provided favorable conditions for new and rapidly mutating viruses to emerge. Similar to the first decade of the new millennium, during which the world witnessed the devastating outbreak of SARS caused by SARS-CoV, the beginning of the second decade was plagued by the emergence of another novel CoV, Middle East respiratory syndrome coronavirus (MERS-CoV), that has caused an outbreak of severe respiratory disease in the Middle East with secondary spread to Europe, Africa, Asia, and North America since 2012 (3, 9). MERS-CoV is similar to SARS-CoV in being a CoV that is likely to have originated from animal reservoirs and crossed interspecies barriers to infect humans (1). The disease, Middle East respiratory syndrome (MERS), was initially called a “SARS-like” illness at the beginning of the epidemic, as both are human CoV infections that manifest as severe lower respiratory tract infection with extrapulmonary involvement and high case-fatality rates (10, 11), whereas the other four CoVs that cause human infections, namely, human coronavirus (HCoV)-OC43, HCoV-229E, HCoV-HKU1, and HCoV-NL63, mainly cause mild, self-limiting upper respiratory tract infections such as the common cold (10). MERS-CoV, like SARS-CoV, is considered by the global health community to be a potential pandemic agent, since person-to-person transmission occurs and effective therapeutic options are limited. However, unlike the SARS epidemic, which rapidly died off after the intermediate amplifying hosts were identified and segregated from humans by closure of wild animal markets in southern China, the MERS epidemic has persisted for more than 2 years with no signs of abatement (3, 12). Detailed analysis of the epidemiological, virological, and clinical aspects of MERS and SARS reveals important differences between the two diseases and identifies unique aspects of MERS-CoV that may help to explain the evolution of the MERS epidemic. A summary of the key differences between the MERS and SARS epidemics is provided in Table 1. In this article, we review the biology of MERS-CoV in relation to its epidemiology, clinical manifestations, pathogenesis, laboratory diagnosis, therapeutic options, immunization, and infection control, in order to identify key research priorities that are important for the control of this evolving epidemic.

TAXONOMY, NOMENCLATURE, AND GENERAL VIROLOGY

MERS-CoV belongs to lineage C of the genus *Betacoronavirus* (βCoV) in the family *Coronaviridae* under the order *Nidovirales* (Fig. 1A). Prior to the discovery of MERS-CoV, the only known lineage C βCoVs were two bat CoVs that are phylogenetically

closely related to MERS-CoV, namely, *Tylonycteris* bat CoV HKU4 (Ty-BatCoV-HKU4) and *Pipistrellus* bat CoV HKU5 (Pi-BatCoV-HKU5), discovered in Hong Kong in 2006 (Fig. 1B) (13–15). MERS-CoV is the first lineage C βCoV and the sixth CoV known to cause human infection. It was designated a novel lineage C βCoV based on the International Committee on Taxonomy of Viruses (ICTV) criteria for CoV species identification using rooted phylogeny. Calculation of pairwise evolutionary distances for seven replicase domains showed that MERS-CoV had an amino acid sequence identity of less than 90% to all other known CoVs at the time when MERS-CoV was discovered (16). Before the virus was formally named MERS-CoV by the Coronavirus Study Group of ICTV, it was also known by other names, including “novel coronavirus,” “human coronavirus EMC,” “human betacoronavirus 2c EMC,” “human betacoronavirus 2c England-Qatar,” “human betacoronavirus 2C Jordan-N3,” and “betacoronavirus England 1,” which represented the places where the first complete viral genome was sequenced (Erasmus Medical Center, Rotterdam, the Netherlands) or where the first laboratory-confirmed cases were identified or managed (Jordan, Qatar, and England) (9, 17–20). Similar to other CoVs, MERS-CoV is an enveloped positive-sense single-stranded RNA virus (16). Its single-stranded RNA genome has a size of approximately 30 kb and a G+C content of 41% and contains 5′-methyl-capped, polyadenylated, polycistronic RNA (16, 20, 21). The genome arrangement of 5′-replicase-structural proteins (spike-envelope-membrane-nucleocapsid)-poly(A)-3′ [i.e., 5′-ORF1a/b-S-E-M-N-poly(A)-3′] is similar to that of other βCoVs and unambiguously distinguishes MERS-CoV from lineage A βCoVs, which universally contain the characteristic hemagglutinin-esterase (HE) gene (16, 20–22). Many of these genes and their encoded proteins are useful diagnostic, therapeutic, or vaccination targets (Fig. 2). There are 10 complete, functional open reading frames (ORFs) expressed from a nested set of seven subgenomic mRNAs carrying a 67-nucleotide (nt) common leader sequence in the genome, eight transcription-regulatory sequences, and two terminal untranslated regions (16, 20, 21). The putative roles and functions of the ORFs and their encoded proteins are derived by analogy to other CoVs (Table 2). Proteolytic cleavage of the large replicase polyproteins pp1a and pp1ab encoded by the partially overlapping 5′-terminal ORF1a/b within the 5′ two-thirds of the genome produces 16 putative nonstructural proteins (nsps), including two viral cysteine proteases, namely, nsp3 (papain-like protease) and nsp5 (chymotrypsin-like, 3C-like, or main protease), nsp12 (RNA-dependent RNA polymerase [RdRp]), nsp13 (helicase), and other nsps which are likely involved in the transcription and replication of the virus (16, 20, 21). The membrane-anchored trimeric S protein is a major immunogenic antigen involved in virus attachment and entry into host cells and has an essential role in determining virus virulence, protective immunity, tissue tropism, and host range (23). The other canonical structural proteins, namely, the E, M, and N proteins, are encoded by ORF6, -7, and -8, respectively, and are involved in the assembly of the virion. The M protein, as well as the papain-like protease and accessory proteins 4a, 4b, and 5, exhibit *in vitro* interferon antagonist activities that may modulate *in vivo* replication efficiency and pathogenesis (24–28).

VIRAL REPLICATION CYCLE

The replication cycle of MERS-CoV consists of numerous essential steps that can be efficiently inhibited by antiviral agents *in vitro* (Fig. 3). CoVs are so named because of their characteristic solar corona (*corona soli*) or “crown-like” appearance observed under electron microscopy, which represents the peplomers formed by trimers of S protein radiating from the virus lipid envelope. The MERS-CoV S protein is a class I fusion protein composed of the amino N-terminal receptor-binding S1 and carboxyl C-terminal membrane fusion S2 subunits (Fig. 2). The S1/S2 junction is the location of a protease cleavage site which is required to activate membrane fusion, virus entry, and syncytium formation. The S1 subunit consists of a C domain, which contains the receptor-binding domain (RBD), and an N domain (29). The RBD of MERS-CoV has been mapped by different groups to a 200- to 300-residue region spanning residues 358 to 588, 367 to 588, 367 to 606, 377 to 588, or 377 to 662 (29–36). Among these RBD-containing fragments, the one that encompasses residues 377 to 588 appears to be the most stable and neutralizing fragment in structural analysis and virus neutralization assays (36). Neutralizing monoclonal antibodies against the RBD potentially inhibit virus entry into host cells and receptor-dependent syncytium formation in cell culture, and vaccines containing the RBD induce high levels of neutralizing antibodies in mice and rabbits (31, 34, 36–43). The S2 subunit contains a fusion peptide, the heptad repeat 1 (HR1) and HR2 domains, a transmembrane domain, and a cytoplasmic domain, which form the stalk region of S protein that facilitates fusion of the viral and cell membranes, which is necessary for virus entry (44, 45). The binding of the S1 subunit to the cellular receptor triggers conformational changes in the S2 subunit, which inserts its fusion peptide into the target cell membrane to form a six-helix bundle fusion core between the HR1 and HR2 domains that approximates the viral and cell membranes for fusion. This fusion process can be inhibited by HR2-based antiviral peptide fusion inhibitors which prevent the interaction between the HR1 and HR2 domains (44, 45).

The key functional receptor of the host cell attached to by the MERS-CoV S protein is dipeptidyl peptidase 4 (DPP4), which is also known as adenosine deaminase-complexing protein 2 or CD26 (46). MERS-CoV is the first CoV that has been identified to use DPP4 as a functional receptor for entry into host cells (1, 46). DPP4 is a multifunctional 766-amino-acid-long type II transmembrane glycoprotein, presented as a homodimer on the cell surface, which is involved in the cleavage of dipeptides (46, 47). It has important roles in glucose metabolism and various immunological functions, including T-cell activation, chemotaxis modulation, cell adhesion, and apoptosis (46, 47). In humans, it is abundantly expressed on the epithelial and endothelial cells of most organs, including lung, kidney, small intestine, liver, and prostate, as well as immune cells, and exists as a soluble form in the circulation (46–48). This broad tissue expression of DPP4 may partially explain the extrapulmonary manifestations seen in MERS. Adenosine deaminase, which is a natural competitive antagonist, and some anti-DPP4 monoclonal antibodies exhibit inhibitory effects on *in vitro* MERS-CoV infection (49, 50).

The energetically unfavorable membrane fusion reaction in endosomal cell entry is overcome by low pH and the pH-dependent endosomal cysteine protease cathepsins and can be blocked by lysosomotropic agents such as ammonium chloride, bafilomycin

A, and cathepsin inhibitors in a cell type-dependent manner (23, 51). Additionally, various host proteases, such as transmembrane protease serine protease 2 (TMPRSS2), trypsin, chymotrypsin, elastase, thermolysin, endoprotease Lys-C, and human airway trypsin-like protease, cleave the S protein into the S1 and S2 subunits to activate the MERS-CoV S protein for endosome-independent host cell entry at the plasma membrane (23, 51–53). Inhibitors of TMPRSS2 can abrogate this proteolytic cleavage and partially block cell entry (23, 51, 52). In some cell lines, MERS-CoV demonstrates the ability to utilize both the cathepsin-mediated endosomal pathway and the TMPRSS2-mediated plasma membrane pathway to enter host cells (51, 52).

In addition to these cellular proteases, furin has recently been identified as another protease that has essential roles in the MERS-CoV S protein cleavage activation (54). Furin and furin-like proprotein convertases are broadly expressed serine endoproteases that cleave the multibasic motifs R_X(R/K/X)_R and process proproteins into their biologically active forms (55). Proprotein convertases, including furin, have been implicated in the processing of fusion proteins and therefore cell entry of various viruses, including human immunodeficiency virus, avian influenza A/H5N1 virus, Marburg virus, Ebola virus, and flaviviruses (55–57). The MERS-CoV S protein contains two cleavage sites for furin at S1/S2 (₇₄₈RSVR₇₅₁) and S2' (₈₈₄RSAR₈₈₇) and exhibits an unusual two-step furin-mediated activation process (Fig. 2) (54). Furin cleaves the S1/S2 site during S protein biosynthesis and the S2' site during virus entry into host cells (54). Furin inhibitors such as decanoyl-RVVKR-chloromethylketone block MERS-CoV entry and cell-cell fusion (54). Treatment of MERS with a combination of inhibitors of the different cellular proteases utilized by MERS-CoV for S activation should be further evaluated in *in vivo* settings.

After cell entry, MERS-CoV disassembles to release the inner parts of the virion, including the nucleocapsid and viral RNA, into the cytoplasm for translation of ORF1a/b into viral polyproteins pp1a and, following –1 ribosomal frameshifting, pp1ab, and replication of genomic RNA (Fig. 3). The characteristic replication structures of CoVs, including double-membrane vesicles and convoluted membranes, are formed by the attachment of the hydrophobic domains of the MERS-CoV replication machinery to the limiting membrane of autophagosomes (58). These structures can be observed at the perinuclear region of the infected cells under electron microscopy (58). The viral papain-like protease and 3C-like protease cotranslationally cleave the large replicase polyproteins pp1a and pp1ab encoded by ORF1a/b into nsp1 to nsp16 (16, 59, 60). These nsps form the replication-transcription complex, where transcription of the full-length positive genomic RNA yields a full-length negative-strand template for synthesis of new genomic RNAs as well as a series of overlapping subgenomic negative-strand templates for synthesis of subgenomic 3' coterminal mRNAs that will be translated to make viral structural and accessory proteins (58). The relative abundance of the subgenomic mRNAs of MERS-CoV is similar to those of other CoVs, with the smallest mRNA, which encodes the N protein, being the most abundant (58). After adequate viral genomic RNA and structural proteins have been cumulated, the N protein assembles with the genomic RNA in the cytoplasm to form the helical nucleocapsid. The nucleocapsid then acquires its envelope by budding through intracellular membranes between the endoplasmic reticulum and Golgi apparatus. The S, E, and M proteins are transported to the budding compartment, where the nucleocapsid probably inter-

TABLE 1 Comparison between MERS and SARS^a

Characteristic	MERS	SARS	References
Epidemiology			
Yr of first identification	2012	2003	2, 9
Geographical origin	Middle East, with imported cases in Europe, Africa, Asia, and North America	South China, with imported cases causing large outbreaks in Canada and Asia	3; http://www.who.int/csr/disease/coronavirus_infections/MERS-CoV_Update_09_May_2014.pdf ; http://www.who.int/csr/disease/coronavirus_infections/MERS-CoV_summary_update_20140611.pdf ua=1
Natural reservoir ^b	Bats (?) (<i>Neoromicia</i> sp. in Africa)	Chinese horseshoe bats (<i>Rhinolophus sinicus</i> and other <i>Rhinolophus</i> spp. in China)	3, 102, 110, 111, 273, 274
Amplification or intermediate host ^b	Dromedary camels (Middle East and Africa)	Game food mammals (civets and raccoon dogs in southern China)	3, 12, 114, 121, 133
Epidemic centers of outbreaks or premises of acquisition	Camel farms (?), hospital or household with MERS patients	Wildlife markets, restaurants, hospitals, laboratories, housing estate with faulty sewage system, hotels, and planes	3, 12, 75, 138, 139, 275–277
Seasonality	May be related to camel breeding season	Winter	3; http://www.who.int/csr/disease/coronavirus_infections/MERS-CoV_Update_09_May_2014.pdf ; http://www.who.int/csr/disease/coronavirus_infections/MERS-CoV_summary_update_20140611.pdf ua=1
Main types of transmission ^c	Animal to human, person to person	Person to person, animal to human	3, 73, 138
In-flight transmission	Not yet documented	A few documented episodes, related to physical proximity to the index patient	3, 277
Modes of transmission	Droplet, contact, airborne (?)	Droplet, contact, airborne	3, 75, 233
Infection control measures	Standard, contact, and droplet precautions; airborne precautions for aerosol-generating procedures	Standard, contact, and droplet precautions; airborne precautions for aerosol-generating procedures	3, 75, 233
Incubation period (days)	2–15	2–14, occasionally up to 21	3, 63, 75, 233
Basic reproduction no. (R_0)	0.3–1.3	0.3–4.1	3, 90, 150, 151, 278–280
Virus-host interaction			
Causative virus	MERS-CoV	SARS-CoV	2, 9, 164, 281
Viral phylogeny	Lineage C βCoV	Lineage B βCoV	2, 9
Host receptor	DPP4 (CD26)	ACE2	46, 282
Major host proteases that activate spike protein	TMPRSS2, cathepsin L, furin	Cathepsin L, TMPRSS2, HAT	44, 51, 52, 54, 283–286
Dominant cell entry pathway	Cell membrane fusion	Endosomal fusion	44, 51, 283, 287
Cytopathic effects	Prominent syncytium formation	Few if any syncytia	2, 3, 23, 60, 116
Spectrum of cell line susceptibility ^d	Broad range of animal and human tissue cells	Only a few human and primate cell lines can be infected	3, 116–118
Viral proteins with interferon antagonist activity	PLpro, accessory proteins 4a, 4b, and 5, and membrane protein	nsP1 protein, PLpro, accessory proteins 3b and 6, and nucleocapsid and membrane proteins	3, 24, 25, 27, 28, 171, 288, 289, 290, 291
Rapid evolution of virus in human	Not yet detected	Overall K_a/K_e ratio of >1 suggests rapid evolution with strong positive selection in human strains associated with deletion of 29-bp signature sequence or 82 bp in ORF8	3, 114, 146, 292
Clinical aspects			
Presenting clinical syndrome	Acute community- or hospital-acquired pneumonia in elderly and patients with multiple comorbidities; upper respiratory tract infection; influenza-like illness, or asymptomatic infection in children and immunocompetent hosts	Acute community- or hospital-acquired pneumonia in immunocompetent and immunocompromised hosts	2, 63, 293
Common extrapulmonary manifestations	Acute renal failure, diarrhea	Diarrhea	63, 160, 195
Radiological changes	Focal to diffuse interstitial ground-glass opacities and/or consolidations	Focal to diffuse ground-glass opacities and/or consolidations with pneumomediastinum	3, 63, 152
Common changes in blood tests	Leukopenia, lymphopenia, thrombocytopenia, impaired liver function at presentation; renal function impairment, leukocytosis, and neutrophilia with progressive illness	Leukopenia, lymphopenia, thrombocytopenia, increased alanine and aspartate aminotransferase levels	3, 63
Severe complications	ARDS, acute renal failure	ARDS	3, 63
Case-fatality rate (%)	>35	~10	3, 63; http://www.who.int/csr/don/17-december-2014-mers/en/
Peak viral load in respiratory secretion	Unclear	~Day 10 after symptom onset	3, 160, 195
Onset of neutralizing antibody	≤12 days after symptom onset	~Day 5–10 after symptom onset	3, 66, 72, 81, 182, 294

Specimens for diagnosis with positive viral RNA (RT-PCR) or culture (cell culture)	Lower respiratory tract—sputum, endotracheal aspirate, and/or bronchoalveolar lavage fluid; upper respiratory tract—nasopharyngeal aspirate or swab, nasal and/or throat swab; extrapulmonary—urine, feces, and/or blood; tissue—biopsied and/or autopsied specimens (findings not yet reported)	Lower respiratory tract—sputum, endotracheal aspirate, and/or bronchoalveolar lavage; upper respiratory tract—nasopharyngeal aspirate or swab, nasal and/or throat swab; extrapulmonary—urine, feces, blood, tears, saliva, sweat, and/or cerebrospinal fluid; tissue—biopsied and/or autopsied specimens	3, 193, 194, 330–332
Criteria for positive RT-PCR test	Follow WHO criteria	Follow WHO criteria	3; http://www.who.int/csr/disease/coronavirus_infections/MERS_Lab_recos_16_Sept_2013.pdf#ua=1
Criteria for positive antibody test	No international standard	4-fold rise in serum (taken at least 14 days apart) neutralizing anti-SARS-CoV antibody titer (often just 4-fold rise in immunofluorescence antibody against fixed whole SARS-CoV if BSL3 facility was not available)	3; http://www.who.int/csr/disease/coronavirus_infections/MERS_Lab_recos_16_Sept_2013.pdf#ua=1
Key treatment measures	Ventilatory support and intensive care (ECMO and hemodialysis)	Ventilatory support and intensive care	3, 88, 203, 233
Antivirals used in humans in nonrandomized trials	Ribavirin and interferon alpha 2b	Interferons (infacon1, interferon beta, leukocytic interferons), combinations of protease inhibitor with ribavirin	3, 206, 215
Active immunization	Vaccines containing RBD of S1 (mice)	Recombinant S protein fragment (mice)	3, 36, 251, 295
Passive immunization	Adoptive transfer of sera containing anti-MERS-CoV S antibodies accelerated virus clearance in mice	Convalescent plasma therapy used in humans	3, 173, 296
Animal models for testing antivirals and vaccines ^e	Common marmoset; transgenic mouse globally expressing human DPP4	Representative models using various mammalian species, including primate and small animal models	3, 167, 333

^a Abbreviations: ACE2, angiotensin-converting enzyme 2; ARDS, acute respiratory distress syndrome; BSL, biosafety level; CoV, coronavirus; DPP4, dipeptidyl peptidase 4; ECMO, extracorporeal membrane oxygenation; HAT, human airway trypsin-like protease; MERS, Middle East respiratory syndrome; ORF, open reading frame; PLpro, papain-like protease; RBD, receptor-binding domain; S, spike; SARS, severe acute respiratory syndrome; TMPRSS2, transmembrane protease serine protease 2.

^b See [Table 5](#) for details on animal reservoirs of MERS-CoV.

^c Both animal (especially dromedary camels)-to-human transmission and person-to-person transmission in nosocomial outbreaks are considered to be important factors for the persistent MERS outbreak. Person-to-person transmission of SARS-CoV in “superspreading events” and major nosocomial outbreaks is considered to be the major transmission type in the large-scale epidemic of SARS.

^d See [Table 6](#) for details on tissue and host tropism of MERS-CoV.

^e See [Table 12](#) for details on other animal models of MERS.

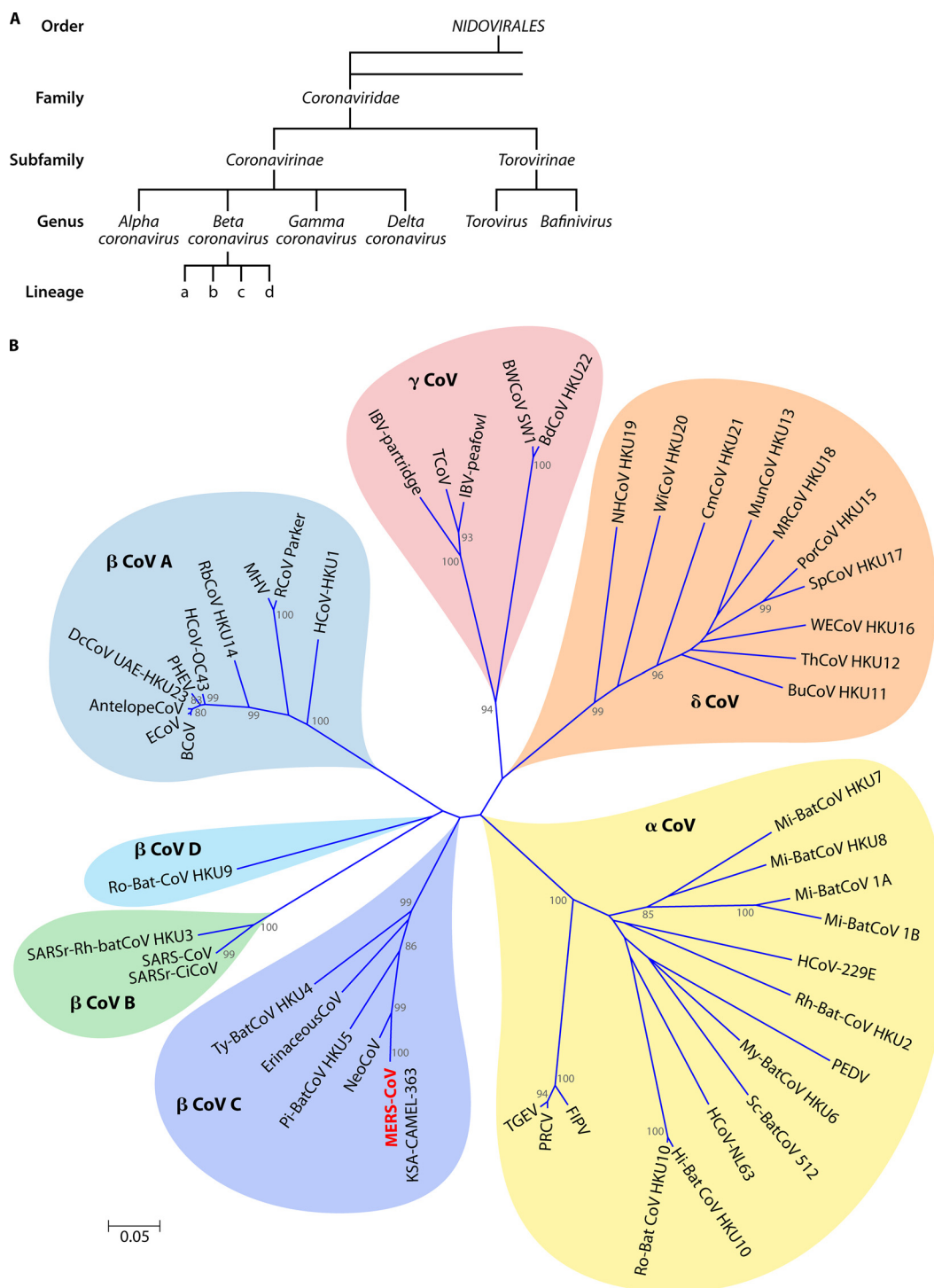


FIG 1 (A) Taxonomy of *Coronaviridae* according to the International Committee on Taxonomy of Viruses. (B) Phylogenetic tree of 50 coronaviruses with partial nucleotide sequences of RNA-dependent RNA polymerase. The tree was constructed by the neighbor-joining method using MEGA 5.0. The scale bar indicates the estimated number of substitutions per 20 nucleotides. Abbreviations (accession numbers): AntelopeCoV, sable antelope coronavirus (EF424621); BCoV, bovine coronavirus (NC_003045); BdCoV HKU22, bottlenose dolphin coronavirus HKU22 (KF793826); BuCoV HKU11, bulbul coronavirus HKU11 (FJ376619); BWCoV-SW1, beluga whale coronavirus SW1 (NC_010646); CMCov HKU21, common-moorhen coronavirus HKU21 (NC_016996); DcCoV UAE-HKU23, dromedary camel coronavirus UAE-HKU23 (KF906251); ECoV, equine coronavirus (NC_010327); Erinaceus-CoV, betacoronavirus *Erinaceus*/VMC/DEU/2012 (NC_022643); FIPV, feline infectious peritonitis virus (AY994055); HCoV-229E, human coronavirus 229E (NC_002645); HCoV-HKU1, human coronavirus HKU1 (NC_006577); HCoV-NL63, human coronavirus NL63 (NC_005831); HCoV-OC43, human coronavirus OC43 (NC_005147); Hi-BatCoV HKU10, *Hipposideros* bat coronavirus HKU10 (JQ989269); IBV-partridge, avian infectious bronchitis virus partridge isolate (AY646283); IBV-peafowl, avian infectious bronchitis virus peafowl isolate (AY641576); KSA-CAMEL-363, KSA-CAMEL-363 isolate of Middle East respiratory syndrome coronavirus (KJ713298); MERS-CoV, Middle East respiratory syndrome coronavirus (NC_019843.3); MHV, murine hepatitis virus

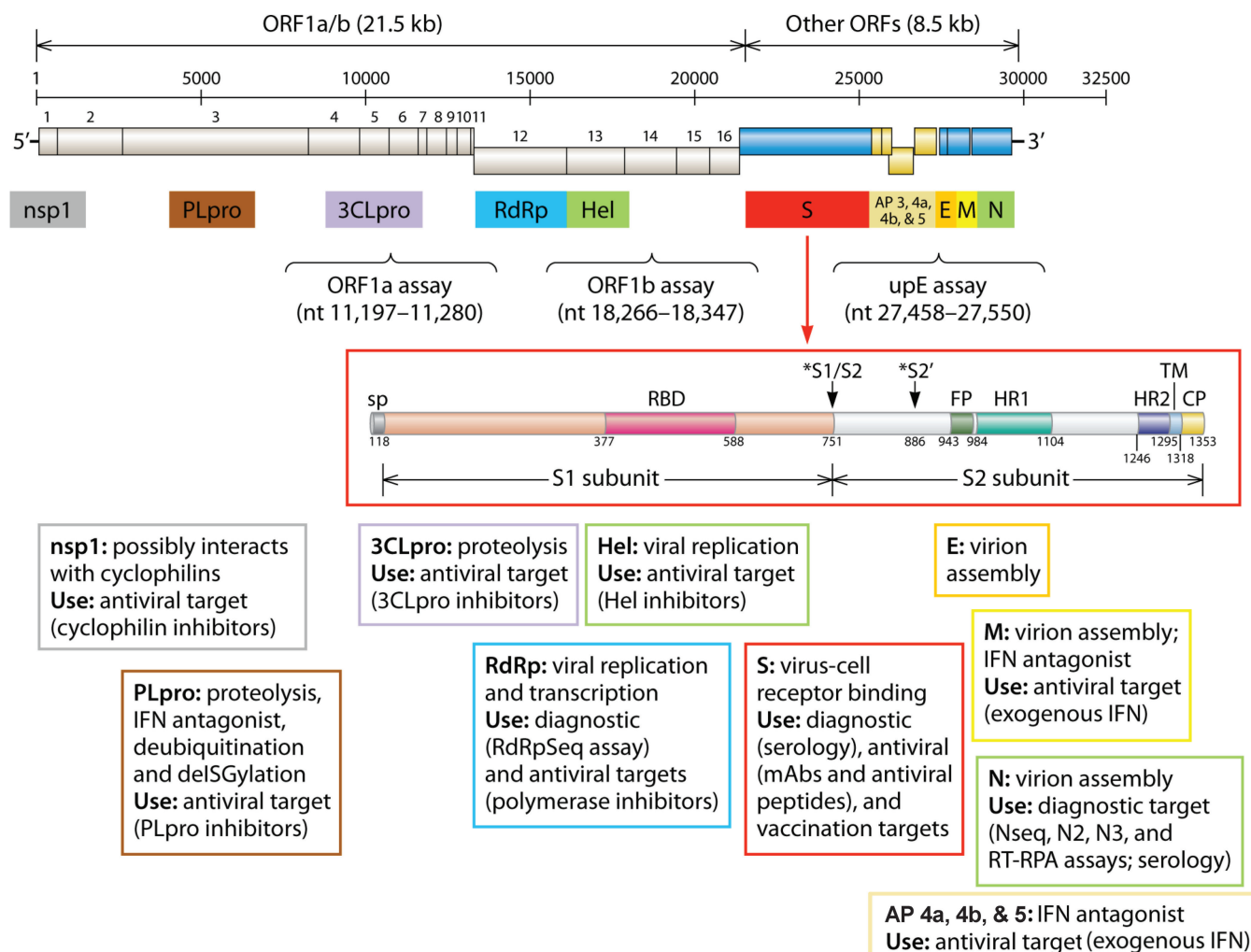


FIG 2 Genome arrangement of MERS-CoV, with emphasis on the clinical applications of the key nonstructural and structural genes and/or gene products. *, furin cleavage sites. Abbreviations: 3CLpro, 3C-like protease; AP, accessory protein; CP, cytoplasmic domain; E, envelope; FP, fusion peptide; Hel, helicase; HR, heptad repeat; IFN, interferon; M, membrane; mAb, monoclonal antibody; N, nucleocapsid; nsp, nonstructural protein; ORF, open reading frame; PLpro, papain-like protease; RBD, receptor-binding domain; RdRp, polymerase; RT-RPA, reverse transcription isothermal recombinase polymerase amplification; S, spike; SP, signal peptide; TM, transmembrane domain.

acts with M protein to generate the basic structure and complexes with the S and E proteins to induce viral budding and release from the Golgi apparatus (61). The viral replication cycle is completed when the assembled virion is released through exocytosis to the extracellular compartment.

SEQUENCE OF EVENTS IN THE MERS EPIDEMIC

On 23 September 2012, the World Health Organization (WHO) reported two cases of acute respiratory syndrome with renal failure associated with a novel CoV in two patients from the Middle

(NC_001846); Mi-BatCoV 1A, *Miniopterus* bat coronavirus 1A (NC_010437); Mi-BatCoV 1B, *Miniopterus* bat coronavirus 1B (NC_010436); Mi-BatCoV HKU7, *Miniopterus* bat coronavirus HKU7 (DQ249226); Mi-BatCoV HKU8, *Miniopterus* bat coronavirus HKU8 (NC_010438); MRCoV HKU18, magpie robin coronavirus HKU18 (NC_016993); MunCoV HKU13, munia coronavirus HKU13 (FJ376622); My-BatCoV HKU6, *Myotis* bat coronavirus HKU6 (DQ249224); NeoCoV, coronavirus *Neoromicia*/PML-PHE1/RSA/2011 (KC869678); NHCov HKU19, night heron coronavirus HKU19 (NC_016994); PEDV, porcine epidemic diarrhea virus (NC_003436); PHEV, porcine hemagglutinating encephalomyelitis virus (NC_007732); Pi-BatCoV-HKU5, *Pipistrellus* bat coronavirus HKU5 (NC_009020); PorCoV HKU15, porcine coronavirus HKU15 (NC_016990); PRCV, porcine respiratory coronavirus (DQ811787); RbCoV HKU14, rabbit coronavirus HKU14 (NC_017083); RCoV parker, rat coronavirus Parker (NC_012936); Rh-BatCoV HKU2, *Rhinolophus* bat coronavirus HKU2 (EF203064); Ro-BatCoV-HKU9, *Rousettus* bat coronavirus HKU9 (NC_009021); Ro-BatCoV HKU10, *Rousettus* bat coronavirus HKU10 (JQ989270); SARS-CoV, SARS coronavirus (NC_004718); SARSr-CiCoV, SARS-related palm civet coronavirus (AY304488); SARSr-Rh-BatCoV HKU3, SARS-related *Rhinolophus* bat coronavirus HKU3 (DQ022305); Sc-BatCoV 512, *Scotophilus* bat coronavirus 512 (NC_009657); SpCoV HKU17, sparrow coronavirus HKU17 (NC_016992); TCoV, turkey coronavirus (NC_010800); TGEV, transmissible gastroenteritis virus (DQ443743.1); ThCoV HKU12, thrush coronavirus HKU12 (FJ376621); Ty-BatCoV-HKU4, *Tylonycteris* bat coronavirus HKU4 (NC_009019); WECov HKU16, white-eye coronavirus HKU16 (NC_016991); WiCoV HKU20, wigeon coronavirus HKU20 (NC_016995).

TABLE 2 Nomenclature and putative functional characteristics of MERS-CoV gene products with analogy to SARS-CoV^a

Gene (no. of amino acid residues in product)	Gene product and/or putative functional domain(s)	Characteristics and/or effect on cellular response of host	References
ORF1a/b			
nsp1 (193)	Unknown	May induce template-dependent endonucleolytic cleavage of host mRNA but not viral RNA and may interact with cyclophilins which may be blocked by cyclosporine	16, 20–22, 251, 297, 298
nsp2 (660)	Unknown	May interact with prohibitin 1 and 2, disrupts intracellular signaling	16, 20–22, 251, 299
nsp3 (1,887)	Papain-like protease	Structurally similar to the papain-like protease of SARS-CoV albeit with only 30% sequence identity, consisting of a right-hand-like architecture with palm, thumb, and fingers domains; specific conserved structural features include the ubiquitin-like domain, a catalytic triad consisting of C1594-H1761-D1776, and the ubiquitin-binding domain at the zinc finger; functions: proteolytic processing of the viral replicase polyprotein at 3 sites (nsp1-2, 2-3, and 3-4) to generate nsps that contribute to subgenomic RNA synthesis, deISGylating (ISG15-linked ISGylation) and deubiquitinating (K48- and K63-linked ubiquitination) activities, interferon antagonist (reduces induction of NF-κB, blocks phosphorylation and nuclear translocation of IRF3, and blocks upregulation of cytokines CCL5, interferon beta, and CXCL10 in HEK293T cells)	16, 20–22, 28, 171, 172, 251, 300–303
	ADP-ribose 1''-phosphatase	Putative dephosphorylation of Appr-1''-p, a side product of cellular tRNA splicing, to ADP-ribose	16, 20–22, 251
	Transmembrane domain	Uncertain function, but may be similar to other CoVs, including SARS-CoV, in anchoring the viral replication complex through recruitment of intracellular membranes to form a reticulovesicular network of CMs and DMVs interconnected via the outer membrane with the rough endoplasmic reticulum	16, 20–22, 251, 304
nsp4 (507)	Transmembrane domain	Similar to nsp3 and may help to form part of the viral replication complex	16, 20–22, 251, 304
nsp5 (306)	Main, chymotrypsin-like, or 3C-like protease	Proteolytic processing of the replicative polyprotein at specific sites and forming key functional enzymes such as replicase and helicase	16, 20, 22, 251
nsp6 (292)	Transmembrane domain	Membrane-spanning integral component of the viral replication complex involved in DMV formation; substitutions may lead to resistance to the viral RNA synthesis inhibitor K22	16, 20–22, 251, 304
nsp7 (83)	Unknown	In SARS-CoV, nsp7 and -8 are part of a unique multimeric RNA polymerase complex	16, 20–22, 251, 305
nsp8 (199)	Primase	In SARS-CoV, nsp9 is an essential protein dimer with RNA/DNA binding activity	16, 20–22, 251
nsp9 (110)	Unknown	In SARS-CoV, nsp10 is required for nsp16 to bind both m7GpppA-RNA substrate and S-adenosyl-L-methionine cofactor; nsp16 possesses the canonical scaffold of MTase and associates with nsp10 at 1:1 ratio	16, 20–22, 252, 306
nsp10 (140)	Unknown		16, 20–22, 252, 307
nsp11 (14)	Unknown	Unknown	16, 20–22, 251
nsp12 (933)	RNA-dependent RNA polymerase	Replication and transcription to produce genome- and subgenome-size RNAs of both polarities	16, 20–22, 251
nsp13 (598)	Superfamily 1 helicase Zinc-binding domain	Putative dNTPase and RNA 5'-triphosphatase activities	16, 20–22, 251 16, 20–22, 251

nsp14 (524)	3'-to-5' exonuclease N7-methyltransferase	Putative endoribonuclease activity in the replication of the giant RNA genome	16, 20–22, 251
nsp15 (343)	Nidoviral endoribonuclease specific for U	Putative RNA endonuclease that is essential in the CoV replication cycle	16, 20–22, 251
nsp16 (303)	S-Adenosylmethionine-dependent ribose 2'-O-methyltransferase	In SARS-CoV, nsp16 is critical for capping of viral mRNA and prevents recognition by host sensor molecules	16, 20–22, 251, 308
ORF2 (1,353)	Spike (S) protein	A type I transmembrane glycoprotein displayed on viral membrane surface critical for receptor binding and membrane fusion	16, 20–22, 251
ORF3 (103)	Accessory protein 3	Deletion of ORF3, -4, and -5 accessory cluster showed ~1.5-log reduction in viral titer compared with recombinant MERS-CoV and resulted in enhanced expression of subgenomic gRNA2 encoding the S protein associated with an increased fusion phenotype; not essential for virus replication in Vero A66 and Huh-7 cells	16, 20–22, 187, 251, 309
ORF4a (109)	Accessory protein 4a	A dsRNA-binding protein with a dsRNA-binding domain (residues 3 to 83) that potentially antagonizes host interferon response via inhibition of interferon production (interferon beta promoter activity, IRF-3/7 and NF-κB activation), ISRE promoter element signaling pathways, and/or suppression of PACT-induced activation of RIG-I and MDA5 in an RNA-dependent manner; not essential for virus replication in Vero A66 and Huh-7 cells	16, 20–22, 24, 25, 251, 309
ORF4b (246)	Accessory protein 4b	May have interferon antagonist activity; not essential for virus replication in Vero A66 and Huh-7 cells	16, 20–22, 24–27, 251, 309
ORF5 (224)	Accessory protein 5	Interferon antagonist with no effect on interferon beta promoter activation; not essential for virus replication in Vero A66 and Huh-7 cells	16, 20–22, 27, 187, 251, 309
ORF6 (82)	Envelope (E) protein	Putative ion channel activity and is involved in viral budding and release; essential for efficient virus propagation in Vero A66 and Huh-7 cells	16, 20–22, 251, 309
ORF7 (219)	Membrane (M) protein	Surface protein that incorporates viral components into virions and interacts with N protein in infected cells; interferon antagonist	16, 20–22, 24, 251
ORF8a (413)	Nucleocapsid (N) protein	Interacts with C-terminal domain of M protein for binding and packaging of viral RNA in assembly of the virion	16, 20–22, 251
ORF8b (112)	Unknown	Unknown	16, 20–22, 251

^a The putative functions of the accessory gene products of MERS-CoV and SARS-CoV may not directly correlate, as the accessory genes of these two viruses are not homologous. Abbreviations: CCL5, chemokine ligand 5; CM, convoluted membrane; CoV, coronavirus; CXCL10, chemokine (C-X-C motif) ligand 10; DMV, double membrane vesicle; dNTPase, deoxynucleoside triphosphatase; IRF3, interferon regulatory factor 3; ISG, interferon-stimulated gene; nsp, nonstructural protein.

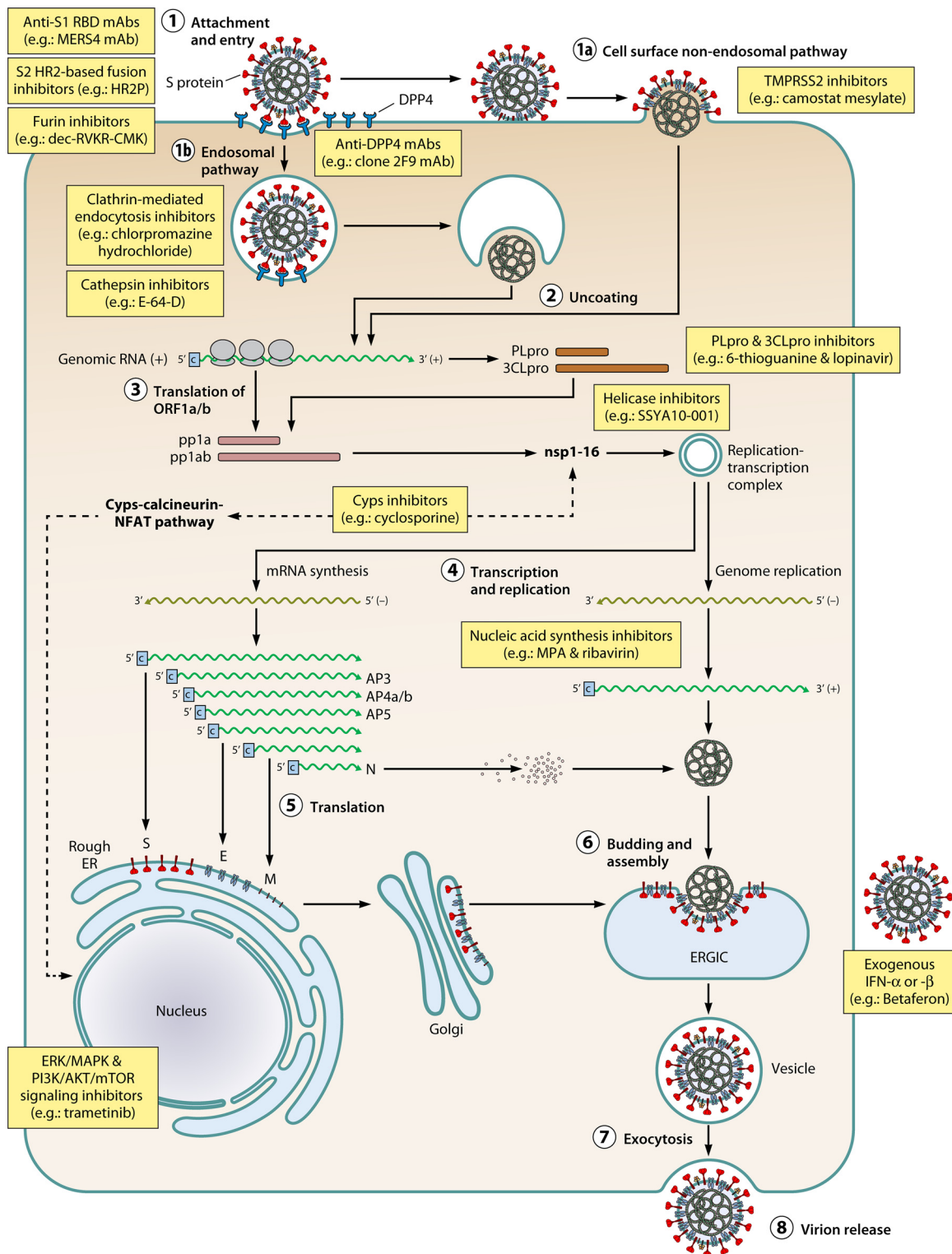


FIG 3 Candidate antiviral agents for MERS-CoV in relation to the viral replication cycle. + and –, positive- and negative-strand RNA, respectively. Abbreviations: AKT, protein kinase B; AP, accessory protein; Cyps, cyclophilins; dec-RVVR-CMK, decanoyl-RVVR-chloromethylketone; DPP4, dipeptidyl peptidase 4; E, envelope; ER, endoplasmic reticulum; ERGIC, endoplasmic reticulum Golgi intermediate compartment; ERK, extracellular signal-regulated kinases; HR2P, heptad repeat 2 peptide; IFN, interferon; M, membrane; mAb, monoclonal antibody; MAPK, mitogen-activated protein kinases; MPA, mycophenolic acid; mTOR, mammalian target of rapamycin; N, nucleocapsid; NFAT, nuclear factor of activated T cells; nsp, nonstructural protein; ORF, open reading frame; PI3K, phosphatidylinositol 3-kinases; S, spike; TMPRSS2, transmembrane protease serine protease 2.

East (Table 3). The viral strains obtained from the respiratory tract specimens of these two epidemiologically unlinked patients shared 99.5% nucleotide identity with each other, with only one nucleotide mismatch in partial replicase gene sequencing (18). In the following week, the WHO and other collaborative health care authorities rapidly responded to the outbreak by providing a unified interim case definition, making the complete genome sequence publicly available in GenBank, and establishing a laboratory diagnostic protocol for real-time reverse transcription-PCR (RT-PCR) using the upE (upstream of E gene) and ORF1b assays (16, 62). With these important tools, sporadic cases were increasingly detected in the Middle East over the subsequent 6 months, including two retrospectively diagnosed cases that occurred in a health care-associated cluster of severe respiratory disease in Zarqa, Jordan, in April 2012 (19, 63–66). Additional cases were also reported in Europe and Africa among patients with recent travel to the Arabian Peninsula and their close hospital and household contacts (18, 67–74). The fear of person-to-person transmission was further heightened by the occurrence of a large-scale outbreak involving over 20 patients in four interrelated hospitals in Al-Hasa, the Kingdom of Saudi Arabia (KSA), from April to May 2013 (75).

In view of the significant epidemiological link of all the reported cases to the region, the ICTV formally named the novel virus MERS-CoV on 15 May 2013 (17). However, the epidemic was not contained within the Middle East as its name implied, and the number of patients and countries involved continued to escalate over the following years (76–81). In particular, there was a sudden surge of over 400 cases in KSA and the United Arab Emirates (UAE) within just 2 months from mid-March to May 2014 as a result of both an increased number of primary cases (possibly related to the weaning season of dromedary camels, a probable zoonotic source of MERS-CoV) and an amplification of the number of secondary cases by several health care-associated outbreaks in the region during the same period (82, http://www.who.int/csr/disease/coronavirus_infections/MERS_CoV_Update_09_May_2014.pdf). As of 26 February 2015, the WHO has reported a total of 1,030 laboratory-confirmed cases of MERS, including 381 deaths. The affected countries with primary cases include KSA, Qatar, Jordan, UAE, Oman, Kuwait, Egypt, Yemen, Lebanon, and Iran in the Middle East. The countries with imported cases include the United Kingdom, Germany, France, Italy, Greece, the Netherlands, Austria, and Turkey in Europe, Tunisia and Algeria in Africa, Malaysia and the Philippines in Asia, and the United States in North America.

EPIDEMIOLOGY

Among the first 699 laboratory-confirmed cases of MERS, 63.5% of the patients were male and the median age was 47 years, with a range of 9 months to 94 years (http://www.who.int/csr/disease/coronavirus_infections/MERS-CoV_summary_update_20140611.pdf). The persistence of the epidemic is postulated to be related to repeated animal-to-human transmissions from at least one type of animal reservoir that is in frequent contact with residents in the region, which are amplified by nonsustained person-to-person transmission in multiple large-scale health care-associated outbreaks and limited household clusters (67, 68, 70, 71, 73–75, 83, 84; http://www.who.int/csr/disease/coronavirus_infections/MERS-CoV_summary_update_20140611.pdf). Human infection has been linked to contact with dromedary camels (*Camelus*

dromedarius) or other humans infected with MERS-CoV, but alternative sources of infection are possible, as many patients did not have an epidemiological link to infected camels or humans. All primary MERS cases were epidemiologically linked to the Middle East, and all secondary cases in other countries were linked to primary cases imported from the Middle East. The incubation period is estimated to be 5.2 days, with a range of 1.9 to 14.7 days, and 95% of infected patients have symptom onset by day 12.4 (63, 75). The serial interval, representing the time between the case's symptom onset and the contact's symptom onset, is estimated to be 7.6 days with a range of 2.5 to 23.1 days and is less than 19.4 days in 95% of the cases (63, 75). The rate of secondary transmission among household contacts of MERS patients is estimated to be about 4% (85).

Risk Factors for Severe Disease

Among the first 536 laboratory-confirmed cases reported by the WHO, 62% were severe cases that required hospitalization (77). Severe cases requiring hospitalization were more commonly seen among primary cases, which mainly consist of older patients with comorbidities. The secondary cases were mostly younger patients and health care workers without comorbidities, but severe nosocomial infection among patients sharing contaminated equipment with improper barrier controls have also been reported (75; http://www.who.int/csr/disease/coronavirus_infections/MERS-CoV_summary_update_20140611.pdf) (Table 4). In a clinical cohort from KSA with 47 severe cases requiring hospitalization, the patients' median age was 56 years. There was a male predominance, with a male-to-female ratio of 3.3 to 1 (63). About 96% of the patients had comorbidities, with the most common being diabetes mellitus (68%), chronic renal disease (49%), hypertension (34%), chronic cardiac disease (28%), and chronic pulmonary disease (26%). Smoking and obesity were reported in 23% and 17% of the patients, respectively. The predominance of older males with comorbidities among severe cases was also reported in other case series at variable rates, depending on the size and setting of the studies (63, 66, 75, 80, 86–89). Furthermore, age of over 50 years, male sex, and the presence of multiple comorbidities were associated with a higher fatality rate (63, 87, 90). Some of these conditions are highly prevalent among residents in the Middle East, for example, diabetes mellitus in nearly 63% of persons at or older than 50 years in KSA (91). Their relative risk of developing severe MERS requires further evaluation in large-scale case-control studies. Patients who develop complications such as acute respiratory distress syndrome requiring hospitalization and/or intensive care are also at risk of fatal outcome (87).

Seroepidemiology

The interim WHO case definition used early in the epidemic was criticized for being focused on identifying severe cases, which might have overestimated the clinical severity and significance of MERS (92). This was supported by the increasing number of asymptomatic and mild cases identified in subsequent enhanced surveillance among contacts of MERS patients in various clusters. It was thus suggested that the genuine epidemiology of MERS-CoV might be more similar to that of HCoV-HKU1 rather than SARS-CoV in that the infection is prevalent in the general population but manifests severely only in the elderly and immunocompromised (93–96). However, seroepidemiological studies conducted so far have refuted this hypothesis, as there is little evidence of past infection among the general population

TABLE 3 Sequence of events with epidemiological importance related to MERS^a

Date ^b	Place or institution	Important event	Reference(s)
19 April 2012	Zarqa, Jordan	First health care-associated cluster: an outbreak of severe respiratory disease among 13 patients and health care workers in an ICU. The index patient and a close contact (ICU nurse) were subsequently confirmed to be infected with MERS-CoV in November 2012.	66
6 June 2012	Jeddah, KSA	First laboratory-confirmed case: a 60-year-old man was admitted to a regional hospital for severe acute community-acquired pneumonia complicated with acute renal failure and later died. A novel CoV was isolated in cell culture of a sputum sample obtained on admission. The virus was initially named human coronavirus-Erasmus Medical Center (HCoV-EMC).	9
3 September 2012	London, UK	First imported case in UK: a 49-year-old man in Qatar with travel history to KSA was transferred from Doha, Qatar to an ICU in London, UK, on 11 September 2012 for severe acute community-acquired pneumonia. A novel CoV was detected in combined nose and throat swab, sputum, and tracheal aspirate samples. The replicase gene fragment of this strain shared 99.5% identity with the first HCoV-EMC strain.	18, 84
23 September 2012	WHO	WHO disease outbreak news: report of the first 2 laboratory-confirmed cases.	http://www.who.int/csr/don/2012_09_23/en/
25 September 2012	WHO	First interim case definition for HCoV-EMC infection issued.	
26 September 2012	EMC, Rotterdam, the Netherlands	First complete genome of HCoV-EMC available in GenBank (accession no. JX869059).	http://www.who.int/csr/don/2012_09_25/en/
27 September 2012	ECDC	Protocols for real-time RT-PCR (upE and ORF1b) assays published in <i>Eurosurveillance</i> .	310
5 October to 14 November 2012	KSA	First household cluster: three household family members of a 70-year-old man with laboratory-confirmed HCoV-EMC infection were hospitalized for severe respiratory disease.	67
9 October 2012	Riyadh, KSA	First survived case: a 45-year-old man who was admitted for severe respiratory disease and renal failure recovered from HCoV-EMC infection.	64
13 October 2012	Essen, Germany	First imported case in Germany.	69
21 December 2012	WHO	First interim recommendations for laboratory testing for HCoV-EMC issued.	http://www.who.int/csr/disease/coronavirus_infections/LaboratoryTestingNovelCoronavirus_21Dec12.pdf?ua=1
24 January to 16 February 2013	UK	First cluster outside the Middle East: a 60-year-old man with recent travel history to KSA was admitted to an ICU for laboratory-confirmed HCoV-EMC. Two of his relatives who were close contacts also developed laboratory-confirmed MERS.	73
5 February 2013	UK	First mild case: the 30-year-old female relative in the UK cluster had only mild, influenza-like illness symptoms and spontaneously recovered.	73
8 March 2013	UAE	First case in UAE.	72
8 April to May 2013	Al-Hasa, KSA	First large-scale cluster: >20 laboratory-confirmed cases of HCoV-EMC were reported in household and hospital contacts in the Eastern Province of KSA.	75
22 April 2013	Valenciennes, France	First imported case in France.	68, 71
6 May 2013	Tunisia	First imported cases in Tunisia.	74
15 May 2013	Coronavirus Study Group, ICTV	Formal naming of the novel CoV as Middle East respiratory syndrome coronavirus.	17

25 May 2013	Italy	First imported case in Italy.	http://www.who.int/csr/don/2013_06_01_ncov/en/
2 June 2013 ^c	Italy	First pediatric case: a 2-year-old girl who was a close contact of the first imported case in Italy (subsequently reclassified as a probable case).	163
9 August 2013	Oman	First report on the detection of anti-MERS-CoV antibodies in dromedaries in the Middle East.	121
23 August 2013	CDC	First report on the detection of a short (182-nt) fragment of the viral RdRp gene from a fecal pellet of a <i>Taphozous perforatus</i> bat in KSA, which showed 100% identity to that of MERS-CoV (strain HCoV-EMC/2012).	109
16 September 2013	CDC	First report on the detection of a MERS-CoV-like virus (<i>Neoromicia coronavirus</i>) with 85.6% nt identity (complete genome) in the fecal sample of a <i>Neoromicia capensis</i> bat in South Africa.	110, 111
26 October 2013	Oman	First case in Oman.	http://www.who.int/csr/don/2013_10_31/en/
17 December 2013	Qatar	First report on the detection of MERS-CoV RNA in nose swabs from dromedaries by RT-PCR.	133
13 February 2014	Kuwait	First case in Kuwait.	http://www.who.int/csr/don/2014_03_20_mers/en/
17 March 2014	Yemen	First case in Yemen.	http://www.who.int/csr/don/2014_05_07_mers_yemen/en/
9 April 2014	Malaysia	First imported case in Malaysia.	78
13 April 2014	The Philippines	First imported case in the Philippines.	http://www.who.int/csr/don/2014_04_17_mers/en/
17 April 2014	Greece	First imported case in Greece.	76
18 April 2014	USA	First imported case in USA.	77, 81
22 April 2014	Egypt	First imported case in Egypt.	http://www.who.int/csr/don/2014_05_01_mers/en/
mid-March to May 2014	KSA and UAE	Sudden surge of >400 cases associated with an increase in the no. of primary cases amplified by several large health care-associated outbreaks in KSA and UAE.	http://www.who.int/csr/disease/coronavirus_infections/MERS-CoV_summary_update_20140611.pdf?ua=1
22 April 2014	Lebanon	First case in Lebanon.	http://www.who.int/csr/don/2014_05_15_mers/en/
1 May 2014	The Netherlands	First imported case in the Netherlands.	79
1 May 2014	Iran	First cases in Iran.	345
23 May 2014	Algeria	First imported cases in Algeria.	http://www.who.int/csr/don/2014_06_14_mers/en/
4 June 2014	KSA	First report on camel-to-human transmission of MERS-CoV.	138
22 September 2014	Austria	First imported case in Austria.	http://www.who.int/csr/don/02-october-2014-mers-arabia/en/
25 September 2014	Turkey	First imported case in Turkey.	http://www.who.int/csr/don/24-october-2014-mers/en/
26 February 2015	WHO	A total of 1,030 laboratory-confirmed cases of MERS, including at least 381 deaths, were reported.	http://www.who.int/csr/don/26-february-2015-mers-saudi-arabia/en/

^a Abbreviations: CoV, coronavirus; CDC, Centers for Disease Control and Prevention; ECDC, European Centre for Disease Prevention and Control; ICTV, International Committee on Taxonomy of Viruses; ICU, intensive care unit; KSA, Kingdom of Saudi Arabia; UAE, United Arab Emirates; UK, United Kingdom; USA, United States of America; WHO, World Health Organization.

^b The date of reported cases represents the date of symptom onset unless otherwise specified.

^c The date of reporting by WHO.

TABLE 4 Underlying comorbidities of patients with laboratory-confirmed MERS^a

Value for clinical cohort described in reference(s):									
Parameter	87	66	63	75	80	88	311	86, 152, 334, 335	
Time period	April 2012 to 22 October 2013	April 2012	1 September 2012 to 15 June 2013	1 March 2013 to 19 April 2013	1 April 2013 to 3 June 2013	May 2013 to August 2013	1 October 2012 to 31 May 2014		
Setting or data source	161 cases reported to WHO	Retrospective outbreak investigation in Jordan	All cases reported by the KSA Ministry of Health to WHO	Outbreak investigation in 4 hospitals in Al-Hasa, KSA	A 350-bed general hospital in KSA	3 intensive care units in KSA	70 cases at a single center in Riyadh, KSA	Case reports or case series	
Underlying comorbidities ^b									
Any	91/120 (75.8%); fatal (86.8%) > nonfatal (42.4%) cases	NA	45/47 (95.7); 28/45 (62.2) fatal	NA	12/12 (100)	NA	57/70 (81.4)	Fatal (40/55; 72.7%) > nonfatal (30/73; 41.1%) cases	NA
Chronic pulmonary disease	NA	NA	12/47 (25.6); 10/12 (83.3) fatal	10/23 (43.5)	6/15 (40.0)	Asthma, 1/12 (8.3)	NA	NA	NA
Chronic renal disease	16/120 (13.3); 20.8% fatal cases; secondary (23.0%) > primary (4.3%) cases	NA	23/47 (48.9); 17/23 (73.9) fatal	NA	5/15 (33.3)	5/12 (41.7); 1/12 (8.3) required dialysis	NA	NA	NA
Chronic cardiac disease	9/120 (7.5); at least 2 fatal; primary (7/47, 14.9%) > secondary (2/61, 3.3%) cases	1/8 (12.5)	13/47 (27.7); 10/13 (76.9) fatal	9/23 (39.1)	8/15 (53.3), including 3/15 (20.0) with CHF	MI, 4/12 (33.3); cardiac surgery, 3/12 (25.0); CHF, 2/12 (16.7); valvular disease, 1/12 (8.3); PVD, 2/12 (16.7)	NA	Chemotherapy-induced cardiomyopathy, 1/7 (14.3)	NA
Diabetes mellitus	12/120 (10.0); 3.8% fatal cases; primary (11/47, 23.4%) > secondary (1/61, 1.6%) cases	NA	32/47 (68.1); 21/32 (65.6) fatal	17/23 (73.9)	13/15 (86.7)	8/12 (66.7)	NA	3/7 (42.9)	NA
Hypertension	NA	2/8 (25.0)	16/47 (34.0); 13/16 (81.3) fatal	NA	NA	6/12 (50.0)	NA	3/7 (42.9)	NA
Obesity	NA	NA	8/47 (17.0); 5/8 (62.5) fatal	5/21 (23.8)	Mean BMI, 32.02 ± 6.78 kg/m ²	Median BMI, 31.8 (21.6 to 46.1) kg/m ² ; 3/12 (33.3) were obese	7/70 (10.0)	1/7 (14.3)	NA
Smoking	NA	2/8 (25.0)	11/47 (23.4); 7/11 (63.6) fatal	NA	NA	4/12 (33.3)	9/70 (12.9)	2/7 (28.6)	NA
Malignancy	NA	NA	1/47 (2.1); fatal	NA	1/15 (6.7)	1/12 (8.3)	NA	2/7 (28.6)	NA
Other	NA	Pregnancy	Immunosuppressive therapy, 3/47 (6.4); all 3 fatal	NA	NA	Stroke, kidney and liver transplant, and neuromuscular disease	Pregnancy	Dyslipidemia, 1/7 (14.3); kidney transplant, and HIV infection	NA

^a Abbreviations: BMI, body mass index; CHF, congestive heart failure; HIV, human immunodeficiency virus; KSA, Kingdom of Saudi Arabia; MI, myocardial infarction; NA, not available; PVD, peripheral vascular disease; WHO, World Health Organization.

^b Unless indicated otherwise, data are reported as number with comorbidity/total (percentage with comorbidity).

in the Middle East. Serum anti-MERS-CoV antibodies were not detected in archived serum samples of 2,400 control in- or outpatients without MERS in KSA, suggesting that MERS-CoV was unlikely to be circulating in the general population during the preceding 2 years (9, 90). Similarly, serum neutralizing anti-MERS-CoV antibodies were not detected among 158 children hospitalized for lower respiratory tract infections and 110 adult male blood donors in KSA between May 2010 and December 2012 (97). Even among 226 slaughterhouse workers who had contact with various livestock species that might serve as zoonotic sources of MERS-CoV, neutralizing anti-MERS-CoV antibodies were not detected in serum samples collected in October 2012 (98). Additional region-wide seroepidemiological studies that include large collections of archived samples from earlier time points may determine the true prevalence and clinical severity of MERS among residents in the affected areas.

Animal Surveillance

Given the sudden emergence of MERS-CoV without definite serological evidence of past exposure in the general population, a novel episode of interspecies transmission of the virus was postulated. An intense hunt for animal reservoirs of MERS-CoV was sparked by the early recognition of the close phylogenetic relationship between MERS-CoV and the prototype lineage C β CoVs, Ty-BatCoV-HKU4 and Pi-BatCoV-HKU5, which suggested the possibility of MERS-CoV being a zoonotic agent (9, 13, 14, 21, 99). Subsequent functional studies showed that Ty-BatCoV-HKU4 also utilizes DPP4 as a functional receptor for cell entry in a pseudotyped virus assay (100, 101). These findings concur with the existing notion that bats are the likely gene sources of most α CoVs and β CoVs, including SARS-CoV (1, 15, 102–107). Recent reports also show a high ratio of nonsynonymous (d_N) to synonymous (d_S) nucleotide substitutions per site in the bat DPP4-encoding genes (108). This adaptive evolution in the bat DPP4 is suggestive of long-term interactions between bats and MERS-CoV-related viruses (108). In addition to Ty-BatCoV-HKU4 and Pi-BatCoV-HKU5, which are found in bats in Hong Kong and southern China, other lineage C β CoVs closely related to MERS-CoV were also identified in different bat species in the Middle East, Africa, Europe, and Central America after the MERS epidemic started (Table 5). The virus that is most closely related to MERS-CoV phylogenetically was a β CoV detected in the fecal pellet of a *Taphozous perforatus* bat caught in Bisha, KSA, near the home of a patient with laboratory-confirmed MERS, which shared 100% nucleotide identity with MERS-CoV by partial RdRp gene sequencing (109). However, this study was limited by the short length of the gene fragment analyzed (182 nucleotides) and its detection in only one of 29 (3.4%) *T. perforatus* bats caught at the same location. Furthermore, no live virus was isolated from any of these bats. Subsequent studies identified a closely related virus, NeoCoV, in the feces of a *Neoromicia capensis* bat in South Africa which had a complete genome sequence sharing 85.6% nucleotide identity with those of MERS-CoVs from infected humans and dromedary camels (110, 111). Based on the estimated evolutionary rate of MERS-CoV, the most recent common ancestor between NeoCoV and human MERS-CoV strains was proposed to exist in bats more than 44 years ago (112). As the same lineage of CoVs are usually found and originate from closely related bat species, the likelihood of MERS-CoV originating from both *T. perforatus* (superfamily *Emballonuroidea*) and vespertilionid bats (*Neoromicia capensis*, *Pipistrellus* sp., and *Tylonycteris pachypus* in

the superfamily *Vespertilionoidea*), which belong to two distantly related superfamilies of insectivorous bats, is low (20, 110, 111). Interestingly, European hedgehogs (*Erinaceus europaeus*) belonging to the order *Eulipotyphla*, which are closely related to bats phylogenetically, also carry high concentrations of a MERS-CoV-related lineage C β CoV, *Erinaceus* CoV, in their feces and intestines (113). Further surveillance and full virus genome sequencing involving a larger population of different bat and bat-related species are required to confirm these preliminary findings.

Besides the possibility of direct interspecies transmission of SARS-CoV from bats to humans, it is postulated that intermediate amplifying animal hosts such as civets and raccoon dogs might also have been important in the transmission of SARS. Therefore, specific intermediate animal hosts of MERS-CoV with frequent contact with infected humans were sought since the early phase of the MERS epidemic (3, 114, 115). In *in vitro* studies, MERS-CoV can replicate efficiently not only in a variety of bat cell lines but also in cell lines originating from other animal species, including camelid, goat, pig, rabbit, horse, and civet (116–118, 336) (Table 6). The host range is determined mainly by the binding of the MERS-CoV S protein to the host receptor DPP4, which is relatively conserved among mammalian species (30, 48, 49, 119, 120). The first *in vivo* evidence to support the presence of an intermediate animal reservoir of MERS-CoV emerged when high titers of serum neutralizing IgG against the MERS-CoV S1 RBD were detected in dromedary camels (121). All 50 Omani dromedary camels were seropositive, compared to fewer than 10% of the Spanish dromedary camels and none of the other common livestock species in the study. This suggested that widespread circulation of MERS-CoV or a closely related virus was present among dromedary camels in this Middle Eastern country. Numerous seroepidemiological studies also demonstrated serological evidence of MERS-CoV infection in dromedary camels in other Middle Eastern countries, including KSA, Qatar, UAE, and Jordan, and also in African countries, including Egypt, Kenya, Nigeria, Ethiopia, Tunisia, Somalia, and Sudan, from where most of the camels found in the Middle East have originated (Table 5). Serological evidence of infection among camels was detected in archived specimens collected in as early as 1992 and 1983 in KSA and eastern Africa, respectively, and was especially prevalent in areas of high dromedary population density (122–133). These findings suggested that unrecognized primary human cases of MERS might also be present outside the Middle East. On the other hand, studies in Qatar and several other countries showed that anti-MERS-CoV antibodies were not detected in the sera of other livestock species tested, including goats, sheep, cows, water buffaloes, swine, and wild birds (http://www.who.int/csr/disease/coronavirus_infections/MERS_CoV_RA_20140613.pdf). Furthermore, it was also shown that the percent seropositivity of neutralizing anti-MERS-CoV antibodies was much lower in juvenile than in adult dromedary camels, suggesting that acutely infected juvenile dromedary camels without neutralizing antibodies might be a more important source for transmission to humans than adult dromedary camels (123, 127).

The significance of camels as the major source of animal-to-human transmission required further virological studies on the pattern of viral shedding in camels and their relationship to laboratory-confirmed human cases (Fig. 4). An investigation of a disease outbreak in dromedary camels in Qatar demonstrated MERS-CoV in nasal swabs, but not rectal swabs or fecal samples,

TABLE 5 Evidence of zoonotic sources of MERS-CoV and closely related CoVs^a

Animal species and region (virus)	Country (area)/specimen collection date	Main findings	Reference(s)
Bats			
Superfamily <i>Vespertilionoidea</i> , family <i>Vespertilionidae</i>			
Asia			
<i>Tylonycteris pachypus</i> (Ty-BatCoV HKU4)	China (Hong Kong)/April 2005 to August 2012	Detected in 29/99 (29.3%) alimentary samples; shared 90.0% (RdRp), 67.4% (S), and 72.3% (N) aa identities with MERS-CoV (HCoV-EMC/2012).	13, 99
<i>Pipistrellus abramus</i> (Pi-BatCoV HKU5)	China (Hong Kong)/April 2005 to August 2012	Detected in 55/216 (25.5%) alimentary samples; shared 92.3% (RdRp), 64.5% (S), and 70.5% (N) aa identities with MERS-CoV (HCoV-EMC/2012).	13, 99
<i>Vespertilio superans</i> (Bat CoV-BetaCoV/SC2013)	China (southwestern part)/June 2013	Detected in 5/32 (15.6%) anal swabs; shared 75.7% (complete genome of 1 strain) nt identity; and 96.7% (816-nt RdRp fragment) and 69.0% (S) aa identities with MERS-CoV (HCoV-EMC/2012).	312
Africa			
<i>Neoromicia capensis</i> (NeoCoV)	South Africa (KwaZulu-Natal and Western Cape provinces)/2011	Detected in 1/62 (1.6%) fecal samples; shared 85.6% (complete genome) nt identity; and 64.6% (S), 89.0% (E), 94.5% (M), and 91.7% (N) aa identities with MERS-CoV from humans and camels, placing them in the same viral species based on taxonomic criteria.	110, 111
Europe			
<i>Pipistrellus</i> , <i>Pipistrellus nathusii</i> , and <i>Pipistrellus pygmaeus</i> (<i>Pipistrellus</i> bat βCoVs)	Romania (Tulcea county) and Ukraine (Kiev region)/2009–2011	Detected in 40/272 (14.7%) fecal samples; shared 98.2% (816-nt RdRp fragment) aa identity with MERS-CoV (HCoV-EMC/2012).	313
<i>Pipistrellus kuhlii</i> , <i>Hypsugo savii</i> , <i>Nyctalus noctula</i> , and an unknown <i>Pipistrellus</i> sp. (βCoVs)	Italy (Lombardia and Emilia regions)/2010–2012	10 βCoVs detected in fecal specimens of <i>Pipistrellus kuhlii</i> (7), <i>Hypsugo savii</i> (1), <i>Nyctalus noctula</i> (1), and an unknown <i>Pipistrellus</i> sp. (1) bats; shared 85.2% to 87% nt identity and 95.3% to 96.1% (329-nt RdRp fragment) aa identity with MERS-CoV (HCoV-EMC/2012).	314
Superfamily <i>Emballonuroidea</i> , family <i>Emballonuridae</i>			
<i>Taphozous perforatus</i> (βCoV)	KSA (Bisha)/October 2012	A βCoV detected in 1/29 (3.4%) fecal samples; shared 100% nt identity (182-nt RdRp fragment) with MERS-CoV (HCoV-EMC/2012).	109
Superfamily <i>Molossoidea</i> , family <i>Molossidae</i>			
<i>Nyctinomops laticaudatus</i> (Mex_CoV-9)	Mexico (Campeche)/2012	Detected in 1/5 (20.0%) rectal swabs; shared 96.5% (329-nt RdRp fragment) aa identity with MERS-CoV (HCoV-EMC/2012).	315
Superfamily <i>Noctilionoidea</i> , family <i>Mormoopidae</i>			
<i>Pteronotus davyi</i> (BatCoV-P.davyi49/Mexico/2012)	Mexico (La Huerta)/2007–2010	Detected in 1/4 (25.0%) intestinal samples; shared 71.0% (439-nt RdRp fragment) nt identity with MERS-CoV (HCoV-EMC/2012).	316
Superfamily <i>Rhinolophoidea</i> , family <i>Nycteridae</i>			
<i>Nycteris gambiensis</i> (<i>Nycteris</i> bat CoV)	Ghana (Bouyem, Forikrom, and Kwamang)/2009–2011	Detected in 46/185 (24.9%) fecal samples; shared 92.5% aa identity (816-nt RdRp fragment) with MERS-CoV (HCoV-EMC/2012).	313
Hedgehogs			
Europe			
<i>Erinaceus europaeus</i> (<i>Erinaceus</i> CoV)	Northern Germany/unknown date	Two clades detected in 146/248 (58.9%) fecal samples; shared 89.4% (816-nt RdRp fragment), 58.2% (S), 72.0% (E), 79.4% (M), and 72.1% (N) aa identities with MERS-CoV (HCoV-EMC/2012); RNA concn was higher in the intestine and fecal samples than in other solid organs, blood, or urine, suggestive of viral replication in the lower intestine and fecal-oral transmission; 13/27 (48.2%) sera contained nonneutralizing antibodies.	113

KSA (countrywide)/1992 to 2010 and November to December 2013	Serum Ab: 150/203 (73.9%) (2013) and 72%–100% (1992 to 2010); adults (95%) > juveniles (55%). Viral RNA: nasal > rectal swabs; juveniles (36/104; 34.6%) > adults (15/98; 15.3%). Virus isolation: two nasal swabs cultured in Vero E6 cells.	123, 137
KSA (Riyadh and Al Ahsa)/2012 to 2013	Serum NAb: 280/310 (90.3% with titer \geq 1:20); adults (233/245; 95.1%) > juveniles (47/65; 72.3%).	127
KSA (Jeddah)/3 November 2013	Direct camel-to-human transmission: phylogenetic (identical full genome sequences of patient strain and an epidemiologically linked camel strain) and serological (the virus was circulating in the epidemiologically linked camels but not in the patient before the human infection occurred) evidence.	138
KSA (Jeddah)/14 November to 9 December 2013	Serum Ab: 4-fold rise in paired sera in 2/9 (22.2%). Viral RNA: detected in nasal swabs of both camels (upE and ORF1a).	128
KSA (Al-Hasa)/November 2013 to February 2014 (peak calving season)	Serum NAb: 280/310 (90.3%). Viral RNA: nasal > fecal specimens. Viral genome: highly stable with an estimated mutation rate of 0 nt substitutions per site per day. Clinical: both calves and adults could be infected; symptoms included mild respiratory symptoms (cough, sneezing, respiratory discharge), increased body temp, and decreased appetite; acute infection was not associated with prolonged viremia or viral shedding.	129
UAE (Dubai)/2003 and 2013	Serum Ab: 151/151 (100%) (2003) and 481/500 (96.2%) (2013); high titers of NAb > 1:640 in 509/651 (78.2%).	124
UAE (Dubai)/February to October 2005	Serum NAb: 9/11 (81.8%).	125
Oman/March 2013 and Spain (Canary Islands)/April 2012 to May 2013	Serum Ab: 50/50 (100%) of Omani and 15/105 (14.3%) of Spanish camels; all 50/50 (100%) of Omani (titers 1/320 to 1/2560) and 9/105 (9%) of Spanish camels had NAb (titers 1/20 to 1/320).	121
Oman (countrywide)/December 2013	Viral RNA: high concentrations in nasal and conjunctival swabs of 5/76 (6.6%) camels (\geq 2 gene targets).	317
Jordan (al Zarqa governorate)/June to September 2013	Serum NAb: 11/11 (100%).	126
Qatar/17 October 2013	Serum NAb: 14/14 (100%); titers 1/160 to 1/5120. Viral RNA: 5/14 (35.7%) nasal swabs by 3 gene targets (upE, N, and ORF1a), 1/14 (7.1%) by 2 gene targets, and 5/14 (35.7%) by 1 gene target. Viral genome: 3/5 samples shared 100% identity (357-nt S fragment) with sequences from 2 epidemiologically linked patients; further sequencing of 4.2-kb concatenated fragments of a camel strain and 2 epidemiologically linked patient strains; only 1 nt difference in ORF1a and 1 nt difference in ORF4b.	133
Qatar (Doha)/February 2014	Viral RNA: 1/53 (1.9%) nasal swabs from an 8-month-old camel (1/53, 1.9%) (upE and N). Viral genome: complete genome (MERS-CoV camel/Qatar_2_2014) shared 99.5% to 99.9% nt identities with other camel and patient strains.	131
Qatar (Al Shahaniya and Dukhan)/April 2014	Serum and milk Ab: all 33 camels had IgG in serum and milk. Viral RNA: detected in the nose swabs and/or feces of 7/12 camels and the milk of 5/7 of these camels in Al Shahaniya.	144
KSA (Al Hasa, As Sulayyil, Hafar Al-Batin, Medina)/1993, Egypt/2014, and Australia (central Australia and Queensland)/2014	Serum NAb: 118/131 (90.1%) of KSA camels and 0/25 (0%) of Australian camels.	135

(Continued on following page)

TABLE 5 (Continued)

Animal species and region (virus)	Country (area)/specimen collection date	Main findings	Reference(s)
Africa <i>Camelus dromedarius</i>	Somalia/1983 to 1984, Sudan/June and July 1983, Egypt/June and July 1997	Serum NAb: Somalia (70/86, 81.4%), Sudan (49/60, 81.0%), and Egypt (34/43, 79.1%) by MNT.	132
	Kenya/1992 to 2013	Serum Ab: 213/774 (27.5%), including 119/774 (15.4%) with NAb; seropositive camels were found in all sampling sites throughout the study period; increased seroprevalence was significantly correlated with increased camel population density.	130
	Nigeria/2010 to 2011, Tunisia/2009 and 2013, and Ethiopia/2011 to 2013	Serum Ab: Nigeria (94.0% of adults) and Ethiopia (93.0% of juveniles and 97.0% of adults); lower rates in Tunisia (54.0% of adults and 30.0% of juveniles).	318
	Egypt (Cairo and Qalyubia governorate)/June 2013	Serum NAb: 103/110 (93.6% with titer \geq 1:20) by MNT and 108/110 (98% with titer \geq 1:20) by spike ppNT.	122
	Egypt (Alexandria, Cairo, and Nile Delta region)/June to December 2013	Serum NAb: 48/52 (92.3% with titers between 1:20 and \geq 1:640); 0/179 abattoir workers. Viral RNA: 4/110 (3.6%) nasal swabs (upE and ORF1a).	134

^a Abbreviations: aa, amino acid; concn, concentration; KSA, Kingdom of Saudi Arabia; N, nucleocapsid; NAb, neutralizing antibody; nt, nucleotide; ORF, open reading frame; MNT, microneutralization test; RT-PCR, reverse transcription-PCR; ppNT, pseudoparticle neutralization test; RBD, receptor-binding domain; RdRp, RNA-dependent RNA polymerase; S, spike; UAE, United Arab Emirates.

of three of 14 (21.4%) camels by RT-PCR sequencing (133). The nucleotide sequences of a 940-nucleotide ORF1a fragment and a 4.2-kb concatenated gene fragment of these camel strains were very similar to those of two epidemiologically linked human strains. This study, however, was not able to conclusively establish the direction of transmission or exclude the presence of a third source of infection. Subsequently, the detection of MERS-CoV in dromedary camels was reported in a number of studies conducted in different areas in the Middle East, which provided further insights into the viral shedding kinetics in camels (123, 128, 129, 131, 134). In agreement with the lower frequency of neutralizing anti-MERS-CoV antibodies in juvenile camels, the rate of detection of MERS-CoV RNA in the nasal and/or rectal swabs of juvenile camels was higher than in those of adult camels (123). These findings may partially explain the absence of serum neutralizing anti-MERS-CoV antibodies among camel abattoir workers, who have contacted predominantly adult camels (135, 136). These serological surveys should be confirmed by virus neutralization assays. Nevertheless, infected adult camels might still be a source of human infection. Similar to the case for HCoVs and other respiratory viruses that can cause repeated infections in humans over a lifetime, MERS-CoV shedding could be observed in camels with preexisting serum antibodies, suggesting that prior infection and passively acquired maternal antibodies might not provide complete protection from MERS-CoV infection and/or reinfection in camels (129). The fact that the majority of amino acid residues critical for receptor binding are identical between most human and camel strains further supports the potential of the dromedary MERS-CoVs to infect humans despite differences in clinical manifestations of infected humans and camels (129, 131). The higher positivity rate of MERS-CoV RNA in nasal swabs than in rectal swabs or fecal samples and the isolation of MERS-CoV from cultures of nasal swabs but not rectal swabs of camels in Vero E6 cells correlated with the predominantly upper respiratory tract symptoms in acutely infected symptomatic camels (129, 137). Together with the genetic stability of MERS-CoV in camels, these serological and virological data from animal surveillance support the hypothesis that MERS-CoV likely originated from bats in Africa and then crossed species barriers to infect camels in the greater Horn of Africa many years ago. Infected camels were then transported to the Middle East, where they transmitted the virus to nonimmune humans to cause the epidemic (111).

The strongest evidence of direct cross-species transmission of MERS-CoV from camels to humans was provided in a study reporting the isolation of the virus from a dromedary camel which had a complete genome sequence identical to that of a human strain from a patient who developed MERS after close contact with sick camels that had rhinorrhea (138). Serological tests showed seropositivity in the camels but not in the patient before the human infection occurred (138). The air sample collected from the camel barn on the same day when a sick camel tested positive for MERS-CoV, but not on the subsequent 2 days, was also positive for MERS-CoV RNA by RT-PCR (139). This suggests that the virus may persist in the air surrounding infected animals or humans for less than 24 h, although viral infectivity is uncertain because the virus was not culturable from the air sample. Another similar study also reported a human case of MERS that developed after the patient had contact with sick camels with respiratory symptoms (128). Comparison of eight RT-PCR fragments, constituting 15% of the virus genomes derived from the infected

camel and from an epidemiologically linked patient, showed nearly 100% nucleotide identity (128). The genomes of both the camel and human strains of MERS-CoV contained unique nucleotide polymorphism signatures not found in any other known MERS-CoV sequences and therefore supported direct cross-species transmission (128). Preliminary results from an ongoing investigation in Qatar showed that people working closely with camels, including farm workers, slaughterhouse workers, and veterinarians, may be at higher risk of developing MERS than those who do not have regular contact with camels (http://www.who.int/csr/disease/coronavirus_infections/MERS_CoV_RA_20140613.pdf). Notably, while these studies support camel-to-human transmission, a bidirectional mode of transmission cannot be completely excluded at this stage.

In spite of these examples that support the hypothesis of direct camel-to-human cross-species transmission of MERS-CoV, a number of important questions remain unresolved at this stage. First, it is uncertain whether camels are intermediate amplification hosts or the natural reservoirs of MERS-CoV. Although bats are postulated to be the natural host of most β CoVs, including MERS-CoV, the detection of anti-MERS-CoV antibodies in archived sera of camels dating back to more than 28 years ago in eastern Africa and more than 20 years ago in KSA, the high genetic stability of MERS-CoV in camels, and the high sequence nucleotide identities between camel and human strains of MERS-CoV suggest that the virus was well adapted and circulating in camels for a long time (123, 129). While some have suggested the concentration of camel herding activities in the urban areas of the Arabian Peninsula to be a contributing factor for increased camel and human interactions in recent years, the exact reason why human infection was not reported until 2012 remains elusive (337). Notably, a different novel lineage A β CoV, named dromedary camel CoV UAE-HKU23, has also been discovered in the fecal samples of dromedary camels in Dubai, UAE, recently (140). Further surveillance studies may provide novel insights into the role of this unique camelid species, which also has heavy-chain antibodies as a humoral defense, in the emergence of novel CoVs (141). Another unresolved question is whether an alternative source may be present but undetected at this stage. It is noteworthy that a significant proportion of laboratory-confirmed human cases did not have a clear history of contact with camels (83, 142). Evaluation of other animal species endemic in the region using validated serological and virological assays should be conducted. Finally, the route of transmission of MERS-CoV from camels to humans remains unknown at this stage. Droplet transmission appears likely, as evidenced by the high viral loads in the nasal and conjunctival swabs of camels and the surrounding air samples. However, viral shedding in nasal secretions is usually short-lasting during acute infection, which may limit viral transmission by this route (129). Direct contact with other infected bodily fluids, including blood and feces, is also possible, but viral shedding in these samples is also transient in acute infection (129). Foodborne transmission through ingestion of infected unpasteurized camel milk, in which MERS-CoV can survive for at least 48 h at 4°C or 22°C, has also been suggested. However, it has yet to be definitively proven that camels actively shed MERS-CoV in their milk, as contamination by feces, nasal secretions, or calf saliva containing the virus cannot be completely excluded (143). The presence of neutralizing antibody in milk may also limit the virus' infectivity *in vivo* (144). In human MERS cases without direct exposure to camels, contact with environments contaminated with infected

camel secretions and aerosol transmission are other possibilities that warrant further investigations (139, 145).

Molecular Epidemiology

Detailed analysis of the molecular evolution and spatiotemporal distribution of genomes of human and animal strains of MERS-CoV provides useful information for detecting viral adaptation to animal-to-human and person-to-person transmissions, identifying zoonotic and other sources of human infections, and assessing the pandemic potential of the virus. Comparative analysis of 65 complete or near-complete genomes of human MERS-CoV strains identified early in the epidemic from June 2012 to September 2013 estimated the evolutionary rate of the coding regions of the viral genome to be 1.12×10^{-3} (95% confidence interval, 8.76×10^{-4} to 1.37×10^{-3}) substitutions per site per year (146). The time to the most recent common ancestor (TMRCA) of MERS-CoV was estimated to be March 2012 (95% confidence interval, December 2011 to June 2012) (112, 146). Compared with the genome of one of the earliest human MERS-CoV strains, the genomes of the MERS-CoV strains obtained from patients diagnosed between October 2012 and June 2013 showed various nucleotide changes in the last third of the genomes, which represent potential amino acid changes in the accessory proteins and the S protein encoded at nucleotide positions 21000 to 25500 (112). Specifically, codon 1020 at the HR1 domain of the S gene was identified to be under strong episodic selection among different geographical lineages with either a histidine or arginine at this position (112, 146). Although the amino acid variations are not predicted to change the alpha helical structure of this region, the histidine and arginine provide an endosomal protonated residue and a potential endosomal protease cleavage site, respectively, that may affect the S protein membrane fusion activity (146). Codon 158 at the N-terminal domain and codon 509 at the RBD of the S gene are also noted to be under weaker positive selection (146). As mutations in the RBD of the S protein of CoVs may be associated with changes in the transmissibility across and within species, the phenotypic changes associated with these genomic variations should be ascertained (3, 29, 147–149).

In addition to the results of animal surveillance studies and investigations of human MERS outbreaks, genomic analysis also supports the hypothesis that MERS-CoV is transmitted from both animal to human and from person to person. Among genomes of sporadic human MERS cases, numerous distinct phylogenetic clades and genotypes exist, which likely represent separate instances of incursions from animals to humans (112). Indeed, at least four clades of MERS-CoV were identified in KSA, with three of them apparently no longer widely circulating during May to September 2013 (146). In a large health care-associated outbreak in Al-Hasa, person-to-person transmissions were supported by genomic analysis in at least 8 of 13 patients (75, 112). Two phylogenetically distinct MERS-CoV strains were detected in a family cluster in Riyadh, KSA, in October 2012, suggesting that at least two distinct lineages of MERS-CoV were circulating in Riyadh during this time period and that human clusters might involve multiple sources with more than one virus lineage (112). The genomic diversity of MERS-CoV detected in patients from the same locality and the geographical dispersion of MERS-CoV lineages in the Middle East suggest the presence of multiple mobile infection sources such as animal reservoirs, infected animal products, and/or infected patients in the regions of the epidemic (146).

TABLE 6 Tissue and host tropism of MERS-CoV demonstrated in cell culture systems^a

Cell culture system	Anatomic site or animal species	Main findings ^b	Reference
Cell lines			
Human cell types			
Lower respiratory tract			
A549	Lung adenocarcinoma	Replication with increased viral load (~1–2), N protein expression, and CPE	116
Calu-3	Polarized bronchial epithelium	Replication with increased viral load (~4–5), N protein expression, and CPE (cell rounding, detachment, and prominent syncytium formation)	116
		Replication in Calu-3 cells with increased viral load (~5–6) and CPE at 24 hpi; infection and release of virions through both the apical and basolateral routes	184
HFL	Embryonic lung fibroblasts	Replication with increased viral load (~4–5), N protein expression, and CPE	116
Differentiated HTBE	Human tracheobronchial epithelium	Replication with increased viral load (~2.5–4.5) in differentiated HTBE cells; virions released exclusively from the apical and not from the basolateral side	185
Nondifferentiated HTBE	Human tracheobronchial epithelium	Replication with increased viral load (<1) in nondifferentiated but much less than that observed in differentiated HTBE cells	185
HAE	Pseudostratified human airway epithelium	Productive infection in HAE cultures peaks at 48 hpi: host cell factors required for cell entry, RNA synthesis, and virus assembly and release are available in human	186
		Replication in HAE; lung fibroblasts, type II pneumocytes, and microvascular endothelial cells; most efficient in HAE and lung fibroblasts	187
HBEpC	Human primary bronchial epithelium	Replication with increased viral load (~0.5–1) (~1,000-fold-lower concentrations of virus progeny than in HBEpC) and without CPE	157
Kidney			
HEK 293	Human embryonic kidney	Replication with increased viral load (~4–5), N protein expression, and CPE	116
769-P	Renal cell adenocarcinoma	Replication with increased viral load (~3–4)	117
HREpC	Human primary kidney epithelium	Replication with increased viral load (~3–4) (~1,000-fold-higher concentrations of virus progeny than in HBEpC) and CPE (rounding and detachment of cells with cell death in the majority of cells after only 20 hpi)	157
Colon			
Caco-2	Colorectal adenocarcinoma	Replication with increased viral load (~4–5), N protein expression, and CPE (cell rounding, detachment, and prominent syncytium formation)	116
LoVo	Metastatic colonic adenocarcinoma	Replication in LoVo cells with increased viral load (~5–6) and CPE at 4 days p.i.	184
Liver			
Huh-7	Hepatocellular carcinoma	Replication with increased viral load (~4–5), N protein expression and CPE (cell aggregates with marked shrinkage)	116
Neuromuscular			
NT2	Neurocommitted teratocarcinoma	Replication with increased viral load (~2–3) but no N protein expression and CPE	116
Immune			
THP-1	Peripheral blood monocytes from AML	Replication with increased viral load (<1) but no N protein expression and CPE	116
U937	Monocytes from histiocytic lymphoma	Replication with increased viral load (<0.5) but no N protein expression and CPE	116
H9	T lymphocytes from T-cell leukemia	Replication with increased viral load (<0.5) but no N protein expression and CPE.	116
Jurkat_CD26DPP4+	Human T lymphocytes transfected with a human DPP4-encoding plasmid	Conversion from nonsusceptible state to susceptible state with productive viral infection after plasmid transfection	184
His-1	Malignant histiocytoma	Replication with increased viral load (~3–4), N protein expression, and CPE	116
Nonhuman cell types			
Primates			
LLC-MK2	Rhesus monkey kidney	Replication with increased viral load (~4–5), N protein expression, and CPE	116
Vero	African green monkey kidney	Replication with increased viral load (~4–5), N protein expression, and CPE	116
Vero-TMPRSS2	African green monkey kidney cells expressing TMPRSS2	Early appearance of large syncytia at 18 hpi and virus particle-induced cell-cell fusion at 3 hpi	52

Vero E6	African green monkey kidney	Replication with increased viral load (~4–5) and N protein expression; slower and less obvious CPE than in Vero cells	58, 116
COS-7 with DPP4	African green monkey fibroblasts transfected with a human DPP4-encoding plasmid	Conversion from non-susceptible state to susceptible state with productive viral infection after plasmid transfection	46
Bats			
RoNi/7	Old World bat (<i>Rousettus aegyptiacus</i>) kidney	Replication with increased viral load (~3–4)	117
PipNi/1	Old World bat (<i>Pipistrellus pipistrellus</i>) kidney	Replication with increased viral load (~1–2)	117
PipNi/3	Old World bat (<i>Pipistrellus pipistrellus</i>) kidney	Replication with increased viral load (~1–2)	117
RhiLu	Old World bat (<i>Rhinolophus landeri</i>) lung	Replication with increased viral load (~2–3)	117
MyDauNi/2	Old World bat (<i>Myotis daubentonii</i>) kidney	Replication with increased viral load (~1–2)	117
CarNi/1	New World bat (<i>Carollia perspicillata</i>) kidney	Replication with increased viral load (<0.5)	117
EFF	New World bat (<i>Eptesicus fuscus</i>) embryo	Susceptible to MERS-CoV pseudovirus infection	23
EidNi/41.3	Old World bat (<i>Eidolon helvum</i>) adult kidney	Replication with increased viral load (~10 ⁶ PFU/ml)	319
EpoNi/22.1	Old World bat (<i>Epomops buettikoferi</i>) adult kidney	Replication with increased viral load (~10 ⁴ PFU/ml)	319
HypLu/45.1	Old World bat (<i>Hypsingathus monstrosus</i>) fetal lung	Replication with increased viral load (~10 ⁵ PFU/ml)	319
HypNi/1.1	Old World bat (<i>Hypsingathus monstrosus</i>) fetal kidney	Replication with increased viral load (~10 ⁵ PFU/ml)	319
PESU-B5L	New World bat (<i>Pipistrellus subflavus</i>) adult lung	Did not support productive MERS-CoV infection unless transfected with a plasmid expressing human DPP4	319
RO5T	Old World bat (<i>Rousettus aegyptiacus</i>) embryo	Did not support productive MERS-CoV infection unless transfected with a plasmid expressing human DPP4	319
RO6E	Old World bat (<i>Rousettus aegyptiacus</i>) embryo	Did not support productive MERS-CoV infection unless transfected with a plasmid expressing human DPP4	319
RoNi/7.1	Old World bat (<i>Rousettus aegyptiacus</i>) adult kidney	Replication with increased viral load (~10 ⁶ PFU/ml)	319
RoNi/7.2	Old World bat (<i>Rousettus aegyptiacus</i>) adult kidney	Replication with increased viral load (~10 ⁶ PFU/ml)	319
Tb1Lu	New World bat (<i>Tadarida brasiliensis</i>) adult lung	Did not support productive MERS-CoV infection unless transfected with a plasmid expressing human DPP4	319
Camelids			
TT-R.B	Arabian camel (<i>Camelus dromedarius</i>) umbilical cord	Replication with increased viral load (~1) but without production of infectious virus particles	118
LGK-1-R	Alpaca (<i>Llama pacos</i>) kidney	Replication with increased viral load (~2–3) and production of infectious virus particles	118
Other mammals			
ZLu-R	Goat (<i>Capra hircus</i>) lung	Replication with increased viral load (~1–2) and production of infectious virus particles	118
ZN-R	Goat (<i>Capra hircus</i>) kidney	Replication with increased viral load (~3–4) and production of infectious virus particles	118
PK-15	Pig kidney	Replication with increased viral load (~4–5), N protein expression, and CPE	116
PS	Pig kidney	Replication with increased viral load (<1)	117
RK-13	Rabbit kidney	Replication with increased viral load (~1–2) but no N protein expression and CPE	116
CL-1	Civet lung fibroblasts	Replication with increased viral load (~1–2), N protein expression, and CPE	116
PN-R	Horse kidney	Replication with production of infectious virus progeny, increased viral load (~7–8), and CPE	336
PFN-R	Horse kidney	Replication with production of infectious virus progeny, increased viral load (~7–8), and CPE	336
MDCK with human DPP4	Dog kidney transfected with a human DPP4-encoding plasmid	Conversion from non-susceptible state to susceptible state with productive viral infection after plasmid transfection	46
LR7 with human DPP4	Mouse fibroblasts transfected with a human DPP4-encoding plasmid	Conversion from non-susceptible state to susceptible state with productive viral infection after plasmid transfection	46
CRFK with human DPP4	Cat kidney cortex epithelium transfected with a human DPP4-encoding plasmid	Conversion from non-susceptible state to susceptible state with productive viral infection after plasmid transfection	46

(Continued on following page)

TABLE 6 (Continued)

Cell culture system	Anatomic site or animal species	Main findings ^b	Reference
BHK with human DPP4	Baby hamster kidney cells expressing human DPP4	Conversion from nonsusceptible state to susceptible state after transfection with a human but not hamster or ferret DPP4-encoding expression vector	48
Primary ferret kidney with human DPP4	Primary ferret kidney cells expressing human DPP4	Conversion from nonsusceptible state to susceptible state with after transfection with a human but not hamster or ferret DPP4-encoding expression vector	48
<i>Ex vivo</i> organ or cell cultures			
Respiratory tract			
Lower respiratory tract	Human lung	Infection and replication in most cell types of the human alveolar compartment (ciliated and nonciliated cells in simple columnar and simple bronchial epithelia, type I and II pneumocytes, endothelial cells of large and small pulmonary vessels, but not alveolar macrophages)	188
	Human bronchus and lung	Productive replication in both human bronchial and lung <i>ex vivo</i> organ cultures (nonciliated bronchial epithelium, bronchiolar epithelial cells, alveolar epithelial cells, and endothelial cells); virions were found within the cytoplasm of bronchial epithelial cells, and budding virions were found in alveolar epithelial cells (type II)	189
	Human lung	Infection of airway epithelial cells (pneumocytes and epithelial cells of terminal bronchioles, endothelial cells, and lung macrophages)	190
	Human bronchus and lung	The respiratory tropisms of human and dromedary MERS-CoV strains in <i>ex vivo</i> human bronchus and lung culture were similar	338
Immune cells			
Peripheral blood mononuclear cells	Human MDMs	Productive infection and replication in MDMs with increased viral load (~3–4) and aberrant induction of inflammatory cytokines and chemokines (higher expression levels of IL-12, IFN- γ , IP-10, MCP-1, MIP-1 α , IL-8, CCL-5, MHC class I, and costimulatory molecules than SARS-CoV-infected MDMs)	190
	Human MoDCs	Productive infection of MoDCs with increased viral load (~2–3) and significantly higher expression levels of inflammatory cytokines and chemokines (IL-12, IFN- γ , IP-10, CCL-5, MHC class II, and the costimulatory molecule CD86) than SARS-CoV-infected MoDCs	192

^a Abbreviations: AML, acute monocytic leukemia; CCL, chemokine C-C motif ligand; CPE, cytopathic effects; p.i., postinfection; hpi, hours postinfection; IFN, interferon; IP, interferon- γ -induced protein; MCP, monocyte chemoattractant protein; MDM, monocyte-derived macrophage; MHC, major histocompatibility complex; MIP, macrophage inflammatory protein; MoDC, monocyte-derived dendritic cell; N, nucleocapsid; TMPRSS2, transmembrane protease serine protease 2.

^b Values of viral loads are presented as log₁₀ virus genome copies equivalents per ml of cell culture supernatant unless otherwise specified.

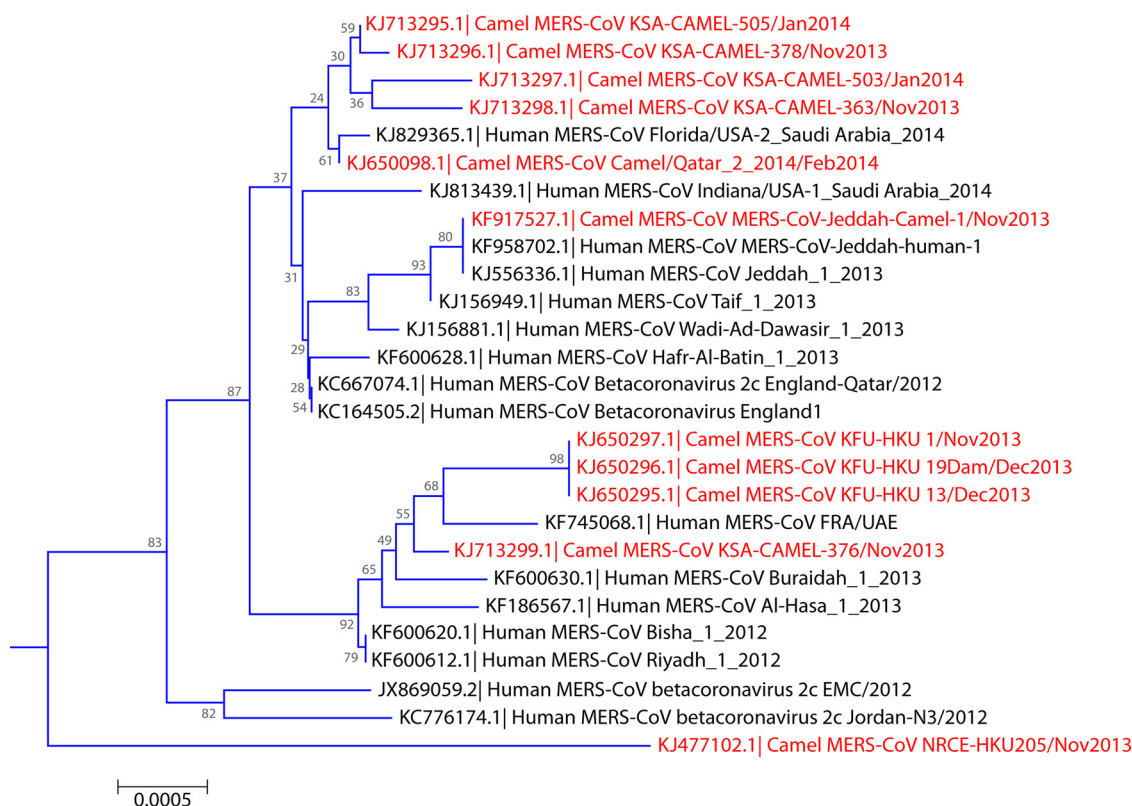


FIG 4 Phylogenetic tree of the complete genomes of 27 representative human (black) and camel (red) MERS-CoV strains rooted by NeoCoV (KC869678.4). The tree was constructed by the neighbor-joining method using MEGA 5.0. The scale bar indicates the estimated number of substitutions per 2,000 nucleotides.

This hypothesis fits well with the evidence of MERS-CoV infection in dromedary camels, which are an important vehicle for transportation of goods and travelers, as well as a food source, in the Middle East. Notably, quasispecies of MERS-CoV within single samples have been detected in samples from dromedary camels but not humans or Vero cell isolates from the same animal (137). Further studies using next-generation high-throughput sequencing are required to confirm the presence of quasispecies and clonal virus populations within individual human cases, which may help identify specific genotypes that can pass the bottleneck selection to cause cross-species transmission from camels to humans and help explain the relative rarity of human cases despite the widespread circulation of MERS-CoV in dromedary camels for prolonged periods in the Middle East and North Africa (137).

Mathematical Modeling

Mathematical modeling has been widely used to predict the spread and pandemic potential of emerging viruses. Although the interval for data accumulation may diminish the predictive value of mathematical modeling and its impact on epidemiological control or policy setting, these studies provide a preliminary estimate of the pandemic potential of emerging viruses if enough data are included in the calculations. Three real-time predictions of the spread of MERS-CoV have been conducted for the current epidemic and have estimated the basic reproduction number (R_0), the number of secondary cases per index case in a fully susceptible population, to be 0.30 to 0.77 (150), 0.60 to 0.69 (90), or 0.8 to 1.3 (151), compared to about 0.8 for preepidemic SARS-CoV. These

estimates imply the occurrence of a subcritical epidemic in the Middle East, which is unlikely to sustain person-to-person transmission of MERS-CoV, especially when infection control measures are implemented (150). The estimated daily rate of MERS-CoV introductions into the human population in the Middle East is 0.12 to 0.85, and the expected yearly incidence of MERS introduction was estimated to be between 160 and 320 cases per year (90, 150). Clearly, these estimations are, at most, only modestly accurate for a number of reasons. First, these studies were conducted early in the epidemic when the total number of laboratory-confirmed cases was only less than one-tenth of that reported by the WHO as of 26 February 2015 (90, 150, 151). This low number limited the accuracy of the predictions, as a sufficient caseload is required to calculate the basic parameters for estimation of the worst- and best-case scenarios to gauge the magnitude of the epidemic. The omission of large clusters may underestimate the R_0 (90). Second, most of the cases reported in the early period of the epidemic were biased toward including more severe cases. The increasingly recognized number of asymptomatic or mildly symptomatic cases identified through enhanced surveillance programs may further underestimate the R_0 (90). Finally, the R_0 may also be affected by community demographics, contact structure, large gatherings such as the Hajj, and exportation of patients from the relatively less populated Middle East to densely populated areas such as Southeast Asia (78, 90). Indeed, a more recent study that included more than 700 cases of MERS showed that the R_0 was much higher at 2.0 to 6.7 in large health care-associated outbreaks

TABLE 7 Clinical, laboratory, and radiological features of MERS^a

Value for clinical cohort described in reference(s):						
Parameter	66	63	75	80	88	311
Time period	April 2012	1 September to June 2013	1 March 2013 to 15 June 2013	1 April 2013 to 3 June 2013	May 2013 to August 2013	1 October 2012 to 31 May 2014
Setting or data source	Retrospective outbreak investigation in Jordan	All cases reported by the KSA Ministry of Health to WHO	Outbreak investigation in 4 hospitals in Al-Hasa, KSA	A 350-bed general hospital in KSA	3 intensive care units in KSA	70 cases at a single center in Riyadh, KSA
Clinical features ^b						Case reports or case series
Systemic						
Fever > 38°C	8/9 (88.9)	46/47 (97.9)	20/23 (87.0)	6/15 (40.0)	8/12 (66.7)	6/7 (85.7)
Chills and/or rigors	1/9 (11.1)	41/47 (87.2)	NA	1/15 (6.7)	NA	NA
Respiratory						
Rhinorrhea	1/9 (11.1)	2/47 (4.3)	NA	NA	1/12 (8.3)	NA
Sore throat	NA	10/47 (21.3)	20/23 (87.0)	1/15 (6.7)	1/12 (8.3)	NA
Cough	8/9 (88.9)	39/47 (83.0)	NA	NA	10/12 (83.3)	38/70 (54.3)
Sputum	NA	17/47 (36.2)	NA	NA	2/12 (16.7)	23/70 (23.9)
Hemoptysis	NA	8/47 (17.0)	NA	1/15 (6.7)	1/12 (8.3)	NA
Wheezing	NA	NA	NA	2/15 (13.3)	2/12 (16.7)	NA
Chest pain	4/9 (44.4)	7/47 (14.9)	NA	1/15 (6.7)	NA	NA
Dyspnea	5/9 (55.6)	34/47 (72.3)	11/23 (47.8)	10/15 (66.7)	11/12 (91.7)	4/7 (57.1)
Renal						
Acute renal failure	NA	NA	NA	NA	7/12 (58.3)	7/7 (100) in one cohort; and 9/12 (75.0) in another with at least 6/9 (75.0) fatal; median time = 11 ± 2 days from symptom onset
Gastrointestinal						
Nausea	NA	10/47 (21.3)	NA	NA	1/12 (8.3)	NA
Vomiting	NA	10/47 (21.3)	4/23 (17.4)	1/15 (6.7)	NA	NA
Diarrhea	NA	12/47 (25.5)	5/23 (21.7)	1/15 (6.7)	2/12 (16.7)	NA
Abdominal pain	NA	8/47 (17.0)	NA	NA	Acute abdomen (3/12, 25.0%); ischemic bowel requiring hemicolectomy (1) and negative laparotomies (2)	1/7 (14.3)
Other symptoms						
Myalgia	NA	15/47 (31.9)	NA	1/15 (6.7)	NA	1/7 (14.3)
Headache	NA	6/47 (12.8)	NA	1/15 (6.7)	2/12 (16.7)	9/70 (12.9)
Malaise	3/9 (33.3)	NA	NA	NA	2/12 (16.7)	29/70 (41.4)
Complications						
Coinfections						
Bacterial and fungal	NA	0/47 (0)	NA	NA	<i>Staphylococcus aureus</i> (1/12, 8.3%) and <i>Streptococcus pneumoniae</i> (1/12, 8.3%)	<i>Klebsiella pneumoniae</i> , <i>S. aureus</i> , <i>S. epidermidis</i> , <i>Acinetobacter</i> sp., <i>Pseudomonas aeruginosa</i> , <i>Aspergillus fumigatus</i> , and candidemia (<i>Candida albicans</i> and <i>C. glabrata</i>)
Viral	NA	0/47 (0)	NA	NA	Influenza B virus (1/12, 8.3%)	Influenza A/H1N1/2009 virus (1) and type 2 parainfluenza virus (2)

ICU admission ^c	4/8 (50.0)	42/47 (89.4)	18/23 (78.3); time from symptom onset = 5 days (1 to 10 days)	8/15 (53.3)	12/12 (100); time from symptom onset to ICU admission = 2 days; duration = 30 days (7 to 104 days)	49/70 (70.0)	60/133 (45.1)
Mechanical ventilation ^c	2/8 (25.0)	34/47 (72.3); time from presentation = 7 days (3 to 11 days)	18/23 (78.3); time from symptom onset = 7 days (3 to 11 days)	NA	12/12 (100); time from symptom onset to mechanical ventilation = 4.5 days; duration = 16 days (4 to 30 days)	49/70 (70.0)	NA
Other	Pericarditis, pleural and pericardial effusions, arrhythmias (SVT and VT), and delirium	NA	NA	NA	Vasopressors: (8/12, 66.7%)	Delirium (18/70, 25.7%); seizure (6/70, 8.6%), arrhythmias (11/70, 15.7%), pneumothorax (5/70, 7.1%), rhabdomyolysis (10/70, 14.3%)	Second-trimester stillbirth at 5 mo of gestation
Death ^c	2/8 (25.0); time from symptom onset = 16.5 days	28/47 (59.6); time from presentation = 14 days (5 to 36 days); CFR increased with increased age	At least 15/23 (65.2); time from symptom onset = 11 days (5 to 27 days)	13/17 (76.5)	7/12 (58.3) at day 90 after symptom onset	42/70 (60.0)	291/837 (34.8) (April 2012 to 23 July 2014) (86)
Laboratory features							
Hematological abnormalities							
Leukocytosis	NA	NA	3/23 (13.0)	2/17 (11.8)	NA	Yes	NA
Leukopenia	2/7 (28.6)	7/47 (14.9)	2/23 (8.7)	1/17 (5.9)	NA	NA	3/7 (42.9)
Normal neutrophil count	NA	43/47 (91.5)	NA	NA	NA	Yes	NA
Lymphocytosis	NA	5/47 (10.6)	NA	NA	NA	NA	NA
Lymphopenia	6/7 (85.7)	16/47 (34.0)	NA	6/17 (35.3)	9/12 (75.0) on ICU admission and 11/12 (91.7) during ICU stay	Yes (median lymphocyte count, $0.85 \times 10^9/\text{liter}$)	7/7 (100)
Thrombocytosis	NA	NA	1/23 (4.3)	NA	NA	NA	NA
Thrombocytopenia	NA	17/47 (36.2)	4/23 (17.4)	NA	2/12 (16.7) on ICU admission and 7/12 (58.3) during ICU stay	NA	3/7 (42.9)
Other	DIC	NA	NA	NA	NA	DIC (10, 14.3%), anemia (median, 10.7 g/dl), neutropenia	Anemia, increased PT, increased APTT, increased INR, and DIC
Biochemical abnormalities							
Elevated serum ALT	NA	5 (10.6)	NA	3/17 (17.6)	2/12 (16.7) on ICU admission and 5/12 (41.7) during ICU stay	22/70 (31.4)	NA
Elevated serum AST	NA	7/47 (14.9)	3/13 (23.1)	9/17 (52.9)	2/12 (16.7) on ICU admission and 8/12 (66.7) during ICU stay	22/70 (31.4); median, 59 IU/liter	NA
Elevated serum LDH	NA	23/47 (48.9)	NA	8/17 (47.1)	NA	NA	NA
Other	NA	NA	NA	NA	NA	Hypalbuminemia	Hyponatremia, hyperkalemia, hypoalbuminemia, and increased serum urea, creatine kinase, troponin, C-reactive protein, and procalcitonin levels

(Continued on following page)

TABLE 7 (Continued)

Value for clinical cohort described in reference(s):		66	63	75	80	88	311	9, 18, 64, 67, 69, 71–73, 86, 152, 157, 320
Parameter	Radiological findings	7/7 (100) had CXR lesions in ≤3 days of presentation (unilateral/bilateral increased bronchovascular markings, consolidation, elevated diaphragm, and cardiomegaly with pericardial effusion)	47/47 (100) had CXR lesions (mild to extensive unilateral/bilateral increased bronchovascular markings, air space opacities, patchy infiltrates, interstitial changes, patchy to confluent air space consolidation, nodular opacities, reticular opacities, reticulonodular shadows, pleural effusion, and total opacification of lung segments and lobes)	20/23 (87.0) had CXR lesions at presentation (increased bronchovascular markings, unilateral/bilateral infiltrates, and diffuse reticulonodular shadows)	Single (6/15; 40.0%) and multiple (9/15; 60.0%) CXR infiltrates; interstitial infiltrates (10/15; 66.7%) and cardiomegaly (8/15; 53.3%)	12/12 (100) had CXR lesions (unilateral to bilateral diffuse air space infiltrates)	Bilateral (53/66; 80.3%) and unilateral (10/66; 15.2%) CXR lesions	Bilateral (6/7; 85.7%) and unilateral (1/7; 14.3%) CT lesions; ground-glass opacities and consolidations (5/7; 71.4%); isolated ground-glass opacities (1/7; 14.3%); isolated consolidation (1/7; 14.3%); smooth septal thickening (3/7; 42.9%); lower lung-predominant (5/7; 71.4%); none had tree-in-bud pattern, cavitation, or intrathoracic lymphadenopathy

^a Abbreviations: ALT, alanine aminotransferase; APTT, activated partial thromboplastin time; AST, aspartate aminotransferase; CRAB, carbapenem-resistant *Acinetobacter baumannii*, CT, computerized tomography scan; CXR, chest radiograph; DIC, disseminated intravascular coagulation; ICU, intensive care unit; INR, international normalized ratio; KSA, the Kingdom of Saudi Arabia; LDH, lactate dehydrogenase; mo, month; MRSA, methicillin-resistant *Staphylococcus aureus*; NA, not available; SVT, supraventricular tachycardia; UK, United Kingdom; VRE, vancomycin-resistant enterococci, VT, ventricular tachycardia; WHO, World Health Organization.

^b Unless indicated otherwise, data are reported as number with feature/total (percentage with feature).

^c Values represent median time intervals.

in KSA in spring 2014 (339). Updated mathematical modeling using the latest available epidemiological and virological data may increase the accuracy of these estimates.

CLINICAL MANIFESTATIONS

The early reports of MERS have focused on severe cases, which typically presented as acute pneumonia with rapid respiratory deterioration and extrapulmonary manifestations (Table 7). Few clinical and radiological features can reliably differentiate MERS from acute pneumonia caused by other microbial agents (80). The common presenting symptoms of MERS are nonspecific, and include feverishness, chills, rigors, sore throat, nonproductive cough, and dyspnea. Other symptoms of respiratory tract infections, including rhinorrhea, sputum production, wheezing, chest pain, myalgia, headache, and malaise, may also be present. Rapid clinical deterioration with development of respiratory failure usually occurs within a few days after these initial symptoms (80). Physical signs at the time of deterioration may include high fever, tachypnea, tachycardia, and hypotension. Diffuse crepitations may be present on chest auscultation, but they may be disproportionately mild compared with radiological findings (68).

Chest radiograph abnormalities are found in nearly all severe cases and often progress from a mild unilateral focal lesion to extensive multifocal or bilateral involvement, especially of the lower lobes as the patient deteriorates (63). The radiological changes are nonspecific and indistinguishable from other viral pneumonias associated with acute respiratory distress syndrome (ARDS), and they include air space opacities, segmental, lobar, or patchy consolidations, interstitial ground-glass infiltrates, reticulonodular shadows, bronchial wall thickening, increased bronchovascular markings, and/or pleural and pericardial effusions (Table 7). Rarely, pneumonia may be an incidental finding in the chest radiograph and may precede the sudden deterioration in respiratory function in patients who are harboring a “walking pneumonia” with minimal respiratory tract symptoms (63, 68). The most common thoracic computerized tomography (CT) scan features are bilateral, predominantly basilar, and subpleural air-space involvement, with extensive ground-glass opacities and occasional septal thickening and pleural effusions (152). Tree-in-bud pattern, cavitation, and lymph node enlargement have not been reported. Fibrotic changes, including reticulation, traction bronchiectasis, subpleural bands, and architectural distortion, may be found in thoracic CT scans performed 3 weeks after symptom onset. These different changes in thoracic CT scan throughout the course of disease are suggestive of organizing pneumonia and may mimic those seen in other viral pneumonias such as influenza (4, 8, 153–156).

Various extrapulmonary manifestations involving multiple body systems have been reported in MERS (Table 7). Acute renal impairment was the most striking feature in the early reports (9, 18). This finding was confirmed in subsequent sporadic reports and at least three case series that provided specific details on renal function, in which more than half of the patients developed acute renal impairment at a median time of around 11 days after symptom onset, with most requiring renal replacement therapy (88, 152, 157). This is unique among CoV infections of human. For SARS, only around 6.7% of patients developed acute renal impairment, mainly due to hypoxic injury, at a median duration of 20 days after symptom onset, and 5% required renal replacement therapy (158, 159). The exceptionally high incidence of this dis-

tinctive manifestation of MERS is likely multifactorial. These factors include the high prevalence of background chronic renal impairment among severe cases and the renal tropism of MERS-CoV (63, 116, 157). The presence of MERS-CoV RNA in urine also supports the possibility of direct renal involvement, but the exact incidence and prognostic significance of this finding are unknown at present (72).

As in humans infected with SARS-CoV and animals infected with other CoVs, patients infected with MERS-CoV may have enteric symptoms in addition to respiratory tract involvement (3, 160, 161). Gastrointestinal symptoms were found in more than a quarter of hospitalized cases in a large cohort in KSA (63). Diarrhea is the most common symptom and occurs in 6.7% to 25.5% of severe cases. Nausea, vomiting, and abdominal pain may also occur. The detection of viral RNA in fecal samples has been reported, but longitudinal studies on the pattern of viral shedding are lacking (72). It remains to be determined whether cases of acute abdomen presenting as ischemic bowel or negative findings on laparotomy result from hypoxic damage or direct viral invasion of the gastrointestinal tract (88).

Other extrapulmonary features of MERS include hepatic dysfunction, pericarditis, arrhythmias, and hypotension (66). Hematological abnormalities include leukopenia or leukocytosis, usually accompanied by lymphopenia with normal neutrophil count, and thrombocytopenia. Compared to other patients with pneumonia, patients with MERS are more likely to have a normal leukocyte count on admission (80). Anemia, coagulopathy, and disseminated intravascular coagulation have also been reported (64, 66, 72). Elevated levels of serum transaminases, lactate dehydrogenase, potassium, creatine kinase, troponin, C-reactive protein, and procalcitonin and reduced levels of serum sodium and albumin are seen occasionally.

Complications of MERS include bacterial, viral, and/or fungal coinfections, ventilator-associated pneumonia, septic shock, delirium, and possibly stillbirth (9, 69, 71, 73) (Table 7). Respiratory failure with ARDS and multiorgan dysfunction syndrome are not uncommon, and the majority of such patients require admission to the intensive care unit at a median of 2 to 5 days from symptom onset. The median time from symptom onset to invasive ventilation and/or extracorporeal membrane oxygenation (ECMO) in these patients is 4.5 to 7 days, which is at least 6 days earlier than that for SARS (63, 66, 75, 88, 162). The duration of stay in the intensive care unit is often prolonged, with a median of 30 days (range, 7 to 104 days). The case-fatality rate is up to 25.0% to 76.5% in various cohorts (Table 7).

With enhanced surveillance of health care-associated and family contacts of MERS patients, an increasing number of asymptomatic and mild cases have been identified. Most of these patients are young, healthy female health care workers or children who do not have any comorbidities (65, 163). Among 402 patients identified in the recent clusters that occurred in KSA between 11 April 2014 and 9 June 2014, 109 (27.1%) were health care workers. Of note, though many were either asymptomatic or mildly symptomatic, more than one-third developed moderate to severe disease requiring hospitalization, and nearly 4% died (http://www.who.int/csr/disease/coronavirus_infections/MERS-CoV_summary_update_20140611.pdf). Severe and even fatal cases have also been reported among infected children, especially in those who have underlying diseases such as cystic fibrosis and Down's syndrome with con-

genital heart disease and hypothyroidism (163). Therefore, even young health care workers and children with MERS should be monitored closely for clinical deterioration.

HISTOPATHOLOGY AND PATHOGENESIS

The pathogenesis of MERS is understudied and poorly understood. Serial sampling for characterization of the innate and adaptive immune responses is lacking in human cases of MERS. Due to religious and cultural reasons, postmortem examination was seldom performed in Islamic patients who died of MERS, and no postmortem findings have been reported so far. Thus, the current understanding on the histopathology and pathogenesis of MERS is limited to findings in *in vitro*, *ex vivo*, and from animal experiments.

Histological Changes

In rhesus macaques infected with MERS-CoV, macroscopic changes of acute pneumonia, including multifocal to coalescent bright red palpable nodules with congestion, occurred throughout the lower respiratory tract in necropsy lung tissues collected on day 3 postinfection (164–166). On day 6 postinfection, these inflamed areas progressed into dark reddish purple lesions. Microscopically, the changes resembled those seen in mild to severe acute interstitial pneumonia, characterized by alveolar infiltration by small to moderate numbers of macrophages and fewer neutrophils with occasional multinucleate syncytia, and thickening of alveolar septa by edema fluid and fibrin on day 3 postinfection. Lesions similar to those described in early bronchiolitis obliterans, with organizing pneumonia consisting of aggregates of fibrin, macrophages, and sloughed pulmonary epithelium that occluded small airways, and multifocal perivascular infiltrates of inflammatory cells within and adjacent to the affected areas of lungs were also reported. On day 6 postinfection, moderate to marked microscopic changes, including type II pneumocyte hyperplasia, alveolar edema, and hyaline membranes of fibrin, were observed (165). *In situ* hybridization and immunohistochemistry demonstrated viral RNA and antigen, respectively, in type I and II pneumocytes, alveolar macrophages, and occasionally round mononuclear cells and stellate cells within the cortex of the mediastinal lymph nodes, but not in pulmonary endothelial cells, on both days 3 and 6 postinfection (165, 166). Infected cells were not observed in the kidneys, brains, hearts, livers, spleens, and large intestines of the infected rhesus macaques (166). Common marmosets infected with MERS-CoV showed similar but more severe histological findings. In necropsied lungs of common marmosets euthanized on day 3 to 4 postinfection, extensive transcriptional evidence of pulmonary fibrosis was present (167). In rhesus macaques immunosuppressed using cyclophosphamide and dexamethasone with depleted T and B cells and disrupted splenic and mesenteric lymph node architectures, MERS-CoV replicated more efficiently and affected more tissues than in nonimmunosuppressed controls. Interestingly, the immunosuppressed animals had fewer histological changes associated with infection despite having higher virus replication in the lungs, suggesting that immunopathology might also play a key role in MERS (168).

Innate Immune Response

Immune evasion is an important strategy utilized by CoVs to overcome the innate immune response for efficient replication in the host. MERS-CoV is capable of inhibiting recognition, delaying

interferon induction, and dampening interferon-stimulated gene (ISG) expression in polarized human bronchial epithelia (Calu-3) cells until peak viral titers have been reached (169). While MERS-CoV triggers an activation of pattern recognition receptors that is similar to that with SARS-CoV, their subsequent levels of interferon induction in Calu-3 cells are markedly different (170). This may be related to the different structural and accessory proteins of the two viruses that act as interferon antagonists. Instead of the papain-like protease, accessory proteins 3b and 6, nsp1, M, and N proteins, which are the major putative interferon antagonists of SARS-CoV, the papain-like protease encoded by nsp3 of ORF1a/b, M protein encoded by ORF7, and accessory proteins 4a, 4b, and 5 encoded by ORF4a, -4b, and -5, respectively, of MERS-CoV antagonize interferons *in vitro* (3, 24, 25, 27, 28, 171). Among them, the MERS-CoV accessory protein 4a, a double-stranded RNA (dsRNA)-binding protein, exhibits potent antagonistic activity at multiple levels of the interferon response, including the prevention of interferon beta synthesis through the inhibition of interferon promoter activation and interferon regulatory factor 3 (IRF3) function, and inhibition of the interferon-stimulated response element (ISRE) promoter signaling pathway in human (HEK-293T) and/or primate kidney (Vero) cells (24). Specifically, it inhibits PACT-induced activation of retinoic acid-inducible gene 1 (RIG-I) and melanoma differentiation-associated protein 5 (MDA5), which are key cytosolic recognition receptors of virus-derived RNAs (25). Furthermore, preliminary data show that MERS-CoV, but not SARS-CoV, may employ an additional mechanism to antagonize ISG via altered histone modification, which affects a diverse spectrum of biological processes, including gene regulation (169). With the attenuated interferon response at the cellular level, the virus may then employ the deISGylating and deubiquitinating activities of its papain-like protease to take over the host metabolic apparatus (28, 171, 172). Efficient viral replication may follow and result in cell damage through direct virus-induced cytolysis or immunopathology via dysregulated proinflammatory cytokine induction.

In addition to these *in vitro* data, the roles of the different branches of the innate immune response have been assessed in a limited number of animal models and patients. MERS-CoV infection is more severe in knockout C57BL/6 and BALB/c mice with impaired type I interferon or Toll-like receptor signaling than in those with impaired RIG-I-like receptor signaling, suggesting that the former signaling pathways are more important for controlling the infection (173). The depletion of natural killer cells, a major cellular component of the innate immune response, does not significantly affect the clinical disease severity or viral clearance kinetics (173). In rhesus macaques, the innate immune response occurs and resolves very rapidly after MERS-CoV inoculation. A type I interferon response is observed on days 1 and 2 and disappears on day 3 postinfection (165, 174). Robust but transient up-regulation of the expression levels and elevated serum levels of proinflammatory cytokines and chemokines, including interleukin-6 (IL-6), chemokine (C-X-C motif) ligand 1 (CXCL1), and matrix metalloproteinase 9 (MMP9), are associated with chemotaxis and activation of neutrophils, as evidenced by increased numbers of neutrophils in the blood and lungs of the infected animals (165). In humans who develop severe MERS, significant differences are noted between the innate immune responses in fatal and nonfatal cases. Compared to a patient who survived, a patient who died from MERS induced lower expression levels of

RIG-I and MDA-5, which led to decreased expression levels of IRF3 and IRF7 (175). This was associated with a major decrease in the amount of mRNA and protein of interferon alpha in serum and bronchoalveolar lavage fluid. Additionally, the antigen presentation pathway was broadly downregulated and affected type I and II major histocompatibility (MHC) genes, which were associated with significantly lower expression levels of the key cytokines involved in the activation of lymphocytes into CD4⁺ Th1 cells, including IL-12 and interferon gamma (175, 176). Increased levels of IL-17A and IL-23 in the serum and bronchoalveolar lavage fluid within the first week after symptom onset and persistent uncontrolled secretion of the type I interferon-triggered CXCL10 and IL-10 beyond the first week after symptom onset were noted in fatal MERS cases and might be associated with poor outcome as in SARS and other respiratory viral infections (175, 177–180). A poorly coordinated innate immune response with ineffective activation of the adaptive immune response that failed to clear MERS-CoV viremia appeared to be associated with fatal outcome (175, 181).

Adaptive Immune Response

Systematic study on the adaptive immune response to MERS in large cohorts of human cases is lacking. T-cell deficiency or combined T- and B-cell deficiencies, but not B-cell deficiency alone, were found to be associated with persistent infections and lack of virus clearance in C57BL/6 and BALB/c mice transduced with adenoviral vectors expressing human DPP4, highlighting the important role of T cells in acute clearance of MERS-CoV (173). In terms of antibody-mediated immunity which is essential for protection against subsequent challenge by the virus, the CD8 T-cell response to the immunodominant epitopes located in the MERS-CoV S protein was shown to peak at days 7 to 10 postinfection and exhibits only a low level of cross-reactivity with the T-cell response to SARS-CoV infection (173). In rhesus macaques infected with MERS-CoV, serum neutralizing antibodies are detected on as early as day 7 postinfection, reaching a peak titer on day 14 postinfection and decreasing slightly in titer on day 28 postinfection (166). In patients with MERS, high titers of serum neutralizing antibodies can be detected on day 12 and persist for at least 13 months after symptom onset (66, 72, 81, 182). Both IgM and IgG against S and N proteins are detectable in the sera of infected patients on day 16 after symptom onset, with the titer of IgG being at least 10 times higher than that of IgM, suggesting that the initial IgM antibody response is likely mounted before this time period (72). IgG titers peaked at 3 weeks after symptom onset, while IgM titers remained elevated between 2 to 5 weeks after symptom onset in a patient (183). Notably, anti-MERS-CoV antibodies were undetectable in the sera collected on days 26 and 32 after symptom onset from a patient who died, suggesting that an inadequate antibody response may be associated with poor clinical outcome (66). The exact onset and changes in titer of serum neutralizing anti-MERS-CoV antibodies should be further evaluated in subsequent clinical cohorts consisting of patients with different severities and outcomes. Moreover, given the *in vitro* observation that the viral fitness and evolution may be restricted by the immunodominance of the anti-MERS-CoV-RBD neutralizing antibody response that blocks binding to human DPP4, B-cell-associated antibodyome studies from MERS patients should be performed to further assess the role that immunoglobulin polymorphisms play

in determining the protective antibody repertoire and clinical outcomes (40).

Organ-Specific Pathology and Systemic Virus Dissemination

Although *in vitro* cell line studies and even *ex vivo* organ cultures may not completely represent *in vivo* scenarios, they have provided insightful clues to explain the pathogenesis involved in the pulmonary and extrapulmonary manifestations of MERS before findings from animal models and postmortem examination are available (Table 6). The *in vitro* observation that MERS-CoV replicates more efficiently in a variety of lower respiratory tract cell lines than in upper respiratory tract cell lines and the inability of the human bronchial epithelium to mount a timely and adequate innate immune response against MERS-CoV infection in the absence of professional cytokine-producing cells, including dendritic cells and macrophages, may partially explain the high incidence of severe cases in MERS (116, 157, 170, 184–187). The finding in *ex vivo* culture systems that MERS-CoV is capable of infecting most cell types of the human alveolar compartment, including nonciliated and possibly ciliated epithelial cells, type I and II pneumocytes, and endothelial cells of pulmonary vessels, further supports the notion that all the host cell factors necessary for viral replication are available in the human lung (186, 188–190). Additionally, MERS-CoV can also infect pulmonary vascular endothelial cells and lung macrophages, which corroborates the clinical observation of systemic dissemination of the virus with viremia in severe cases (190).

Besides lower respiratory tract cells, MERS-CoV also exhibits a peculiar tropism for renal cells that is not seen with any other CoVs associated with human infections and is not explainable by the expression of their respective host cell receptors. Avian nephropathogenic infectious bronchitis virus may cause lymphoplasmacytic interstitial nephritis, but rarely pneumonia, in broiler chickens (191). MERS-CoV replicates efficiently to about 5 logs above the baseline titer, with abundant N protein expression and prominent cytopathic effects (CPE) within 72 h after infection of human embryonic kidney cells (116). In primary kidney epithelial cells and primary bronchial epithelial cells infected with either MERS-CoV or SARS-CoV, pronounced CPE with rounding, detachment, and death of the majority of cells occurs only in primary kidney epithelial cells infected with MERS-CoV, although viral replication was detectable with both viruses (157). The concentration of infectious MERS-CoV progeny in primary kidney epithelial cells was almost 1,000-fold higher than that in primary bronchial epithelial cells (157). Together with the clinical observation that MERS-CoV RNA may be detectable in the urine without viremia almost 2 weeks after symptom onset, these *in vitro* findings suggest that the kidney may be a potential site of autonomous virus replication (72, 157). Comparable findings are also observed in many bat and primate kidney cell lines, although clinical disease in these animals is much milder than in humans and viral RNA is not detectable in the kidneys of infected rhesus macaques (116, 117). *Ex vivo* kidney culture may help to elucidate the specific pathways involved in virus-host cell interactions affecting different cell types, such as podocytes in the renal cortex and others in the medulla, which are often involved in renal disease pathogenesis.

In view of the pronounced systemic inflammatory response with multiorgan involvement and hematological abnormalities seen in patients with MERS, the specific roles of immune cells in the pathogenesis of the disease have been investigated. Among the immune cells, human histiocytes efficiently support viral replica-

tion, with N protein expression *in vitro* as early as day 1 postinfection, while increased viral RNA levels without N protein expression are detectable in human monocyte and T lymphocyte cell lines (116). Correspondingly, *ex vivo* culture systems of human monocyte-derived dendritic cells and macrophages confirm that MERS-CoV can productively infect both of these important professional antigen-presenting cell types with high-level and persistent induction of immune cell-recruiting cytokines (190, 192). This leads to recruitment and infiltration of a large number of immune cells into the infected lung tissues, as is seen clinically. Moreover, the sequestration of lymphocytes at infected tissues resulting from the induction of CXCL10 and monocyte chemoattractant protein 1 (MCP-1) may also explain the marked peripheral lymphopenia that is commonly seen in MERS (190). Together with the wide distribution of DPP4 in different human cell types, the ability of MERS-CoV to hijack these professional antigen-presenting cells as vehicles for systemic dissemination to and induction of immunopathology at various organs may help to explain the unusually severe multiorgan involvement in MERS.

LABORATORY DIAGNOSIS

There are no pathognomonic clinical, biochemical, or radiological features that reliably differentiate MERS from other causes of acute community- or hospital-acquired pneumonia. Nucleic acid amplification assays are the most widely used method to provide laboratory confirmation of MERS with a short turnaround time using a unified testing protocol that was established early on in the epidemic. The WHO criteria for a laboratory-confirmed case include either a positive RT-PCR result for at least two different specific targets on the MERS-CoV genome or one positive RT-PCR result for a specific target on the MERS-CoV genome and an additional different RT-PCR product sequenced, confirming identity to known sequences of MERS-CoV (Table 8) (http://www.who.int/csr/disease/coronavirus_infections/MERS_Lab_recos_16_Sept_2013.pdf?ua=1). Isolation of infectious MERS-CoV from respiratory tract specimens, and possibly also blood, urine, and fecal samples, also confirms the diagnosis, but virus isolation has a longer turnaround time than nucleic acid amplification assays and requires experienced staff for interpretation of CPE and confirmation of infection by RT-PCR or immunostaining. Serological assays for detection of specific neutralizing anti-MERS-CoV antibodies in paired sera, taken at the acute and convalescent phases 14 to 21 days apart, also provide evidence of infection, but none of the serological assays developed so far has been thoroughly validated or compared against each other. Furthermore, viral culture and neutralizing antibody detection assays using whole virus require biosafety level 3 (BSL3) containment, which is not widely available in standard clinical microbiology laboratories.

Specimen Collection

The ideal clinical specimen for laboratory diagnosis is one which can be readily obtained by noninvasive means and contains a large number of infected cells with high viral load. Although lower respiratory tract specimens, including tracheal aspirate and bronchoalveolar lavage specimens, contain higher viral loads and genome yields than upper respiratory tract specimens and sputum, they require invasive procedures for collection and may not be easily obtainable in the early phase of illness (71, 72, 193). Therefore, upper respiratory tract specimens, including nasopharyngeal aspirate or swabs and oropharyngeal swabs are the most com-

TABLE 8 Characteristics of nucleic acid amplification tests for laboratory diagnosis of MERS^a

Diagnostic method (target gene)	Clinical specimen(s)	Recommended use	Technical LOD	Remarks	Reference(s)
upE assay (upstream of E gene)	Respiratory swab, sputum, and endotracheal aspirate	Screening	1.6 to 3.4 RNA copies/reaction	Most widely used test globally	310
ORF1a assay (ORF1a gene)	BAL fluid, NPA	Confirmatory for upE-positive samples	4.1 RNA copies/reaction	As sensitive as upE assay	62, 69
RealStar MERS-CoV RT-PCR kit 1.0	Aspiration tube flushed with PBS, BAL fluid, mouth exudates, nose exudates, stool, urine, CVC flushed with PBS	Screening	upE assay, 5.3 copies/reaction; ORF1a assay, 9.3 copies/reaction	As sensitive as the in-house upE and 1A assays; rapid and less labor-intensive than the in-house assays	321
ORF1b assay (ORF1b gene)	Respiratory swab, sputum, and endotracheal aspirate	Confirmatory for upE-positive samples	64 RNA copies/reaction	Less sensitive than upE and 1A assays; no overlap with those of known pan-CoV assays	310
RdRpSeq assay (RdRp gene and sequencing)	BAL fluid, NPA	Screening (pan-CoV RT-PCR) and confirmatory (sequencing)	0.3 to 3.0 PFU/ml	May cross-react with other βCoVs as the gene target is highly conserved	62, 69
NSeq assay (N gene and sequencing)	BAL fluid, NPA	Screening (RT-PCR) and confirmatory (sequencing)	0.03 to 0.3 PFU/ml	Highly sensitive and specific for MERS-CoV; may have deletion or mutation in the amplified fragment	62, 69
N2 assay (N gene)	URT, LRT, serum, stool	Screening with upE to enhance sensitivity and specificity	5 to 10 RNA copies/reaction	As sensitive as upE assay	322
N3 assay (N gene)	URT, LRT, serum, stool	Confirmatory for upE- or N2-positive samples	5 to 10 RNA copies/reaction	As sensitive as upE assay	322
RT-RPA assay (N gene)	No clinical specimen; culture supernatant	Field use (point-of-care test)	10 RNA copies/reaction	As sensitive as RT-PCR, faster TAT (≤30 min), and mobile	199
RT-LAMP	Medium containing pharyngeal swabs (healthy adults) mixed with MERS-CoV	Field use	3.4 RNA copies/reaction	As sensitive as upE and ORF1a assays, faster TAT (≤30 min)	200

^a Abbreviations: BAL, bronchoalveolar lavage; CoV, coronavirus; CVC, central venous catheter; Ig, immunoglobulin; LOD, lower limit of detection; LRT, lower respiratory tract; N, nucleocapsid; NPA, nasopharyngeal aspirate; ORF, open reading frame; RdRp, RNA-dependent RNA polymerase; RT-LAMP, reverse transcription loop-mediated isothermal amplification; RT-PCR, reverse transcription isothermal recombinase polymerase amplification; TAT, turnaround time; URT, upper respiratory tract.

monly collected specimens in suspected cases of MERS. Clinical specimens from extrapulmonary sites, especially urine, feces, blood, and/or tissues, may occasionally be positive and should also be collected if available, especially for their possible impact on infection control implementation (71, 72, 81, 175, 181). Notably, the diagnosis of MERS in a Tunisian patient was established by RT-PCR targeting the upE and N genes followed by nucleotide sequencing of RNA from a serum sample collected 10 days after symptom onset, whereas his mini-bronchoalveolar lavage fluid specimen tested negative (74). As for the optimal timing of specimen collection, there is a lack of data on the viral shedding kinetics of MERS-CoV in infected humans over time. Analysis of a limited number of laboratory-confirmed MERS cases suggests that the pattern may be more similar to that of SARS than to that of other HCoV infections (194). Thus, the viral load of MERS-CoV in nasopharyngeal specimens may also peak in the second week of illness rather than at symptom onset (162, 181, 195, 196). Repeated testing of upper and preferably lower respiratory tract specimens at different time points should be performed in suspected cases of MERS even when the first samples have tested negative (77; http://www.who.int/csr/disease/coronavirus_infections/MERS_Lab_recos_16_Sept_2013.pdf?ua=1). Virus shedding in the upper respiratory tract may be found in up to 30% of case contacts with minimal symptoms (197). Severe cases appear to have more prolonged virus shedding than mild cases (197). In critically ill patients who may have detectable MERS-CoV RNA in respiratory tract specimens and/or blood for more than 3 weeks, continued compliance with infection control measures is required during patient care procedures as a precautionary measure despite the presence of serum neutralizing antibody (88, 175, 181, 183). Aerosol-generating procedures for specimen collection should be performed under strict compliance with standard precautions along with additional measures, including the wearing of an N95 respirator, eye shield, long-sleeved gown, and gloves in an adequately ventilated room (http://www.who.int/csr/disease/coronavirus_infections/IPCNCoVguidance_06May13.pdf?ua=1). The specimens should be sent to the laboratory in viral transport medium as soon as possible after collection or be stored at -80°C if a delay in transfer is expected (http://www.who.int/csr/disease/coronavirus_infections/MERS_Lab_recos_16_Sept_2013.pdf?ua=1).

Nucleic Acid Amplification Assays

With the successful isolation and propagation of MERS-CoV and sequencing of its complete genome early in the epidemic, specific primers and a standardized laboratory protocol were rapidly developed and evaluated (198). Several gene targets can be used for RT-PCR as screening and/or confirmatory testing for MERS-CoV (Table 8). The most widely adopted approach uses the upE assay as a screening test, followed by the ORF1a or the ORF1b assay as confirmation. If the ORF1a assay or the ORF1b assay is negative or equivocal despite a positive upE assay, further testing of other specific gene targets, including the N, RdRp, and/or S genes, followed by amplicon sequencing should be performed. If further testing is not available but the patient had a compatible epidemiological and clinical history, then the case is considered to be a probable case of MERS (http://www.who.int/csr/disease/coronavirus_infections/MERS_Lab_recos_16_Sept_2013.pdf?ua=1). Notably, assays targeting the abundant N gene may be more sensitive than those targeting the other genes, although direct comparison with the upE assay in hu-

man clinical specimens has not been performed (133). However, a 6-nt deletion was found in N gene of the strain from the second laboratory-confirmed patient compared to the one obtained from the first patient, and therefore potential false-negative results due to mutations in this region may occur (62). For all positive cases, a second sample should preferably be tested to exclude false-positive results due to amplicon carryover. Other novel diagnostic approaches for MERS which have short turnaround times, high sensitivities, and specificities include reverse transcription loop-mediated isothermal amplification and reverse transcription isothermal recombinase polymerase amplification assays, which may be useful in areas without easy access to laboratories equipped with RT-PCR and/or sequencing technologies (199, 200). Further validation using more clinical specimens is required to assess their field performance.

Antibody Detection Assays

A number of assays for detection of nonneutralizing and neutralizing antibodies to MERS-CoV proteins have been developed but require further validation because some antibodies against β CoVs are generally known to cross-react within the genus (Table 9). Indeed, cross-reacting antibodies have been found not only in immunofluorescence assays but also in virus neutralization tests, which are considered to be the most specific method of antibody detection (201, 202). Therefore, the European Centre for Disease Prevention and Control recommends against testing for immunofluorescent antibodies unless convalescent-phase plasma is available to look for a 4-fold increase in antibody titer, because false-positive results may arise in single tests. Cases with positive serology in the absence of PCR testing or sequencing should be considered probable only if they meet the other criteria of the case definition (http://www.who.int/csr/disease/coronavirus_infections/MERS_Lab_recos_16_Sept_2013.pdf?ua=1). Nevertheless, antibody detection assays are important for retrospective diagnosis in clinically and epidemiologically suspicious cases with negative molecular test results, particularly in those with only upper respiratory tract specimens being tested. It can also be used for monitoring the evolution of epidemics in human and animal seroepidemiological studies and for contact tracing in outbreak investigations (126). The development of high-throughput, non-whole-virus-based assays such as enzyme-linked immunosorbent and pseudoparticle neutralization assays that do not require BSL3 containment facilities may increase their utility, especially in rural parts of the Middle East and other affected areas.

Antigen Detection Assays

The development of antigen detection assays for MERS-CoV has been reported mainly in histopathological confirmation in infected tissues of animals and in cell cultures with positive CPE (165, 166, 173). Recently, an immunochromatographic assay based on the detection of the abundantly expressed MERS-CoV N protein by highly selective monoclonal antibodies has been developed for the rapid qualitative detection of MERS-CoV antigen in nasal swabs of dromedary camels. Compared to the upE RT-PCR assay, this antigen detection assay has a sensitivity of 93.9% and a specificity of 99.6% (340). Similar assays were found to be highly sensitive and specific for the laboratory diagnosis of SARS from sera and nasopharyngeal samples from patients and have the potential advantages of being non-labor-intensive and relatively high throughput without requiring a BSL3 containment facility (3). More information on the timing of serum neutralizing anti-

TABLE 9 Characteristics of antibody detection assays for laboratory diagnosis of MERS and related seroepidemiological data in humans^a

Diagnostic method (detection target)	Antigen used	Sources of tested sera	Cross-reactivity	Main findings	Reference(s)
IFA					
Indirect IFA (anti-MERS-CoV Ab)	Whole virus	2 laboratory-confirmed cases and 85 blood donors	1/85 (1.2%) cross-reactive IgM in blood donors; detected in cells overexpressing recombinant S or N proteins	Better cell morphology; used as a screening test in a 2-stage protocol	62, 69, 182
		130 blood donors and 226 slaughterhouse workers (Jeddah and Makkah, KSA)	8/226 slaughterhouse workers had cross-reactive Ab in IFA	No evidence of widespread circulation of MERS-CoV in Jeddah and Makkah, KSA	98
		Animal handlers, SARS patients, and healthy blood donors in southern China	2/94 (2.1%) of animal handlers, 17/28 (60.7%) SARS patients, and 0/152 (0%) of healthy blood donors had cross-reactive anti-MERS-CoV Ab	An epitope around the HR2 domain of the S2 subunit may induce cross-reactivity in IFA against βCoV _s	202
IFA on Vero B4 cells (anti-MERS-CoV Ab)	Recombinant S and N proteins	2 serum samples from 1 patient (wk 3 and 8)	None in samples from a few German blood donors; detected in cells overexpressing recombinant S or N proteins	Does not require optimization of infection dose and duration and BSL3 containment	62, 69
		1 laboratory-confirmed case and 85 contacts	None	Helps to confirm the positive tests in conventional IFA	182
ELISA (anti-S and anti-N Ab)	S and N proteins expressed in VRP	Mouse sera	Cross-reactive anti-N Ab against MERS-CoV and other lineage 2c βCoV _s ; little cross-reactive anti-S Ab; no cross-reactive anti-N or anti-S Ab between MERS-CoV and SARS-CoV or αCoV _s	Strain-specific anti-S responses with very low level of cross-reactivity within or across CoV subgroups; cross-reactive anti-N Ab within but not across CoV subgroups	201
Western blotting (anti-S and anti-N Ab)	Recombinant S and N proteins expressed in VRP	2 serum samples from 1 patient (wk 3 and 8)	Not tested	Confirms the presence of anti-S and anti-N Ab detected in IFA	62
	S and N proteins expressed in VRP	Mouse sera	Cross-reactive anti-N Ab against MERS-CoV and other lineage C βCoV _s ; little cross-reactive anti-S Ab; no cross-reactive anti-N or anti-S Ab between MERS-CoV and SARS-CoV or αCoV _s	Strain-specific anti-S responses with very low level of cross-reactivity within or across CoV subgroups; cross-reactive anti-N Ab within but not across CoV subgroups	201
Protein microarray	Soluble S1 subunit of S protein	Patients with MERS, SARS, and/or other human CoV infections and sera from cynomolgus macaques and rabbit infected with MERS-CoV	None	Allows 1-stage, high-throughput, testing with minimal sample requirement and can use dried blood spots for testing to facilitate sample transfer	323
Neutralization test					
PRNT (anti-MERS-CoV Ab)	Whole virus	1 laboratory-confirmed case and 85 contacts	None	Used as a confirmatory test in a 2-stage protocol	194
		130 blood donors and 226 slaughterhouse workers (Jeddah and Makkah, KSA)	8/226 slaughterhouse workers had cross-reactive Ab in IFA but not PRNT	PRNT is more specific than IFA	182
		Patients with MERS, SARS, and/or other human CoV infections and sera from camels and other animals	None in human samples	Used as a confirmatory test in a 2-stage protocol	98
PRNT (anti-S and anti-N Ab)	S and N proteins expressed from VRP	Mouse sera and 1 patient with MERS	Very low levels of cross-neutralization of MERS-CoV by mouse antisera to SARS-CoV using high concentrations of serum	S but not N protein is the major determinant of neutralizing Ab response to MERS-CoV; N proteins of CoV _s cross-react within but not between subgroups; S proteins of CoV _s have little cross-neutralization or cross-reactivity within subgroup 2c or any other subgroup	121
					201

Neutralization of MERS-CoV S-driven transduction (anti-S Ab)	S proteins expressed by lentiviral vectors	Sera from hospitalized children and male blood donors in KSA	None	Estimated MERS-CoV seroprevalence in the study area was <2.3% in children during 2010 to 2011 and <3.3% in male adults in 2012	51, 97
Microneutralization assay (neutralizing anti-MERS-CoV Ab)	Whole virus	Animal handlers, SARS patients, and healthy blood donors in southern China	0/94 (0%), 7/28 (25.0%) of SARS patients, and 0/152 (0%) of healthy blood donors had low-titer cross- reactive neutralizing anti-MERS- CoV Ab	An epitope around the HR2 domain of the S2 subunit may induce cross-reactive neutralizing Ab against βCoV s	202
ppNT assay (neutralizing anti-S Ab)	S pseudoparticle expressed by a replication- incompetent HIV containing a luciferase reporter gene	Human sera from general populations in Egypt and Hong Kong, MERS and SARS patients, swine and wild bird sera from Hong Kong, and animal sera from Egypt	None in human samples	10 times less sensitive than the ppNT assay	122
		Human sera from general populations in Egypt and Hong Kong, MERS and SARS patients, swine and wild bird sera from Hong Kong, and animal sera from Egypt	None in human samples	10 times more sensitive than the conventional microneutralization assay, does not require BSL3 containment	122

^a Abbreviations: Ab, antibody; BAL, bronchoalveolar lavage; BSL, biosafety level; CPE, cytopathic effects; CVC, central venous catheter; ELISA, enzyme-linked immunosorbent assay; HIV, human immunodeficiency virus; HR2, heptad repeat 2; Ig, immunoglobulin; IFA, immunofluorescence assay; KSA, Kingdom of Saudi Arabia; LRT, lower respiratory tract; MNT, microneutralization test; N, nucleocapsid protein; NPA, nasopharyngeal aspirate; ppNT, pseudoparticle neutralization; PNRT, plaque reduction neutralization test; RT-PCR, reverse transcription isothermal recombinase polymerase amplification; S, spike; TAT, turnaround time; TCID₅₀, 50% tissue culture infective dose; URT, upper respiratory tract; VRP, Venezuelan equine encephalitis virus replicons.

body kinetics and viral shedding patterns in different human and camel specimens is required to optimize these antigen detection assays for clinical and epidemiological studies.

Viral Culture

In contrast to other CoVs causing human infections, which are difficult to culture in *in vitro* systems, MERS-CoV grows rapidly in a wide range of human and nonhuman cell lines (Table 6) (116–118). Indeed, the first identification of MERS-CoV was achieved by inoculation of the patient's sputum sample in monkey kidney cell lines, including LLC-MK2 and Vero cell lines, for detection of CPE, before specific nucleic acid amplification assays were developed (9). MERS-CoV produces focal CPE with rounded refractile cells in various susceptible cell lines on day 5 after inoculation during primary isolation and on as early as day 1 on subsequent passage (116). These changes then spread throughout the cell monolayers, leading to rounding and detachment of cells within 24 to 48 h. Additionally, syncytium formation caused by fusion activity of the MERS-CoV S protein at neutral pH may be observed in LLC-MK2, Calu-3, Caco-2, and Huh-7 cell lines and Vero cells expressing TMPRSS2 (9, 52, 58, 116). Transmission electron microscopy of MERS-CoV-infected cells shows CoV-induced membrane structures that support RNA synthesis, including convoluted membranes surrounded by double-membrane vesicles measuring 150 to 320 nm with dense inner cores, in the perinuclear region, which is typical of cellular changes of CoV infection (58). Although the clinical use of viral culture for MERS-CoV is limited by the lack of BSL3 facilities in most satellite hospitals, the ease of growing the virus in cell culture systems has greatly facilitated study on its pathogenesis and development of antiviral agents in reference research laboratories.

CLINICAL MANAGEMENT AND ANTIVIRALS

As in the case of other human CoV infections, including SARS, specific antiviral agents with proven efficacy in randomized controlled trials are lacking for MERS (203, 204). Supportive care remains the mainstay of treatment for severe MERS cases with respiratory failure and extrapulmonary complications. ECMO has been increasingly used in severe viral pneumonia, including some cases of MERS (18, 71, 153, 154, 156, 205). However, procedure-related factors, such as the requirements of technical expertise and specific equipment, and patient factors, including the presence of multiple comorbidities and coagulopathy, may limit its use, especially among patients in rural parts of the Middle East and Africa. Other forms of assisted ventilation and pulmonary rescue therapy, including mechanical ventilation using a lung-protective strategy with a small tidal volume, noninvasive positive pressure ventilation, and inhaled nitric oxide, have been tried for SARS and influenza with ARDS (3, 153). However, data on their efficacies in MERS are lacking (88, 206). Due to the apparently high incidence of acute and acute-on-chronic renal failure in patients with severe MERS, renal replacement therapy has been frequently used and was essential for tiding the patient over the oliguric phase (64, 88, 206). Circulatory failure is supported by the use of inotropes and volume expansion (206). Broad-spectrum antibacterials and neuraminidase inhibitors against influenza are used empirically before the diagnosis of MERS is established (206). Antimicrobials guided by interval surveillance or sepsis work-up should be used to treat secondary nosocomial infections in those with prolonged hospitalization and invasive ventilation or opportunistic infections in patients who are immunocompromised, especially those who receive

TABLE 10 Antiviral agents and immunomodulators against MERS-CoV^a

Study type and antiviral agent and/or immunomodulator	Drug class and/or target	Study setting and methods (virus strain)	Main finding(s)	Reference(s)
<i>In vitro</i> studies				
Interferons				
IFN, universal type I	Exogenous IFN	Vero E6 (Hu/Jordan-N3/2012)	IC ₅₀ = 113.8 U/ml	324
Pegylated IFN- α	Exogenous IFN	Vero (HCoV-EMC/2012)	Decreased CPE at ≥ 1 ng/ml	58
IFN- α 2a	Exogenous IFN	Vero E6 (Hu/Jordan-N3/2012)	IC ₅₀ = 160.8 U/ml	324
IFN- α 2b	Exogenous IFN	Vero (HCoV-EMC/2012)	IC ₅₀ = 58.08 μ g/ml	208
		LLC-MK2 (HCoV-EMC/2012)	IC ₅₀ = 13.26 μ g/ml	208
		Vero E6 (Hu/Jordan-N3/2012)	IC ₅₀ = 21.4 U/ml	324
IFN- α 2b (Intron A)	Exogenous IFN	Vero (HCoV-EMC/2012)	IC ₅₀ = 6709.79 IU/ml	209
IFN- β 1a (Avonex)	Exogenous IFN	Vero (HCoV-EMC/2012)	IC ₅₀ = 5073.33 IU/ml	209
IFN- β 1a (Rebif)	Exogenous IFN	Vero (HCoV-EMC/2012)	IC ₅₀ = 480.54 IU/ml	209
IFN- β 1b (Betaferon)	Exogenous IFN	Vero (HCoV-EMC/2012)	IC ₅₀ = 17.64 IU/ml	209
IFN- γ	Exogenous IFN	Vero E6 (Hu/Jordan-N3/2012)	IC ₅₀ = 1.37 U/ml	324
Cyclophilin inhibitor		Vero E6 (Hu/Jordan-N3/2012)	IC ₅₀ = 56.5 U/ml	324
Cyclosporine	Inhibitor of cyclophilins and their interactions with nsp1	Vero (HCoV-EMC/2012)	Complete inhibition of infection at 9 μ M cyclosporine	58
Viral protease inhibitors				
Lopinavir	3C-like protease inhibitor	Huh-7 (HCoV-EMC/2012)	Partial and complete inhibition of infection at 7.5 μ M and 15 μ M cyclosporine, respectively	58
		Huh-7 (HCoV-EMC/2012)	IC ₅₀ = 8.0 μ M, SI = 3.1; 2 other MERS-CoV strains (MERS-HCoV/KSA/UK/Eng-2/2012 and MERS-HCoV/Qatar/UK/Eng-1/2012) tested were less sensitive; inhibition of a postentry step	212
N3	3C-like protease inhibitor	Not available	IC ₅₀ = 0.28 μ mol/liter	222
CE-5	3C-like protease inhibitor	HEK293T (HCoV-EMC/2012)	IC ₅₀ = 12.5 μ M	223
GRL-001	3C-like protease inhibitor	Vero (Hue/England-N1/2012)	Completely blocked viral replication at early time points (<24 hpi), decreased viral decreased replication by \sim 100-fold at 24 hpi, and decreased virus-induced cytopathology in infected cells	224
6-Mercaptopurine	Competitive papain-like protease inhibitor	Peptide cleavage and deubiquitination assays (purified papain-like protease HCoV-EMC/2012)	Inhibition of the proteolytic activity and deubiquitination of MERS-CoV papain-like protease; may act synergistically with mycophenolic acid	341
6-Thioguanine	Competitive papain-like protease inhibitor	Peptide cleavage and deubiquitination assays (purified papain-like protease HCoV-EMC/2012)	Inhibition of the proteolytic activity and deubiquitination of MERS-CoV papain-like protease; may act synergistically with mycophenolic acid	341
Helicase inhibitor SSYA10-001	Helicase inhibitor	Vero E6 (Hu/Jordan-N3/2012)	IC ₅₀ = 25 μ M, SI \geq 20	225
Cellular protease inhibitors Camostat mesylate	TMPSR2 inhibitor	Vero-TMPSR2 (HCoV-EMC/2012)	Decreased cell entry by \sim 15-fold (10 μ M) and inhibited syncytium formation in a dose-dependent manner (1 to 100 μ M)	52
		Calu-3 (HCoV-EMC/2012)	Decreased cell entry by \sim 10-fold (10 μ M), inhibited the multistep growth of the virus by \sim 90-fold (10 μ M) to \sim 270-fold (100 μ M), and delayed virus-induced cell death by 2 (10 μ M) to 5 (100 μ M) days	52
Leupeptin	Protease inhibitor	Calu-3 (HCoV-EMC/2012)	Decreased virus entry into cells (10 and 100 μ M)	52

E-64-D	Broad-spectrum cathepsin inhibitor	Vero E6 (Hu/Jordan-N3/2012)	IC ₅₀ = 1.275 μM	211
EST	Cathepsin inhibitor	Vero-TMPRSS2 (HCoV-EMC/2012)	Decreased virus entry into cells by ~3-fold (10 μM)	52
Cathepsin L inhibitor III	Cathepsin L-specific inhibitor	Vero E6 and LLC-MK2 (HCoV-EMC/2012)	Decreased entry of MERS-CoV pseudovirus by 97%	23
MDL-28170	Cathepsin B and L inhibitor	MRC5 (HCoV-EMC/2012)	MERS-CoV S-mediated transduction was blocked	51
Decanoyl-RV/KR-chloromethylketone	Furin inhibitor	Huh-7, MRC-5, WI-38, Vero, and NHBE cells (HCoV-EMC/2012)	Dose-dependent and significantly decreased virus infection in various cell types	54
Nucleic acid and/or protein synthesis inhibitors				
Anisomycin	Protein and DNA synthesis inhibitor by inhibiting peptidyl transferase or 80S ribosome system	Vero E6 (Hu/Jordan-N3/2012)	IC ₅₀ = 0.003 μM	211
Cycloheximide	Protein synthesis inhibitor	Vero E6 (Hu/Jordan-N3/2012)	IC ₅₀ = 0.189 μM	211
Emetine dihydrochloride hydrate	Protein synthesis inhibitor by binding to 40S ribosomal subunit	Vero E6 (Hu/Jordan-N3/2012)	IC ₅₀ = 0.014 μM	211
Gemcitabine hydrochloride	Nucleoside analogue and DNA synthesis inhibitor	Vero E6 (Hu/Jordan-N3/2012)	IC ₅₀ = 1.216 μM	211
Homoharringtonine (omacetaxine mepesuccinate)	Protein synthesis inhibitor	Vero E6 (Hu/Jordan-N3/2012)	IC ₅₀ = 0.0718 μM	211
K22	Specifically targets membrane-bound viral RNA synthesis	HAE (HCoV-EMC/2012)	Decreased viral replication by >4-logs and substantial reduction of dsRNA (50 μM)	304
Mycophenolic acid	Inhibitor of IMPDH and depletion of guanosine and deoxyguanosine nucleotide pools; noncompetitive inhibitor of MERS-CoV papain-like protease	Vero (HCoV-EMC/2012)	IC ₅₀ = 0.17 μg/ml	209
Ribavirin	Nucleoside polymerase inhibitor	Vero E6 (Hu/Jordan-N3/2012)	IC ₅₀ = 2.87 μM	324
		Vero (HCoV-EMC/2012)	IC ₅₀ = 41.45 μg/ml	208
		Vero (HCoV-EMC/2012)	IC ₅₀ = 9.99 μg/ml	209
		LLC-MK2 (EMC/2012)	IC ₅₀ = 16.33 μg/ml	208
		Vero E6 (Hu/Jordan-N3/2012)	IC ₅₀ ≥ 250 μM	324
mAbs against spike protein				
Mersmab1	mAb against RBD of S1 subunit of S protein	Huh-7 (HCoV-EMC/2012)	Blocked entry of MERS-CoV S-mediated pseudovirus into cells with ND ₅₀ < 0.16 μg/ml	37
		Vero E6 (HCoV-EMC/2012)	Neutralizing inhibitory activity with ND ₅₀ < 2 μg/ml	37
		Calu-3 (HCoV-EMC/2012)	Neutralizing activity with CPE inhibition	37
MERS-4 mAb	mAb against RBD of S1 subunit of S protein	Huh-7 (IC ₅₀) and COS7 (syncytium formation) (HCoV-EMC/2012)	Inhibited syncytium formation and neutralizing inhibitory activity with IC ₅₀ = 0.37 nM (pseudovirus) and 3.33 nM (live)	39
MERS-27 mAb	mAb against RBD of S1 subunit of S protein	Huh-7 (IC ₅₀) and COS7 (syncytium formation) (HCoV-EMC/2012)	Neutralizing inhibitory activity with IC ₅₀ = 63.96 nM (pseudovirus) and 13.33 nM (live)	39
m336 mAb	mAb against RBD of S1 subunit of S protein	Vero (live virus) and DPP4-expressing Huh-7 (pseudovirus) (HCoV-EMC/2012)	Neutralizing inhibitory activity with IC ₅₀ < 0.01 μg/ml (live) and 0.07 μg/ml (pseudovirus); inhibited RBD-DPP4 binding (IC ₅₀ = 0.034 μg/ml)	38
m337 mAb	mAb against RBD of S1 subunit of S protein	Vero (live virus) and DPP4-expressing Huh-7 (pseudovirus) (HCoV-EMC/2012)	Neutralizing inhibitory activity with IC ₅₀ < 0.01 μg/ml (pseudovirus) and < 10 μg/ml (live); inhibited RBD-DPP4 binding (IC ₅₀ = 0.044 μg/ml)	38

(Continued on following page)

TABLE 10 (Continued)

Study type and antiviral agent and/or immunomodulator	Drug class and/or target	Study setting and methods (virus strain)	Main finding(s)	Reference(s)
m337 mAb	mAb against RBD of S1 subunit of S protein	Vero (live virus) and DPP4-expressing Huh-7 (pseudovirus) (HCoV-EMC/2012)	Neutralizing inhibitory activity with $IC_{50} < 0.1 \mu\text{g/ml}$ (pseudovirus) and $< 1 \mu\text{g/ml}$ (live); inhibited RBD-DPP4 binding ($IC_{50} = 0.041 \mu\text{g/ml}$)	38
1E9 scFvFc	Single-chain variable domain fragment against RBD of S1 subunit of S protein fused with hFc	Vero (live virus) and hDPP4-expressing 293T (pseudovirus) cells (HCoV-EMC/2012)	Neutralizing inhibitory activity ($IC_{50} = 3.21 \mu\text{g/ml}$)	40
1F8 scFvFc	Single-chain variable domain fragment against RBD of S1 subunit of S protein fused with hFc	Vero (live virus) and hDPP4-expressing 293T (pseudovirus) cells (HCoV-EMC/2012)	Neutralizing inhibitory activity ($IC_{50} = 6.27 \mu\text{g/ml}$)	40
3A1 scFvFc	Single-chain variable domain fragment against RBD of S1 subunit of S protein fused with hFc	Vero (live virus) and hDPP4-expressing 293T (pseudovirus) cells (HCoV-EMC/2012)	Neutralizing inhibitory activity ($IC_{50} = 1.46 \mu\text{g/ml}$)	40
3B12 scFvFc	Single-chain variable domain fragment against RBD of S1 subunit of S protein fused with hFc	Vero (live virus) and hDPP4-expressing 293T (pseudovirus) cells (HCoV-EMC/2012)	Neutralizing inhibitory activity ($IC_{50} = 1.25 \mu\text{g/ml}$)	40
3C12 scFvFc	Single-chain variable domain fragment against RBD of S1 subunit of S protein fused with hFc	Vero (live virus) and hDPP4-expressing 293T (pseudovirus) cells (HCoV-EMC/2012)	Neutralizing inhibitory activity ($IC_{50} = 2.00 \mu\text{g/ml}$)	40
3B11 scFvFc	Single-chain variable domain fragment against RBD of S1 subunit of S protein fused with hFc	Vero (live virus) and hDPP4-expressing 293T (pseudovirus) cells (HCoV-EMC/2012)	Neutralizing inhibitory activity ($IC_{50} = 1.83 \mu\text{g/ml}$)	40
M14D3 scFvFc	Single-chain variable domain fragment against RBD of S1 subunit of S protein fused with hFc	Vero (live virus) and hDPP4-expressing 293T (pseudovirus) cells (HCoV-EMC/2012)	Neutralizing inhibitory activity ($IC_{50} = 4.30 \mu\text{g/ml}$)	40
mAbs against DPP4				
Clone 2F9 mAb	mAb against DPP4	Huh-7 (strain?)	Near-complete inhibition of nsp4 expression in infected cells	50
Clone YS110 mAb	mAb against DPP4	Huh-7 (strain?)	Partial inhibition of nsp4 expression in infected cells	50
Inhibitors of clathrin-mediated endocytosis				
Astemizole	Antihistamine and anticholinergic; inhibitor of clathrin-mediated endocytosis	Vero E6 (Huh/Jordan-N3/2012)	$IC_{50} = 4.884 \mu\text{M}$	211, 213
Clomipramine hydrochloride	Tricyclic antidepressant; inhibitor of clathrin-mediated endocytosis	Vero E6 (Huh/Jordan-N3/2012)	$IC_{50} = 9.332 \mu\text{M}$	211, 213
Chlorpromazine	Antipsychotic (phenothiazine); inhibitor of clathrin-mediated endocytosis	Huh-7 (HCoV-EMC/2012)	$IC_{50} = 4.9 \mu\text{M}$, SI = 4.3; inhibition of an early step with or without another postentry step in the replicative cycle	212, 213
Fluphenazine hydrochloride	Antipsychotic (piperazine); inhibitor of clathrin-mediated endocytosis	Vero E6 (Huh/Jordan-N3/2012)	$IC_{50} = 9.514 \mu\text{M}$	211, 213
Promethazine hydrochloride	Antihistamine and antipsychotic (phenothiazine); inhibitor of clathrin-mediated endocytosis	Vero E6 (Huh/Jordan-N3/2012)	$IC_{50} = 5.868 \mu\text{M}$	211, 213
Tamoxifen citrate	Estrogen receptor inhibitor; inhibitor of clathrin-mediated endocytosis	Vero E6 (Huh/Jordan-N3/2012)	$IC_{50} = 11.802 \mu\text{M}$	211, 213
		Vero E6 (Huh/Jordan-N3/2012)	$IC_{50} = 10.117 \mu\text{M}$	211, 213

Thiothixene	Antipsychotic (thioxanthene); inhibitor of clathrin-mediated endocytosis	Vero E6 (Hu/Jordan-N3/2012)	IC ₅₀ = 9.297 μ M	211, 213
Triflupromazine hydrochloride	Antipsychotic (phenothiazine); inhibitor of clathrin-mediated endocytosis	Vero E6 (Hu/Jordan-N3/2012)	IC ₅₀ = 5.758 μ M	211, 213
Other cell entry inhibitors				
HR2P peptide	HR2-based fusion inhibitor; inhibitor of clathrin-mediated endocytosis	Vero (HCoV-EMC/2012)	IC ₅₀ = 0.6 μ M	44, 213
P1 peptide	HR2-based fusion inhibitor	Calu-3 (HCoV-EMC/2012)	IC ₅₀ = 0.6 μ M	44
		HFL (HCoV-EMC/2012)	IC ₅₀ = 13.9 μ M	44
		Huh-7 (HCoV-EMC/2012)	Inhibited MERS-CoV pseudovirus with IC ₅₀ = 3.013 μ M	45
S377-588-Fc protein	Recombinant truncated RBD of S protein fused with human IgG Fc fragment	Calu-3 (HCoV-EMC/2012)	Complete CPE inhibition (25 μ g/ml)	42
HP-HSA	3-Hydroxyphthalic anhydride-modified human serum albumin targeting HIV-1 gp120 and/or CD4 receptor	Huh-7 and NBL-7 (MERS-CoV pseudovirus expressing full-length S protein of HCoV-EMC/2012)	Around 90% of pseudovirus entry inhibition (20 μ M); minimal cytotoxicity in Huh-7 cells at up to 100 μ M	41
ADS-J1	Small-molecule entry inhibitor targeting HIV gp41	Huh-7 and NBL-7 (MERS-CoV pseudovirus expressing full-length S protein of HCoV-EMC/2012)	CC50 = 26.9 μ M, IC50 = 0.6 μ M, and SI = 45	41
C34	Peptidic HIV entry inhibitor	Huh-7 and NBL-7 (MERS-CoV pseudovirus expressing full-length S protein of HCoV-EMC/2012)	Around 50% of pseudovirus inhibition at 20 μ M in NBL cells but no activity in Huh-7 cells	41
T20	Peptidic HIV entry inhibitor	Huh-7 and NBL-7 (MERS-CoV pseudovirus expressing full-length S protein of HCoV-EMC/2012)	Around 50% of pseudovirus inhibition at 20 μ M in NBL cells but no activity in Huh-7 cells	41
Adenosine deaminase	Natural DPP4 ligand	Huh-7 (HCoV-EMC/2012)	Dose-dependent inhibition of MERS-CoV infection	49
		Human DPP4 plasmid-transfected MDCK (HCoV-EMC/2012)	Blocks S1 binding and MERS-CoV infection despite expression of DPP4	49
Miscellaneous				
Amodiaquine	Histamine N-methyltransferase inhibitor	Vero E6 (Hu/Jordan-N3/2012)	IC ₅₀ = 6.212 μ M	211
Benztropine mesylate	Anticholinergic	Vero E6 (Hu/Jordan-N3/2012)	IC ₅₀ = 16.627 μ M	211
Chloroquine	Antiparasitic	Huh-7 (HCoV-EMC/2012)	IC ₅₀ = 3.0 μ M, SI = 19.4; Inhibition of an early step in the replicative cycle	212
		Vero E6 (Hu/Jordan-N3/2012)	IC ₅₀ = 6.275 μ M	211
		Vero E6 (Hu/Jordan-N3/2012)	IC ₅₀ = 12.646 μ M	211
Chlorphenoxamine hydrochloride	Antihistamine and anticholinergic	Huh-7 (HCoV-EMC/2012)	45% inhibition (10 μ M)	214
Dabrafenib	Raf inhibitor	Vero E6 (Hu/Jordan-N3/2012)	IC ₅₀ = 5.468 μ M	211
Dasatinib	Tyrosine kinase inhibitor (ABL1 pathway)	Calu-3 (HCoV-EMC/2012)	Dose-dependent CPE inhibition (1 to 10 μ M) and viral yield reduction (2.5 to 40 μ M); treatment before infection unnecessary; extended therapeutic window (≥ 20 h); inhibitory effects starts at 6 hpi; CC ₅₀ > 50 μ M; changed DPP4 expression pattern on the membrane of Calu-3 cells	325
ESI-09	Epac-specific inhibitor			
Everolimus	mTOR inhibitor	Vero E6 (HCoV-EMC/2012)	Dose-dependent CPE inhibition and viral yield reduction	325
Flupirilene	Antipsychotic (diphenylbutylpiperidine)	Huh-7 (HCoV-EMC/2012)	56% to 59% inhibition (10 μ M)	214
		Vero E6 (Hu/Jordan-N3/2012)	IC ₅₀ = 7.477 μ M	211

(Continued on following page)

TABLE 10 (Continued)

Study type and antiviral agent and/or immunomodulator	Drug class and/or target	Study setting and methods (virus strain)	Main finding(s)	Reference(s)
Hydroxychloroquine sulfate	Antiparasitic	Vero E6 (Hu/Jordan-N3/2012)	IC ₅₀ = 8.279 μ M	211
Imatinib mesylate	Tyrosine kinase inhibitor (ABL1 pathway)	Vero E6 (Hu/Jordan-N3/2012)	IC ₅₀ = 17.689 μ M	211
Loperamide	μ -Opioid receptor agonist	Huh-7 (HCoV-EMC/2012)	IC ₅₀ = 4.8 μ M, SI = 3.2; inhibition of an early step in the replication cycle	212
Mefloquine	Inhibition of heme polymerase; serotonin agonist	Vero E6 (Hu/Jordan-N3/2012)	IC ₅₀ = 7.416 μ M	211
Miltefosine	AKT inhibitor	Huh-7 (HCoV-EMC/2012)	28% inhibition (10 μ M)	214
SB203580	Kinase inhibitor	Vero E6 (HCoV-EMC/2012)	Pretreatment of infected cells with SB203580 decreased 15% and 7% of the log ₁₀ viral titer at 24 hpi and 48 hpi, respectively	176
Selumetinib	ERK/MAPK signaling inhibitor	Huh-7 (HCoV-EMC/2012)	>95% inhibition (10 μ M)	214
Sorafenib	Raf inhibitor	Huh-7 (HCoV-EMC/2012)	93% inhibition (10 μ M)	214
Terconazole	Sterol metabolism inhibitor	Vero E6 (Hu/Jordan-N3/2012)	IC ₅₀ = 12.203 μ M	211
Thiethylperazine maleate	Antiemetic (phenothiazine)	Vero E6 (Hu/Jordan-N3/2012)	IC ₅₀ = 7.865 μ M	211
Toremifene citrate	Estrogen receptor inhibitor	Vero E6 (Hu/Jordan-N3/2012)	IC ₅₀ = 12.915 μ M	211
Trametinib	ERK/MAPK signaling inhibitor	Huh-7 (HCoV-EMC/2012)	>95% inhibition (0.1 μ M)	214
Triptanorol	Sterol metabolism inhibitor	Vero E6 (Hu/Jordan-N3/2012)	IC ₅₀ = 5.283 μ M	211
Combination treatment				
Ribavirin/IFN- α 2b (1:5)	Nucleoside polymerase inhibitor/exogenous IFN	Vero (HCoV-EMC/2012)	Additional decreased viral titer by 0.40 to 2.16 logs with ribavirin	208
Mycophenolic acid/IFN- β 1b	IMPDH inhibitor/exogenous IFN	Vero (HCoV-EMC/2012)	IC ₅₀ of mycophenolic acid = 1.7–2.8 times lower with 6.25–12.5 IU/ml of IFN- β 1b; IC ₅₀ of IFN- β 1b 1.1–1.8 times lower with 0.016–0.063 μ g/ml of mycophenolic acid	209
MERS-4 and MERS-27 mAbs	mAbs against RBD of S1 subunit of S protein	Huh-7 (HCoV-EMC/2012)	Synergistic neutralizing effect against pseudovirus	39
Animal experiments				
Ribavirin/IFN- α 2b	Nucleoside polymerase inhibitor/exogenous IFN	Rhesus macaques (HCoV-EMC/2012); regimen, loading dose of 30 mg/kg of ribavirin i.v. and 5 MIU/kg of IFN- α 2b s.c., followed by 10 mg/kg q8h of ribavirin i.m. and 5MIU/kg of IFN- α 2b s.c. q16h until 72 hpi	Compared to untreated, infected macaques, treated macaques had no breathing abnormalities, minimal radiological evidence of pneumonia, lower levels of serum and pulmonary proinflammatory markers, few viral genome copies, lower expression of inflammatory genes, and less severe histopathological changes in lungs	174
Poly(I:C)	TLR3 agonist	Ad5-hDPP4-transduced mice (HCoV-EMC/2012)	Accelerated virus clearance from lungs of infected mice	173
Human trials				
Ribavirin/IFN- α 2b/corticosteroid	Nucleoside polymerase inhibitor/exogenous interferon/corticosteroid	5 critically ill MERS patients; regimen, oral ribavirin, s.c. IFN- α 2b, and i.v. and/or oral corticosteroid (methylprednisolone and/or prednisolone)	Mean age = 57.6 (24–81) yr; 3 males and 2 females; admitted 4 (2–10) days after symptom onset; all had comorbidities; time between admission and antiviral treatment = 16.8 (11–21) days and corticosteroid 15.8 (6–22) days; side effects = hemolytic anemia, thrombocytopenia, pancreatitis, increased lipase, and deranged liver and renal function tests; all died after a mean of 39.6 (32–52) days after admission	326

Ribavirin/IFN- α 2b \pm corticosteroid	Nucleoside polymerase inhibitor/exogenous IFN \pm corticosteroid	2 epidemiologically linked MERS patients; regimen, oral ribavirin and s.c. IFN- α 2b for 2 weeks (and 500 mg of methylprednisolone i.v. q24h for 3 days for index case)	Both the index case (treatment) and contact (prophylaxis) had clinical and radiological improvement after receiving ribavirin and IFN- α 2b	210
Ribavirin/IFN- α 2a	Nucleoside polymerase inhibitor/exogenous IFN \pm corticosteroid	20 severe MERS patients; regimen, oral ribavirin for 8–10 days and 180 μ g/wk of pegylated IFN- α 2a for 2 wk, 11/19 (58%) patients received corticosteroid	Compared to the comparator group (28 severe MERS patients who received supportive care only), the treatment group had significantly improved survival at 14 days but not 28 days after the diagnosis of MERS; significantly greater reduction in hemoglobin level was noted in the treatment group	206
Ribavirin/lopinavir/IFN- α 2a	Nucleoside polymerase inhibitor/protease inhibitor/exogenous IFN	1 severe MERS patient; regimen, 1,200 mg of oral ribavirin q8h and lopinavir/ritonavir (400/100 mg) q12h for 8 days, and 180 μ g/wk of pegylated IFN- α 2a for 2 wk	Viremia resolved 2 days after initiation of antiviral treatment (started on day 13 of illness); persistent virus shedding in respiratory tract secretions until fourth week of illness	183

^a Abbreviations: ABL1, Abelson murine leukemia viral oncogene homologue 1; Ad5-hDPP4, adenovirus expressing human host-cell receptor dipeptidyl peptidase 4; AKT, protein kinase B; CC₅₀, 50% inhibition of cell survival; DPP4, dipeptidyl peptidase 4; Epac, exchange proteins directly activated by cyclic AMP; ERK/MAPK, extracellular signal-regulated kinases/mitogen-activated protein kinases; HAE, primary human airway epithelia; hFc, constant region fragment of human IgG; hpi, hours postinfection; HR, heptad repeat; IC₅₀, 50% maximal inhibitory concentration; IFN, interferon; IMPDH, IMP dehydrogenase; i.v., intravenous; mAb, monoclonal antibody; MIU, mega-international units; mTOR, mammalian target of rapamycin; ND₅₀, 50% neutralization dose; nsp, nonstructural protein; RBD, receptor-binding domain; S, spike; s.c., subcutaneous; SI, selectivity index; TLR3, Toll-like receptor 3; TMPRSS2, type II transmembrane serine protease.

corticosteroid for immunomodulation. As in SARS, an immunosuppressive dose of corticosteroid should not be given because of its potential side effects and immunosuppression. Only a stress dose of corticosteroid should be considered in patients with refractory shock and relative adrenal insufficiency (http://www.who.int/csr/disease/coronavirus_infections/InterimGuidance_ClinicalManagement_NovelCoronavirus_11Feb13u.pdf?ua=1).

The improvement in outcome of MERS, with a case-fatality rate of over 35%, depends on the development of effective antiviral treatment for suppression of viral load. Candidate antiviral agents are identified using three general approaches (Table 10). The first and fastest approach is to test drugs with broad-spectrum antiviral activities, including those with reported activities against other CoVs associated with human infection, particularly SARS-CoV. This approach has identified numerous agents, including interferons, ribavirin, and cyclophilin inhibitors (58, 207, 208). Type I interferons, which are important in the innate immunity against CoV infection, exhibit anti-MERS-CoV activity in various cell lines and also in rhesus macaques. MERS-CoV is 50 to 100 times more sensitive to pegylated interferon alpha than SARS-CoV in cell culture (58). Moreover, the combination of interferon alpha 2b and ribavirin, a purine nucleoside analogue that inhibits GTP synthesis and viral RNA polymerase activity that has been widely used to treat SARS, has exhibited synergistic effects against MERS-CoV in cell cultures (208, 209). In rhesus macaques infected with MERS-CoV, this combination reduces virus replication, moderates the host inflammatory response, and improves clinical outcome (174). However, the regimen's efficacy in humans remains uncertain. In a small cohort of MERS cases in KSA, all five patients who received a combination of interferon alpha 2b, ribavirin, and corticosteroid died. The delayed commencement of the antiviral regimen for at least 2 weeks after symptom onset in these patients might have reduced the treatment benefit, as another patient who received treatment early on the day of admission survived, though MERS-CoV RNA remained detectable in his sputum samples until day 12 of treatment (210). A more recent retrospective cohort study showed that 20 adult patients with severe MERS who received oral ribavirin and pegylated interferon alpha 2a (Pegasys; Roche Pharmaceuticals, Basel, Switzerland) for 8 to 10 days (initiated at a median of 3 days after diagnosis) had significantly better survival rates at 14 days but not at 28 days after diagnosis than 28 historical controls who received supportive care only (206). Possible reasons for the lack of a long-term survival benefit in the treatment group include the small number of patients in the study and the fact that both ribavirin and pegylated interferon have high 50% effective concentrations (EC₅₀) against MERS-CoV relative to their peak serum concentrations achievable at clinically relevant dosages. Cyclophilin inhibitors, such as cyclosporine, are known to have antiviral activity against numerous human and animal CoVs, including SARS-CoV. However, the clinical relevance of cyclosporine for treating MERS is likely limited, as the drug's peak serum level achievable with clinically relevant dosages is below its EC₅₀ for MERS-CoV (58).

The second approach to identify candidate antivirals for MERS involves screening of chemical libraries that comprise large numbers of existing drugs or databases that contain information on transcriptional signatures in different cell lines. The advantages of this approach include the commercial availability, known pharmacokinetics, and well-reported safety profiles of the identified

drugs. The first agent with potent *in vitro* anti-MERS-CoV activity identified by this method was mycophenolic acid, an antirejection drug used in organ transplantation with broad-spectrum antiviral activities that acts by inhibiting IMP dehydrogenase and depleting the lymphocyte guanosine and deoxyguanosine nucleotide pools (209). The combination of mycophenolic acid and interferon beta 1b shows synergistic activity against MERS-CoV in Vero cells. The desirable pharmacokinetics of mycophenolic acid compared to ribavirin warrants further evaluation, although the potential inhibitory effect on the immune system and therefore neutralizing antibody production should be fully assessed in animal models before use in humans. The very low EC₅₀ compared with the peak serum level achieved at routine clinical dosages suggests that even a very low dose may be effective without inducing significant immunosuppression. A fatal case of MERS was reported in a renal transplant recipient who was receiving antirejection therapy consisting of prednisone, mycophenolate mofetil, and cyclosporine, but the dosage, serum drug level of mycophenolate mofetil, and resulting lymphocyte count were not reported (68, 175). Following the identification of mycophenolic acid as an inhibitor of MERS-CoV replication *in vitro*, many other drugs have been found to exhibit *in vitro* anti-MERS-CoV activity in Vero and/or Huh-7 cells using a similar drug discovery approach. These drugs belong to a number of major pharmacological categories, including peptidic or small-molecule HIV entry inhibitors, antiparasitics, antibacterials, and inhibitors of clathrin-mediated endocytosis, neurotransmitters, estrogen receptor, kinase signaling, lipid or sterol metabolism, protein processing, and DNA synthesis or repair (41, 176, 211–214). However, none of them has been tested in animal models for MERS, and many of them have doubtful clinical relevance in human infection because of unachievable peak serum levels in relation to their EC₅₀ against MERS-CoV. Two notable exceptions which warrant further evaluation in clinical trials are lopinavir and chloroquine. Lopinavir, which is routinely available as a lopinavir-ritonavir combination, shows inhibitory effects on MERS-CoV infection *in vitro* in Huh-7 cells at concentrations observed in blood during clinical use and has a well-established toxicity profile (212; http://www.hpa.org.uk/webc/HPAwebFile/HPAweb_C/1317139281416). Moreover, lopinavir-ritonavir has been used successfully in the treatment of SARS in a case-control study (215). Viremia resolved after 2 days of combinational lopinavir-ritonavir, pegylated interferon, and ribavirin therapy in a MERS patient (183). However, virus shedding in the airway was persistent despite treatment (183). Chloroquine is an antimalarial drug that inhibits MERS-CoV *in vitro* in Huh-7 and Vero E6 cells at a concentration achievable by standard clinical oral dosage through multiple possible mechanisms, including inhibition of the pH-sensitive cathepsin L-cell entry pathway through elevation of endosomal pH (211, 212, 216; http://www.hpa.org.uk/webc/HPAwebFile/HPAweb_C/1317139281416). However, previously chloroquine has not been shown to work in BALB/c mice infected by SARS-CoV, possibly due to the lack of inhibition of other cell entry pathways utilized by the virus (217).

The third approach to identify treatment for MERS requires the development of specific antiviral agents based on novel insights into the viral genome and structural biology of MERS-CoV (218, 219). Understandably, the development of such candidate drugs is more time-consuming than that in the first two approaches. However, these tailor-made antiviral agents represent the most specific and possibly most effective therapeutic options against MERS-CoV. Of particular interests are agents that target

the MERS-CoV S protein, which has essential roles in virus-host cell receptor interaction and immunogenicity. A number of potent monoclonal antibodies targeting different epitopes on the RBD in the S1 subunit of the MERS-CoV S protein have been identified by biopanning of ultralarge nonimmune human antibody libraries displayed in yeast or phage baited by the RBD (37–40). These monoclonal antibodies bind to the RBD with 10- to 450-fold-higher affinity than does the RBD to the human DPP4, conferring broader and higher neutralizing activity. The production of these monoclonal antibodies in high titers may help to overcome the potential cultural hurdle in collecting large amounts of convalescent-phase plasma from patients in the Middle East and the possibility of adverse outcomes associated with immune enhancement with low antibody titer previously observed in *in vitro* and animal experiments on SARS (220, 221). Moreover, possible selection of virus mutants capable of escaping from antibody-mediated neutralization may be mitigated by using divergent combinations of two or more synergistically acting neutralizing monoclonal antibodies that target non-cross-resistant epitopes on the RBD (40). *In vitro* inhibition of S protein-mediated cell-cell fusion and virus entry into host cell can also be achieved by specially designed antiviral peptides that span the sequence of the HR2 domain of the S2 subunit of the MERS-CoV S protein. Analogous to the HIV fusion inhibitor Enfuvirtide, which binds to glycoprotein 41 of HIV to block membrane fusion and virus entry, the MERS-CoV antiviral peptides block the fusion process of MERS-CoV by preventing the interaction between the HR1 and HR2 domains required for the formation of the heterologous six-helix bundle in viral fusion core formation (44, 45). Other drug candidates that target specific enzymes of MERS-CoV include inhibitors of viral proteases and helicase (222–225, 341). The rapid determination of crystal structure for these enzymes has facilitated the development of candidate drugs to be further tested in animal studies to evaluate their pharmacokinetics and to confirm their *in vivo* inhibitory effects, especially in view of the reported mutations in the papain-like protease of recently circulating MERS-CoV strains (146, 222–225). Inhibition of MERS-CoV infection can also be achieved by agents that target the functional host cell receptor DPP4. Because of the abundance of DPP4 in epithelial and endothelial cells, high titers of monoclonal antibodies against specific binding regions of DPP4, but not the commercially available reversible, competitive DPP4 antagonists such as sitagliptin, vildagliptin, and saxagliptin, efficiently inhibit virus-cell receptor interaction (46, 50). Agents that manipulate the levels of adenosine deaminase, a natural DPP4 antagonist, may also be considered (49). The clinical efficacy of anti-DPP4 monoclonal antibodies and adenosine deaminase analogues remains uncertain because expression of catalytically inactive DPP4 still allows for MERS-CoV infection *in vitro* (226). Furthermore, the risk of physiological disturbances, immunopathology, and T-cell suppression should be assessed in animal studies given the wide distribution of DPP4 in different human cell types and its multiple essential metabolic and immunological functions (227, 228). Alternatively, inhibitors of host cellular proteases, including furin, TMPRSS2, and cathepsins, which affect virus entry into host cells, may be considered. However, the recent finding that cathepsin activity is essential for Ebola virus infection in cell lines but not for viral spread and pathogenesis in mice highlights the necessity to confirm the roles of cellular protease inhibitors in *in vivo* spread of MERS-CoV (229, 230). Alternative host proteases that cleave the

MERS-CoV S protein should also be searched to broaden the range of existing antiviral options (51).

INFECTION CONTROL AND LABORATORY SAFETY

Similar to the case for epidemics caused by other novel emerging respiratory viruses with no herd immunity in the general population and limited effective treatment and immunization options, infection control measures to interrupt the chain of transmission remain the cornerstone to control the MERS epidemic (3, 4, 153, 231–233). Based on the available epidemiological data, the scenario is most compatible with a combination of animal-to-human and person-to-person transmission. In regions of endemicity, multisource sporadic animal-to-human transmissions occur in the community, which may be amplified under special circumstances such as the breeding seasons of dromedary camels. These primary infections may be followed by limited, nonsustained person-to-person transmission among unprotected household contacts (67, 70, 73). When the patients are hospitalized, the infection is introduced into the health care setting, where lapses in infection control measures culminate in large health care-associated outbreaks (66, 68, 71, 75, 234). The infection can then be disseminated beyond the Middle East by air travel of infected patients seeking medical care in countries where the disease is not endemic (150, 235, 236).

In the community setting, the primary goals of infection control are to identify and segregate all zoonotic reservoirs and infected humans from nonimmune persons. Besides dromedary camels, bats, and hedgehogs, other livestock species prevalent in the Middle East should be further surveyed by validated serological and virological tests to exclude unrecognized MERS-CoV infection. Before these data are available, residents in and travelers to the regions of endemicity should generally avoid contacting sick animals and especially camels. Contact with environments contaminated with animal bodily fluids, tissues, or feces should be avoided, as MERS-CoV may be transmitted via direct contact or fomite due to prolonged environmental survival, lasting for at least 48 h at 20°C in 40% relative humidity and 24 h at 30°C in 30% relative humidity (145, 237). Consumption of unpasteurized camel milk should be cautioned against, as MERS-CoV may possibly be shed and survive in the milk of camels with active nasal or fecal virus shedding (143, 144). Early recognition of human cases can be achieved by public education and dissemination of diagnostic tests to health care facilities. Testing should be performed even among asymptomatic or mildly symptomatic persons with known exposures to potential animal reservoirs or laboratory-confirmed human cases. They should also undergo medical surveillance and quarantine in health care facilities or at home until 14 days after the last day of exposure (http://www.who.int/csr/disease/coronavirus_infections/MERS_home_care.pdf; <http://www.cdc.gov/coronavirus/mers/downloads/MERS-Infection-Control-Guidance-051414.pdf>). Air travel should be restricted for laboratory-confirmed cases unless it is necessary to transfer the patient to another country for medical care. In such cases, compliance with infection control measures, including hand hygiene, wearing of personal protective equipment, and standard and transmission-based precautions should be applied by the aircraft staff and accompanying medical personnel. Though there is no documented in-flight transmission of MERS-CoV so far, the risk is estimated to be one new infection in a 5-h

flight in first class and 15 infections from a “superspreader” in a 13-hour flight in economy class (235). Temperature checks at borders and health declarations for travelers are used in some regions, but their value in controlling international spread is unproven. The Hajj, which attracts millions of pilgrims from over 180 countries to gather in Mecca every year, poses a theoretical risk of causing massive outbreaks of MERS, as in the superspreading events of SARS. Though MERS has not been reported among pilgrims attending the annual Hajj in 2012 and 2013, the small number of subjects tested and the lack of samples collected during the pilgrimage are major limitations of the few surveillance studies conducted so far (238–240). Thus, persons at risk of developing severe infection should consider postponing the Hajj until the epidemic is under control (241, 242).

In the hospital setting, triage, early diagnosis, compliance with appropriate infection control measures, prompt isolation of suspected cases, and timely contact tracing of case contacts are the key strategies to prevent nosocomial transmission. Indeed, the disappearance of the three clades of MERS-CoV found earlier in the epidemic suggests the possible effects of enhanced surveillance and early isolation of human cases in successfully interrupting person-to-person transmission (146). In addition to standard, contact, and droplet precautions, airborne precautions should be applied for aerosol-generating procedures such as intubation, noninvasive ventilation, manual ventilation before intubation, bronchoscopy, tracheostomy, and suctioning of the airway (243; http://www.who.int/csr/disease/coronavirus_infections/IPCnCoVguidance_06May13.pdf?ua=1). Designated health care workers and disposable equipment for managing laboratory-confirmed cases in adequately ventilated single rooms or airborne infection isolation rooms should be considered to limit the number of exposed contacts. All health care workers caring for patients with suspected or confirmed MERS should undergo medical surveillance for 14 days after the last day of exposure with daily temperature checks and monitoring of the development of acute respiratory symptoms. Health care workers with laboratory-confirmed MERS should be strictly excluded from patient care, as asymptomatic infection may serve as the source of nosocomial and community outbreaks (70, 342; http://www.who.int/csr/disease/coronavirus_infections/MERS_home_care.pdf; <http://www.cdc.gov/coronavirus/mers/downloads/MERS-Infection-Control-Guidance-051414.pdf>). For exposed health care workers, exclusion from work for the observation period should also be considered, as applied in the medical surveillance of other respiratory tract infections such as pandemic influenza A/H1N1/2009 and avian influenza A/H7N9 (244, 343; <http://www.cdc.gov/coronavirus/mers/downloads/MERS-Infection-Control-Guidance-051414.pdf>). Although it has been suggested that transmission-based precautions for MERS patients may be stopped 24 h after the resolution of symptoms, laboratory testing to exclude persistent virus shedding should be conducted, as viral RNA can be detected in the respiratory tract specimens and/or blood of critically ill patients for over 3 weeks after symptom onset (88, 175, 181, 183, 210). Rarely, asymptomatic cases may also have prolonged virus shedding for more than 5 weeks after case contact (245). The infectivity of such prolonged viral shedding should be further evaluated to optimize infection control strategies. Patients who have no evidence of pneumonia or who have recovered from pneumonia but remain positive for

MERS-CoV RNA by RT-PCR may be discharged from the hospital and isolated at home under appropriate supervision (246). Collection of potentially infectious specimens should be performed by trained staff wearing appropriate personal protective equipment. The specimens should be transported in leak-proof double containers by hand instead of by pneumatic-tube systems (http://www.who.int/csr/disease/coronavirus_infections/IPCnCoVguidance_06May13.pdf?ua=1). To prevent laboratory-related outbreaks as reported with SARS, all laboratories handling live MERS-CoV should strictly comply with WHO standards for BSL3 laboratories.

VACCINATION

Active Immunization

Active immunization to protect at-risk humans and camels is a research priority in the control of MERS because of the lack of herd immunity and effective antivirals for humans. Based on previous experience gained from vaccine design for SARS, which shows the S protein to be one of the major immunogenic components of CoVs, a number of vaccines that target the S protein of MERS-CoV are being developed and evaluated in cell culture or animal experiments (Table 11). A viral vector-based vaccine using recombinant modified vaccinia virus Ankara expressing full-length MERS-CoV S protein induced high levels of neutralizing antibodies in BALB/c mice after intramuscular immunization (247). The possibility of induction of immunopathology, as in the case of a similar viral vector-based vaccine for SARS that led to enhanced hepatitis in ferrets, needs to be carefully assessed in subsequent investigations (221). Alternatively, several candidate recombinant vaccines containing either full-length MERS-CoV S protein or the RBD of the S1 subunit have been studied for their theoretical advantages of safety and ease of consistent production based on constant conditions and well-defined immunogenic fragments. A baculovirus-based expression system and an approach with Venezuelan equine encephalitis virus replicon particles have been successfully applied for the development of full-length MERS-CoV S protein-based recombinant vaccines (173, 248). Identification and exclusion of nonneutralizing epitopes in the immunopredominant domain of the MERS-CoV S protein may help to reduce the risk of antibody-mediated disease enhancement during future optimization of these vaccines (249). RBD-based subunit vaccines have elicited neutralizing activity against MERS-CoV in cell culture-based assays, BALB/c mice, and rabbits (31, 34, 36, 42, 250). Among five different available RBD constructs, a truncated 212-amino-acid (aa) fragment at residues 377 to 588 of RBD fused with human IgG Fc fragment (S377-588-Fc) showed the highest DPP4-binding affinity and induced the highest titers of IgG and neutralizing antibodies in BALB/c mice and rabbits, respectively (36). Intranasal vaccination with this S377-588-Fc showed stronger systemic cellular and local mucosal responses than subcutaneous vaccination (43). Future research directions for these promising subunit vaccine candidates include the optimization of adjuvant substances which are required to increase the immunogenicity of subunit vaccines (251, 344) and the inclusion of chimeric S proteins containing multiple neutralizing epitopes from divergent subgroups, as there are considerable variations in the receptor-binding subdomain region of S1 within subgroups of MERS-CoV and across different CoV groups (201).

Passive Immunization

Passive immunization using convalescent-phase plasma or hyper-immune globulin with high titers of neutralizing antibody has been used for emerging respiratory viral infections, including SARS and pandemic influenza A/H1N1/2009, with relatively few side effects (252–255). The clinical use of such therapy for MERS has not yet been evaluated in randomized controlled trials. MERS-CoV-S-driven transduction in Caco-2 cells is inhibited by convalescent patient serum in a concentration-dependent manner (51). In BALB/c mice transduced by adenoviral vectors expressing human DPP4, adoptive transfer of sera containing anti-MERS-CoV-S antibodies blocked virus attachment and accelerated virus clearance (173). The increasing number of patients recovering from MERS and enhanced international collaboration for the preparation of convalescent-phase plasma samples will accelerate the availability of passive immunization before neutralizing monoclonal antibodies become commercially available.

ANIMAL MODELS AND ANIMALS SUSCEPTIBLE TO MERS-CoV

In contrast to the case for SARS-CoV, which can cause infection in a diverse range of susceptible mammalian species, studies on MERS-CoV have been limited by the lack of animal models which are representative of MERS in humans (Table 12). Koch's postulates for MERS-CoV as a causative agent of MERS were fulfilled with a primate model using rhesus macaques, which demonstrated mild to moderate clinical and histopathological features when compared to severe infection in humans (164). However, clinical signs varied between animals and were usually transient, lasting for only 3 days or less in most animals, which was consistent with the robust but self-limiting inflammatory response and leukocyte activation in blood and lungs of tested animals (165). Recently, common marmosets were also found to be susceptible to MERS-CoV infection, which resembled moderate to severe MERS in humans with viremia and disseminated infection as evidenced by the presence of viral RNA in blood and multiple organs (167). Nevertheless, extrapulmonary manifestations that are commonly seen in human cases of MERS, such as acute renal failure and diarrhea, were absent in both the rhesus macaque and common marmoset models. Jamaican fruit bats infected with MERS-CoV do not develop clinical signs of infection despite having respiratory and intestinal tract virus shedding up to day 9 postinfection (256). Large animals, including camels and goats, were also found to be susceptible to MERS-CoV infection, but they developed predominantly upper respiratory tract symptoms without pneumonia (256–258). Unlike human infection, in which feces and urine might be positive for viral RNA, the extrapulmonary specimens of infected camels and goats were negative. Most small animal models that worked for SARS-CoV, including the BALB/c mouse, Syrian hamster, and ferret, were not susceptible to MERS-CoV infection. Infected animals had minimal clinical signs, no detectable virus in respiratory tract and extrapulmonary specimens, and no seroconversion. These findings suggest that MERS-CoV fails to enter these host cells because of variable DPP4-binding affinities for MERS-CoV S RBD among different species (48). A mouse model using C57BL/6 and BALB/c mice with prior transduction of respiratory epithelial cells with adenoviral vectors expressing human DPP4 inoculated with MERS-CoV intranasally showed virological, immunological, and histopathological features compatible with interstitial pneumonia, but the clinical signs were mild and evidence of infection was confined to the lungs

TABLE 11 Active and passive immunization against MERS^a

Immunization type and vaccine	Vaccine components (virus strain)	Animal model (administration)	Main findings (animal model)	Reference(s)
Active				
MVA-MERS-S	Recombinant modified vaccinia virus Ankara expressing full-length MERS-CoV S protein (HCoV-EMC/2012)	BALB/c mice (2 i.m. immunizations at days 0 and 21)	High levels of NAb were induced	247
VRP-S	Venezuelan equine encephalitis virus replicon particles containing S protein of MERS-CoV (HCoV-EMC/2012)	Ad5-hDPP4-transduced BALB/c mice (2 immunizations in the footpads at days 0 and 28)	Reduction of viral titers to nearly undetectable levels by 1 day p.i.	173
Spike protein nanoparticles	Purified S protein nanoparticles produced in Sf9 cells infected with specific recombinant baculovirus cloned with MERS-CoV S protein gene sequence (Al-Hasa_1_2013)	BALB/c mice, 6–8 wk old (2 i.m. immunizations on days 0 and 21)	Induced NAb in mice receiving MERS-CoV S inoculation with adjuvant matrix M1 or alum but not in those receiving MERS-CoV S inoculation alone (matrix M1 > alum > no adjuvant); NAb levels were not significantly different between regimens consisting of 1 µg and 3 µg and between sera obtained on days 21 and 45	248
S-RBD-Fc	Recombinant protein containing RBD (residues 377–662) of S1 (HCoV-EMC/2012)	Mice (2 s.c. immunizations on days 0 and 14)	Sera of vaccinated mice showed neutralizing activity (>96%) against MERS-CoV pseudo- (Huh-7 cells) and live (Vero E6 cells) virus infection	41
358-588 S1-Fc	RBD (residues 358–588) of S1 fused with human IgG Fc fragment (HCoV-EMC/2012)	Vero cells (inoculation of sera containing polyclonal Ab raised in immunized rabbits)	Polyclonal antibodies against 358–588 S1-Fc variant efficiently neutralized virus infectivity	34
S377-588-Fc	Truncated 212-aa fragment of RBD (residues 377–588) of S1 fused with human IgG Fc fragment (HCoV-EMC/2012)	BALB/c mice, 6–8 wk old (3 s.c. immunizations)	Increased neutralizing IgG1 (Th2) and IgG2a (Th1) Ab responses specific for the RBD in the S1 subunit were induced after each immunization with Montanide ISA 51 adjuvant	31, 42
		BALB/c mice, 4–6 wk old (5 s.c. or i.n. immunizations at days 0, 21, and 42 and 3 and 6 mo)	Similar degree of systemic humoral immune responses, including NAb, and more robust systemic cellular and local (lung) mucosal immune responses compared to those induced by s.c. vaccination with Montanide ISA 51 adjuvant	43
		BALB/c mice, 6–8 wk old (3 s.c. immunizations), and rabbits (3 immunizations)	Among 5 versions of RBD fragments, the S377–588-Fc showed the highest RBD-binding affinity and induced the highest-titer IgG Ab in mice and NAb in rabbits	36
rRBD (combined with different adjuvants)	Recombinant RBD protein containing a 240-aa fragment of RBD (residues 367–606) of S1 (HCoV-EMC/2012) combined with different adjuvants [alum alone, alum plus CpG-ODNs, alum plus poly(I:C), or CpG-ODNs plus IFA]	BALB/c mice, 6–8 wk old (3 i.m. or s.c. immunizations at days 0, 21, and 42)	The combination of rRBD and alum plus CpG-ODNs given by the i.m. route provided the most robust RBD-specific humoral and cellular immunity	250
Passive				
Adoptive transfer of sera	Sera containing anti-MERS-CoV-S Ab (HCoV-EMC/2012)	Ad5-hDPP4-transduced BALB/c mice (sera obtained 2–4 wk after immunization with VRP-S, and transferred into mice i.p. 1 day before infection)	Adoptive transfer of sera containing anti-MERS-CoV S Ab blocked virus attachment and accelerated virus clearance to nearly undetectable levels by 5 days p.i.	173

^a Abbreviations: aa, amino acid; Ab, antibody; Ad5-hDPP4, adenoviral vectors expressing human dipeptidyl peptidase 4; alum, aluminum hydroxide; CpG-ODNs, cysteine-phosphate-guanine oligodeoxynucleotides; p.i., postinfection; IFA, incomplete Freund's adjuvant; i.m., intramuscular; i.n., intranasal; i.p., intraperitoneal; NAb, neutralizing antibody; poly(I:C), polyribonucleic acid; RBD, receptor-binding domain; s, spikes; s.c., subcutaneous; wk, week.

TABLE 12 Animals tested for susceptibility to MERS-CoV in experimental and natural infection^a

Animal species; age	Dose and route of inoculation (virus strain)	Time of evaluation (days)	Clinical, virological, and immunological findings	Histopathological and IHC results	Reference(s)
Susceptible					
Rhesus macaques (<i>Macaca mulatta</i>); 6–10 yr	7×10^6 TCID ₅₀ i.t., i.n., oral, and ocular (HCoV-EMC/2012)	Up to 6	Clinical: mild to moderate symptoms, including nasal swelling, piloerection, decreased bowel opening, increased or decreased respiratory rate, decreased food intake, and hunched posture at 1–6 days p.i.; leukocytosis with neutrophilia and lymphopenia at 1 day p.i. Virological: viral RNA detected in upper and lower respiratory tract specimens, conjunctiva, and lymphoid tissues (mediastinal and tonsils) from 1 day p.i. and in 1 macaque's urogenital swab at 1 day p.i. Immunological: significant upregulation of genes associated with proinflammatory process (IL-6, CXCL1, MMP9); rapid resolution of controlled interferon-mediated innate immune response.	Macroscopic: multifocal to coalescent, mild to marked interstitial pneumonia. Microscopic: thickening of alveolar septae by edema fluid and fibrin with predominantly macrophages; BOOP-like changes with multinucleate syncytia formed by alveolar macrophages, fibrin aggregates, and occluded small airways by sloughed pulmonary epithelium, and perivascular infiltrates of inflammatory cells; type II pneumocyte hyperplasia; hyaline membrane formation. IHC: viral Ag detected in type I and II pneumocytes and macrophages/monocytes or dendritic cells.	164, 165
Rhesus macaques (<i>Macaca mulatta</i>); 2–3 yr	6.5×10^7 TCID ₅₀ i.t. (HCoV-EMC/2012)	Up to 28	Clinical: fever and reduced water intake at 1–2 days p.i.; CXR showed varying degrees of localized infiltration and interstitial markings at 3–5 days p.i. Virological: viral RNA detected in lungs at 3 days p.i. Immunological: neutralizing Ab detected at 7 days p.i. and peaked at 14 days p.i.	Macroscopic: congestion and palpable nodules scattered in distribution. Microscopic: multifocal mild to moderate interstitial pneumonia and exudative changes in lungs. IHC: viral Ag detected in type I and II pneumocytes and alveolar macrophages.	166
Common marmosets (<i>Callithrix jacchus</i>); 2–6 yr	5.2×10^6 TCID ₅₀ i.t., i.n., oral, and ocular (HCoV-EMC/2012)	Up to 55	Clinical: moderate to severe symptoms, including increased respiratory rate, open mouth and/or labored breathing, frothy hemorrhagic discharge from mouth, decreased food intake, and decreased activity level since 1–3 days p.i. and peaking at 4–6 days p.i.; clinical scores returned to baseline by 13 days p.i.; 2/9 animals were euthanized because of severe disease; CXR showed varying degrees of interstitial infiltration at 3–4 days p.i. Virological: viral RNA detected in upper (since 1 day p.i.) and lower respiratory tract specimens, blood, and multiple organs (conjunctiva, lymph nodes, tonsils, kidneys, heart, adrenal glands, liver, spleen, pancreas, colon, ileum, frontal lobe, cerebellum, brain stem, urinary bladder, and testes) since 3 days p.i. Immunological: pulmonary fibrosis as evidenced by activation of pathways associated with chemotaxis and cell migration, cell cycle progression, cell proliferation, fibrogenesis, inflammation, endothelial activation, and tissue repair; upregulation of innate and adaptive immune genes; induction of type I IFNs, IL-2, IL-4, and IL-6; inhibition of type II IFNs, IL-1, and TNF- α .	Macroscopic: multifocal, extensive, severe lesions especially in lower lobes; lungs were firm, failed to collapse, and fluid filled. Microscopic: multifocal to coalescing, moderate to marked acute bronchointerstitial pneumonia centered on terminal bronchioles, with influx of neutrophils and macrophages; thickening of alveolar septa; edema, hemorrhage, and fibrin filled the alveolar spaces (3–4 days p.i.); type II pneumocyte hyperplasia and formation of hyaline membrane (6 days p.i.). IHC: viral Ag detected in affected areas, especially in type I pneumocytes and alveolar macrophages.	167
C57BL/6 and BALB/c mice with Ad5-hDPP4 transduction; 6–12 wk (young) and 18–22 mo (aged)	1×10^7 PFU i.n. (HCoV-EMC/2012)	Up to 14	Clinical: young BALB/c mice failed to gain wt, aged C57BL/6 and BALB/c mice lost wt. Virological: clearance of virus by 6–8 days p.i. in young mice and 10–14 in aged mice. Immunological: requirement of type I IFN induction and signaling, CD8 T cells, and Ab for virus clearance; low level of cross-reactivity between MERS-CoV and SARS-CoV.	Macroscopic: vascular congestion and inflammation. Microscopic: perivascular and peribronchial lymphoid infiltration initially, with progression to an interstitial pneumonia. IHC: viral Ag detected in lungs.	174
Transgenic mice with global expression of hDPP4; 6–7 wk	1×10^6 TCID ₅₀ i.n. (HCoV-EMC/2012)		Clinical: transgenic mice developed progressive wt loss, ruffled fur, lethargy, inactivity, and shallow breathing starting at 2 days p.i. The mortality at 6 days p.i. was 100%. Virological: infectious virus detected in lungs (up to 10^7 TCID ₅₀ /g at 2 days p.i.) and brain (up to 7×10^4 TCID ₅₀ /g at 4 days p.i.); viral RNA detected in lungs, brain, heart, spleen, and intestine. Immunological: elevated mRNA expressions of classic antiviral and proinflammatory cytokines/chemokines.	Macroscopic: red to dark-red discoloration and multifocal consolidation in lungs. Microscopic: moderate bronchointerstitial pneumonitis, multifocal perivascular infiltrates in terminal bronchioles and pulmonary parenchyma with macrophage and lymphocyte infiltration; minimal inflammatory reaction in brain. IHC: viral Ag detected in type I and II pneumocytes, brain microglia, astrocytes, and neuronal cells.	333

Dromedary camels (<i>Camelus dromedarius</i>); 2–5 yr (adults)	10^7 TCID ₅₀ i.t., i.n., and ocular (HCoV-EMC/2012)		Clinical: mild upper respiratory tract symptoms, including rhinorrhea and mild increased temp. Virological: infectious virus detected in nasal (up to 7 days p.i. and 10^6 PFU/ml) and oral (up to 5 days p.i. and 10^2 PFU/ml) swabs; viral RNA detected in nasal (up to 35 days p.i. and 10^6 TCID ₅₀ /ml) and oral (up to 35 days p.i. and 10^4 TCID ₅₀ /ml) swabs. Immunological: neutralizing Ab detected at 14 days p.i. and peaked at 35 days p.i.	258
Goats	NA	NA	Clinical: asymptomatic to mildly symptomatic. Immunological: seroconversion in all 14 goats by 14 days p.i.	257
Jamaican fruit bats	NA	NA	Clinical: no clinical signs or elevation in temp. Virological: virus shedding from respiratory and intestinal tracts for up to 9 days p.i.	256
Nonsusceptible Syrian hamsters (<i>Mesocricetus auratus</i>)	4×10^7 TCID ₅₀ aerosols, 10^3 TCID ₅₀ i.t., or 10^6 TCID ₅₀ i.t. (HCoV-EMC/2012)	Up to 21	Clinical: no significant wt loss or fever. Virological: no viral RNA detected in nasal, oropharyngeal, urogenital, and rectal swabs from 1–11 days p.i. and from lungs, spleen, and mandibular lymph nodes at 2, 4, and 8 days p.i. Immunological: no seroconversion.	327
BALB/c, 129/SvEv, and 129/SvEv STAT1 knockout mice; 8 wk	120 or 1,200 TCID ₅₀ i.n. (HCoV-EMC/2012)	Up to 9	Clinical: no significant wt loss. Virological: no detectable virus in lungs.	328
Ferrets (<i>Mustela putorius furo</i>)	1×10^6 TCID ₅₀ i.n. and i.t. (HCoV-EMC/2012)	Up to 14	Virological: no infectious virus was detected in nose and throat swabs. Immunological: no seroconversion.	49

^a Abbreviations: Ab, antibody; Ad5-hDPP4, adenoviral vectors expressing human dipeptidyl peptidase 4; Ag, antigen; BOOP, bronchiolitis obliterans organizing pneumonia; CXCL1, chemokine C-X-C ligand 1; IFN, interferon; IHC, immunohistochemistry; IL, interleukin; i.n., intranasal; i.t., intratracheal; MMP9, matrix metalloproteinase 9; NA, not available; p.i., postinoculation; S, spike; TCID₅₀, 50% tissue culture infectious dose; temp, temperature; wt, weight.

without extrapulmonary involvement (173). Furthermore, this model requires infection of the mice with the adenoviral vectors prior to every experiment, and it is unknown whether the differences in the targeted cells between the murine and human lungs may affect the immunological response and clinical progress after infection. Nonetheless, this inhaled adenoviral vector method allows the quick use of a wide variety of preexisting genetically modulated mice with immunodeficiencies to dissect the elements of host responses to MERS-CoV and can be used to test candidate drugs and vaccines *in vivo*. It also provides a rapid model for any novel emerging respiratory viruses before appropriate receptor-transgenic mouse models become available. More recently, a small animal model using transgenic mice that globally express human DPP4 has been established (333). The transgenic mice developed severe infection that closely resembled severe human MERS cases. Further characterization and expansion of this transgenic mouse colony will facilitate the evaluation of candidate therapeutic and immunization options for MERS with *in vitro* activity.

CONCLUSIONS

In contrast to the public health chaos in the early phase of the SARS outbreak, the global health community has demonstrated efficient and collaborative efforts to handle the MERS epidemic. The clinical experience gained with SARS and the genomic data accumulated for other human and animal CoVs discovered after SARS have facilitated the rapid development of diagnostic assays, design of candidate antiviral agents and vaccines, rationalization of infection control measures, and identification of zoonotic reservoirs for MERS (93, 104–107, 259–270). The MERS epidemic has greatly enhanced our understanding of coronavirology and provided lessons that will be useful for tackling future CoV outbreaks. Camels are now recognized as an important animal reservoir for lineage A and C βCoVs and other viruses (140, 271, 272). Continued surveillance of novel CoVs among different animal species, especially bats and mammals with frequent close contact with humans, will strengthen our preparedness to face other emerging CoVs resulting from interspecies transmissions in the future. The identification of DPP4 as a functional receptor of MERS-CoV has expanded the list of membrane ectopeptidases known to be targeted by CoVs and has increased our understanding of the pathogenesis of CoV infections. Finally, the newly identified antiviral agents in drug-repurposing programs for MERS represent additional drug candidates that can be evaluated for novel CoVs that lack specific treatment options. Looking ahead, the successful control of the expanding MERS epidemic will depend on the development of an effective camel vaccine to stop ongoing camel-to-human transmissions, compliance with infection control measures, and timely contact tracing to prevent secondary health care-associated outbreaks. The key research priorities to optimize the clinical outcomes of MERS include more in-depth understanding of the pathogenesis from postmortem studies and serial patient samples, testing of antiviral and vaccine candidates in more representative small animal models, and evaluation of the efficacy of currently available therapeutic options in randomized controlled trials in humans. Monitoring of the molecular evolution of MERS-CoV will facilitate early recognition of further viral adaptations for efficient person-to-person transmission.

ACKNOWLEDGMENTS

We thank Patrick Lane of ScEYence Studios for graphic enhancement. We are grateful to Hayes Luk for technical assistance and to Siddharth Sridhar for proofreading the work.

This work is partly supported by the donations of the Hui Hoy and Chow Sin Lan Charity Fund Limited, the National Natural Science Foundation of China/Research Grants Council Joint Research Scheme (project code N_HKU728/14), the Consultancy Service for Enhancing Laboratory Surveillance of Emerging Infectious Disease of the Department of Health, and the Research Fund for the Control of Infectious Diseases commissioned grant, the Food and Health Bureau, Hong Kong Special Administrative Region, China.

REFERENCES

- Chan JF, To KK, Tse H, Jin DY, Yuen KY. 2013. Interspecies transmission and emergence of novel viruses: lessons from bats and birds. *Trends Microbiol* 21:544–555. <http://dx.doi.org/10.1016/j.tim.2013.05.005>.
- Peiris JS, Lai ST, Poon LL, Guan Y, Yam LY, Lim W, Nicholls J, Yee WK, Yan WW, Cheung MT, Cheng VC, Chan KH, Tsang DN, Yung RW, Ng TK, Yuen KY. 2003. Coronavirus as a possible cause of severe acute respiratory syndrome. *Lancet* 361:1319–1325. [http://dx.doi.org/10.1016/S0140-6736\(03\)13077-2](http://dx.doi.org/10.1016/S0140-6736(03)13077-2).
- Cheng VC, Lau SK, Woo PC, Yuen KY. 2007. Severe acute respiratory syndrome coronavirus as an agent of emerging and reemerging infection. *Clin Microbiol Rev* 20:660–694. <http://dx.doi.org/10.1128/CMR.00023-07>.
- To KK, Chan JF, Chen H, Li L, Yuen KY. 2013. The emergence of influenza A H7N9 in human beings 16 years after influenza A H5N1: a tale of two cities. *Lancet Infect Dis* 13:809–821. [http://dx.doi.org/10.1016/S1473-3099\(13\)0167-1](http://dx.doi.org/10.1016/S1473-3099(13)0167-1).
- Yuen KY, Chan PK, Peiris M, Tsang DN, Que TL, Shortridge KF, Cheung PT, To WK, Ho ET, Sung R, Cheng AF. 1998. Clinical features and rapid viral diagnosis of human disease associated with avian influenza A H5N1 virus. *Lancet* 351:467–471. [http://dx.doi.org/10.1016/S0140-6736\(98\)01182-9](http://dx.doi.org/10.1016/S0140-6736(98)01182-9).
- MacNeil A, Rollin PE. 2012. Ebola and Marburg hemorrhagic fevers: neglected tropical diseases? *PLoS Negl Trop Dis* 6:e1546. <http://dx.doi.org/10.1371/journal.pntd.0001546>.
- Marsh GA, Wang LF. 2012. Hendra and Nipah viruses: why are they so deadly? *Curr Opin Virol* 2:242–247. <http://dx.doi.org/10.1016/j.coviro.2012.03.006>.
- To KK, Ng KH, Que TL, Chan JM, Tsang KY, Tsang AK, Chen H, Yuen KY. 2012. Avian influenza A H5N1 virus: a continuous threat to humans. *Emerg Microbes Infect* 1:e25. <http://dx.doi.org/10.1038/emi.2012.24>.
- Zaki AM, van Boheemen S, Bestebroer TM, Osterhaus AD, Fouchier RA. 2012. Isolation of a novel coronavirus from a man with pneumonia in Saudi Arabia. *N Engl J Med* 367:1814–1820. <http://dx.doi.org/10.1056/NEJMoa1211721>.
- Chan JF, Li KS, To KK, Cheng VC, Chen H, Yuen KY. 2012. Is the discovery of the novel human betacoronavirus 2c EMC/2012 (HCoV-EMC) the beginning of another SARS-like pandemic? *J Infect* 65:477–489. <http://dx.doi.org/10.1016/j.jinf.2012.10.002>.
- Chan JF, Lau SK, Woo PC. 2013. The emerging novel Middle East respiratory syndrome coronavirus: the “knowns” and “unknowns.” *J Formos Med Assoc* 112:372–381. <http://dx.doi.org/10.1016/j.jfma.2013.05.010>.
- Woo PC, Lau SK, Yuen KY. 2006. Infectious diseases emerging from Chinese wet-markets: zoonotic origins of severe respiratory viral infections. *Curr Opin Infect Dis* 19:401–407. <http://dx.doi.org/10.1097/01.qco.0000244043.08264.fc>.
- Qiao PC, Wang M, Lau SK, Xu H, Poon RW, Guo R, Wong BH, Gao K, Tsoi HW, Huang Y, Li KS, Lam CS, Chan KH, Zheng BJ, Yuen KY. 2007. Comparative analysis of twelve genomes of three novel group 2c and group 2d coronaviruses reveals unique group and subgroup features. *J Virol* 81:1574–1585. <http://dx.doi.org/10.1128/JVI.02182-06>.
- Woo PC, Lau SK, Li KS, Poon RW, Wong BH, Tsoi HW, Yip BC, Huang Y, Chan KH, Yuen KY. 2006. Molecular diversity of coronaviruses in bats. *Virology* 351:180–187. <http://dx.doi.org/10.1016/j.virol.2006.02.041>.
- Woo PC, Lau SK, Huang Y, Yuen KY. 2009. Coronavirus diversity, phylogeny and interspecies jumping. *Exp Biol Med* (Maywood) 234:1117–1127. <http://dx.doi.org/10.3181/0903-MR-94>.
- van Boheemen S, de Graaf M, Lauber C, Bestebroer TM, Raj VS, Zaki AM, Osterhaus AD, Haagmans BL, Gorbalenya AE, Snijder EJ, Fouchier RA. 2012. Genomic characterization of a newly discovered coronavirus associated with acute respiratory distress syndrome in humans. *mBio* 3(6):e00473–12. <http://dx.doi.org/10.1128/mBio.00473-12>.
- de Groot RJ, Baker SC, Baric RS, Brown CS, Drosten C, Enjuanes L, Fouchier RA, Galiano M, Gorbalenya AE, Memish ZA, Perlman S, Poon LL, Snijder EJ, Stephens GM, Woo PC, Zaki AM, Zambon M, Ziebuhr J. 2013. Middle East respiratory syndrome coronavirus (MERS-CoV): announcement of the Coronavirus Study Group. *J Virol* 87:7790–7792. <http://dx.doi.org/10.1128/JVI.01244-13>.
- Bermingham A, Chand MA, Brown CS, Aarons E, Tong C, Langrish C, Hoschler K, Brown K, Galiano M, Myers R, Pebody RG, Green HK, Boddington NL, Gopal R, Price N, Newsholme W, Drosten C, Fouchier RA, Zambon M. 2012. Severe respiratory illness caused by a novel coronavirus, in a patient transferred to the United Kingdom from the Middle East, September 2012. *Euro Surveill* 17(40):pii=20290. <http://www.eurosurveillance.org/ViewArticle.aspx?ArticleId=20290>.
- Pollack MP, Pringle C, Madoff LC, Memish ZA. 2013. Latest outbreak news from ProMED-mail: novel coronavirus—Middle East. *Int J Infect Dis* 17:e143–144. <http://dx.doi.org/10.1016/j.ijid.2012.12.001>.
- Cotten M, Lam TT, Watson SJ, Palser AL, Petrova V, Grant P, Pybus OG, Rambaut A, Guan Y, Pillay D, Kellam P, Nastouli E. 2013. Full-genome deep sequencing and phylogenetic analysis of novel human betacoronavirus. *Emerg Infect Dis* 19:736–742B.
- Woo PC, Lau SK, Li KS, Tsang AK, Yuen KY. 2012. Genetic relatedness of the novel human group C betacoronavirus to *Tylonycteris* bat coronavirus HKU4 and *Pipistrellus* bat coronavirus HKU5. *Emerg Microbes Infect* 1:e35. <http://dx.doi.org/10.1038/emi.2012.45>.
- Frey KG, Redden CL, Bishop-Lilly KA, Johnson R, Hensley LE, Raviprakash K, Luke T, Kochel T, Mokashi VP, Defang GN. 2014. Full-genome sequence of human betacoronavirus 2c jordan-n3/2012 after serial passage in mammalian cells. *Genome Announc* 2(3):e00324–14. <http://dx.doi.org/10.1128/genomeA.00324-14>.
- Qian Z, Dominguez SR, Holmes KV. 2013. Role of the spike glycoprotein of human Middle East respiratory syndrome coronavirus (MERS-CoV) in virus entry and syncytia formation. *PLoS One* 8:e76469. <http://dx.doi.org/10.1371/journal.pone.0076469>.
- Yang Y, Zhang L, Geng H, Deng Y, Huang B, Guo Y, Zhao Z, Tan W. 2013. The structural and accessory proteins M, ORF 4a, ORF 4b, and ORF 5 of Middle East respiratory syndrome coronavirus (MERS-CoV) are potent interferon antagonists. *Protein Cell* 4:951–961. <http://dx.doi.org/10.1007/s13238-013-3096-8>.
- Siu KL, Yeung ML, Kok KH, Yuen KS, Kew C, Lui PY, Chan CP, Tse H, Woo PC, Yuen KY, Jin DY. 2014. Middle East respiratory syndrome coronavirus 4a protein is a double-stranded RNA-binding protein that suppresses PACT-induced activation of RIG-I and MDA5 in the innate antiviral response. *J Virol* 88:4866–4876. <http://dx.doi.org/10.1128/JVI.03649-13>.
- Matthews KL, Coleman CM, van der Meer Y, Snijder EJ, Frieman MB. 2014. The ORF4b-encoded accessory proteins of Middle East respiratory syndrome coronavirus and two related bat coronaviruses localize to the nucleus and inhibit innate immune signalling. *J Gen Virol* 95:874–882. <http://dx.doi.org/10.1099/vir.0.062059-0>.
- Niemeyer D, Zillinger T, Muth D, Ziebeck F, Horvath G, Suliman T, Barchet W, Weber F, Drosten C, Muller MA. 2013. Middle East respiratory syndrome coronavirus accessory protein 4a is a type I interferon antagonist. *J Virol* 87:12489–12495. <http://dx.doi.org/10.1128/JVI.01845-13>.
- Yang X, Chen X, Bian G, Tu J, Xing Y, Wang Y, Chen Z. 2014. Proteolytic processing, deubiquitinase and interferon antagonist activities of Middle East respiratory syndrome coronavirus papain-like protease. *J Gen Virol* 95:614–626. <http://dx.doi.org/10.1099/vir.0.059014-0>.
- Chen Y, Rajashankar KR, Yang Y, Agnihothram SS, Liu C, Lin YL, Baric RS, Li F. 2013. Crystal structure of the receptor-binding domain from newly emerged Middle East respiratory syndrome coronavirus. *J Virol* 87:10777–10783. <http://dx.doi.org/10.1128/JVI.01756-13>.
- Lu G, Hu Y, Wang Q, Qi J, Gao F, Li Y, Zhang Y, Zhang W, Yuan Y, Bao J, Zhang B, Shi Y, Yan J, Gao GF. 2013. Molecular basis of binding between novel human coronavirus MERS-CoV and its receptor CD26. *Nature* 500:227–231. <http://dx.doi.org/10.1038/nature12328>.
- Du L, Zhao G, Kou Z, Ma C, Sun S, Poon VK, Lu L, Wang L, Debnath

- AK, Zheng BJ, Zhou Y, Jiang S. 2013. Identification of a receptor-binding domain in the S protein of the novel human coronavirus Middle East respiratory syndrome coronavirus as an essential target for vaccine development. *J Virol* 87:9939–9942. <http://dx.doi.org/10.1128/JVI.01048-13>.
32. Jiang S, Lu L, Du L, Debnath AK. 2013. A predicted receptor-binding and critical neutralizing domain in S protein of the novel human coronavirus HCoV-EMC. *J Infect* 66:464–466. <http://dx.doi.org/10.1016/j.jinf.2012.12.003>.
 33. Jiang S, Lu L, Du L, Debnath AK. 2013. Putative conformations of the receptor-binding domain in S protein of hCoV-EMC in complex with its receptor dipeptidyl peptidase-4. *J Infect* 67:156–158. <http://dx.doi.org/10.1016/j.jinf.2013.04.007>.
 34. Mou H, Raj VS, van Kuppeveld FJ, Rottier PJ, Haagmans BL, Bosch BJ. 2013. The receptor binding domain of the new Middle East respiratory syndrome coronavirus maps to a 231-residue region in the spike protein that efficiently elicits neutralizing antibodies. *J Virol* 87:9379–9383. <http://dx.doi.org/10.1128/JVI.01277-13>.
 35. Wang N, Shi X, Jiang L, Zhang S, Wang D, Tong P, Guo D, Fu L, Cui Y, Liu X, Arledge KC, Chen YH, Zhang L, Wang X. 2013. Structure of MERS-CoV spike receptor-binding domain complexed with human receptor DPP4. *Cell Res* 23:986–993. <http://dx.doi.org/10.1038/cr.2013.92>.
 36. Ma C, Wang L, Tao X, Zhang N, Yang Y, Tseng CT, Li F, Zhou Y, Jiang S, Du L. 2014. Searching for an ideal vaccine candidate among different MERS coronavirus receptor-binding fragments. The importance of immunofocusing in subunit vaccine design. *Vaccine* 32:6170–6176. <http://dx.doi.org/10.1016/j.vaccine.2014.08.086>.
 37. Du L, Zhao G, Yang Y, Qiu H, Wang L, Kou Z, Tao X, Yu H, Sun S, Tseng CT, Jiang S, Li F, Zhou Y. 2014. A conformation-dependent neutralizing monoclonal antibody specifically targeting receptor-binding domain in middle East respiratory syndrome coronavirus spike protein. *J Virol* 88:7045–7053. <http://dx.doi.org/10.1128/JVI.00433-14>.
 38. Ying T, Du L, Ju TW, Prabakaran P, Lau CC, Lu L, Liu Q, Wang L, Feng Y, Wang Y, Zheng BJ, Yuen KY, Jiang S, Dimitrov DS. 2014. Exceptionally potent neutralization of Middle East respiratory syndrome coronavirus by human monoclonal antibodies. *J Virol* 88:7796–7805. <http://dx.doi.org/10.1128/JVI.00912-14>.
 39. Jiang L, Wang N, Zuo T, Shi X, Poon KM, Wu Y, Gao F, Li D, Wang R, Guo J, Fu L, Yuen KY, Zheng BJ, Wang X, Zhang L. 2014. Potent neutralization of MERS-CoV by human neutralizing monoclonal antibodies to the viral spike glycoprotein. *Sci Transl Med* 6:234ra259. <http://dx.doi.org/10.1126/scitranslmed.3008140>.
 40. Tang XC, Agnihothram SS, Jiao Y, Stanhope J, Graham RL, Peterson EC, Avnir Y, Tallarico AS, Sheehan J, Zhu Q, Baric RS, Marasco WA. 2014. Identification of human neutralizing antibodies against MERS-CoV and their role in virus adaptive evolution. *Proc Natl Acad Sci U S A* 111:E2018–E2026. <http://dx.doi.org/10.1073/pnas.1402074111>.
 41. Zhao G, Du L, Ma C, Li Y, Li L, Poon VK, Wang L, Yu F, Zheng BJ, Jiang S, Zhou Y. 2013. A safe and convenient pseudovirus-based inhibition assay to detect neutralizing antibodies and screen for viral entry inhibitors against the novel human coronavirus MERS-CoV. *Virol J* 10:266. <http://dx.doi.org/10.1186/1743-422X-10-266>.
 42. Du L, Kou Z, Ma C, Tao X, Wang L, Zhao G, Chen Y, Yu F, Tseng CT, Zhou Y, Jiang S. 2013. A truncated receptor-binding domain of MERS-CoV spike protein potentially inhibits MERS-CoV infection and induces strong neutralizing antibody responses: implication for developing therapeutics and vaccines. *PLoS One* 8:e81587. <http://dx.doi.org/10.1371/journal.pone.0081587>.
 43. Ma C, Li Y, Wang L, Zhao G, Tao X, Tseng CT, Zhou Y, Du L, Jiang S. 2014. Intranasal vaccination with recombinant receptor-binding domain of MERS-CoV spike protein induces much stronger local mucosal immune responses than subcutaneous immunization: implication for designing novel mucosal MERS vaccines. *Vaccine* 32:2100–2108. <http://dx.doi.org/10.1016/j.vaccine.2014.02.004>.
 44. Lu L, Liu Q, Zhu Y, Chan KH, Qin L, Li Y, Wang Q, Chan JF, Du L, Yu F, Ma C, Ye S, Yuen KY, Zhang R, Jiang S. 2014. Structure-based discovery of Middle East respiratory syndrome coronavirus fusion inhibitor. *Nat Commun* 5:3067. <http://dx.doi.org/10.1038/ncomms4067>.
 45. Gao J, Lu G, Qi J, Li Y, Wu Y, Deng Y, Geng H, Li H, Wang Q, Xiao H, Tan W, Yan J, Gao GF. 2013. Structure of the fusion core and inhibition of fusion by a heptad repeat peptide derived from the S protein of Middle East respiratory syndrome coronavirus. *J Virol* 87:13134–13140. <http://dx.doi.org/10.1128/JVI.02433-13>.
 46. Raj VS, Mou H, Smits SL, Dekkers DH, Muller MA, Dijkman R, Muth D, Demmers JA, Zaki A, Fouchier RA, Thiel V, Drosten C, Rottier PJ, Osterhaus AD, Bosch BJ, Haagmans BL. 2013. Dipeptidyl peptidase 4 is a functional receptor for the emerging human coronavirus-EMC. *Nature* 495:251–254. <http://dx.doi.org/10.1038/nature12005>.
 47. Lambeir AM, Durinx C, Scharpe S, De Meester I. 2003. Dipeptidyl-peptidase IV from bench to bedside: an update on structural properties, functions, and clinical aspects of the enzyme DPP IV. *Crit Rev Clin Lab Sci* 40:209–294. <http://dx.doi.org/10.1080/713609354>.
 48. van Doremalen N, Miazgowicz KL, Milne-Price S, Bushmaker T, Robertson S, Scott D, Kinne J, McLellan JS, Zhu J, Munster VJ. 2014. Host species restriction of Middle East respiratory syndrome coronavirus through its receptor dipeptidyl peptidase 4. *J Virol* 88:9220–9232. <http://dx.doi.org/10.1128/JVI.00676-14>.
 49. Raj VS, Smits SL, Procvacia LB, van den Brand JM, Wiersma L, Ouwendijk WJ, Bestebroer TM, Spronken MI, van Amerongen G, Rottier PJ, Fouchier RA, Bosch BJ, Osterhaus AD, Haagmans BL. 2014. Adenosine deaminase acts as a natural antagonist for dipeptidyl peptidase 4-mediated entry of the Middle East respiratory syndrome coronavirus. *J Virol* 88:1834–1838. <http://dx.doi.org/10.1128/JVI.02935-13>.
 50. Ohnuma K, Haagmans BL, Hatano R, Raj VS, Mou H, Iwata S, Dang NH, Bosch BJ, Morimoto C. 2013. Inhibition of Middle East respiratory syndrome coronavirus infection by anti-CD26 monoclonal antibody. *J Virol* 87:13892–13899. <http://dx.doi.org/10.1128/JVI.02448-13>.
 51. Gierer S, Bertram S, Kaup F, Wrensch F, Heurich A, Kramer-Kuhl A, Welsch K, Winkler M, Meyer B, Drosten C, Dittmer U, von Hahn T, Simmons G, Hofmann H, Pohlmann S. 2013. The spike protein of the emerging betacoronavirus EMC uses a novel coronavirus receptor for entry, can be activated by TMPRSS2, and is targeted by neutralizing antibodies. *J Virol* 87:5502–5511. <http://dx.doi.org/10.1128/JVI.00128-13>.
 52. Shirato K, Kawase M, Matsuyama S. 2013. Middle East respiratory syndrome coronavirus infection mediated by the transmembrane serine protease TMPRSS2. *J Virol* 87:12552–12561. <http://dx.doi.org/10.1128/JVI.01890-13>.
 53. Gierer S, Muller MA, Heurich A, Ritz D, Springstein B, Karsten CB, Schendzielorz A, Gnirss K, Drosten C, Pohlmann S. 23 July 2014. Inhibition of proprotein convertases abrogates processing of the MERS-coronavirus spike protein in infected cells but does not reduce viral infectivity. *J Infect Dis* <http://dx.doi.org/10.1093/infdis/jiu407>.
 54. Millet JK, Whittaker GR. 2014. Host cell entry of Middle East respiratory syndrome coronavirus after two-step, furin-mediated activation of the spike protein. *Proc Natl Acad Sci U S A* 111:15214–15219. <http://dx.doi.org/10.1073/pnas.1407087111>.
 55. Thomas G. 2002. Furin at the cutting edge: from protein traffic to embryogenesis and disease. *Nat Rev Mol Cell Biol* 3:753–766. <http://dx.doi.org/10.1038/nrm934>.
 56. Hallenberger S, Bosch V, Anglikar H, Shaw E, Klenk HD, Garten W. 1992. Inhibition of furin-mediated cleavage activation of HIV-1 glycoprotein gp160. *Nature* 360:358–361. <http://dx.doi.org/10.1038/360358a0>.
 57. Shiryaev SA, Remacle AG, Ratnikov BI, Nelson NA, Savinov AY, Wei G, Bottini M, Rega MF, Parent A, Desjardins R, Fugere M, Day R, Sabet M, Pellicchia M, Liddington RC, Smith JW, Mustelin T, Guiney DG, Lebl M, Strongin AY. 2007. Targeting host cell furin proprotein convertases as a therapeutic strategy against bacterial toxins and viral pathogens. *J Biol Chem* 282:20847–20853. <http://dx.doi.org/10.1074/jbc.M703847200>.
 58. de Wilde AH, Raj VS, Oudshoorn D, Bestebroer TM, van Nieuwkoop S, Limpens RW, Posthuma CC, van der Meer Y, Barcena M, Haagmans BL, Snijder EJ, van den Hoogen BG. 2013. MERS-coronavirus replication induces severe in vitro cytopathology and is strongly inhibited by cyclosporin A or interferon-alpha treatment. *J Gen Virol* 94:1749–1760. <http://dx.doi.org/10.1099/vir.0.052910-0>.
 59. Lu L, Liu Q, Du L, Jiang S. 2013. Middle East respiratory syndrome coronavirus (MERS-CoV): challenges in identifying its source and controlling its spread. *Microbes Infect* 15:625–629. <http://dx.doi.org/10.1016/j.micinf.2013.06.003>.
 60. Lei J, Mesters JR, Drosten C, Anemuller S, Ma Q, Hilgenfeld R. 2014. Crystal structure of the papain-like protease of MERS coronavirus reveals unusual, potentially druggable active-site features. *Antiviral Res* 109C:72–82. <http://dx.doi.org/10.1016/j.antiviral.2014.06.011>.
 61. Stadler K, Masignani V, Eickmann M, Becker S, Abrignani S, Klenk HD, Rappuoli R. 2003. SARS—beginning to understand a new virus. *Nat Rev Microbiol* 1:209–218. <http://dx.doi.org/10.1038/nrmicro775>.
 62. Corman VM, Muller MA, Costabel U, Timm J, Binger T, Meyer B,

- Kreher P, Lattwein E, Eschbach-Bludau M, Nitsche A, Bleicker T, Landt O, Schweiger B, Drexler JF, Osterhaus AD, Haagmans BL, Dittmer U, Bonin F, Wolff T, Drosten C. 2012. Assays for laboratory confirmation of novel human coronavirus (hCoV-EMC) infections. *Euro Surveill* 17(49):pii=20334. <http://www.eurosurveillance.org/ViewArticle.aspx?ArticleId=20334>.
63. Assiri A, Al-Tawfiq JA, Al-Rabeeh AA, Al-Rabiah FA, Al-Hajjar S, Al-Barrak A, Flemban H, Al-Nassir WN, Balkhy HH, Al-Hakeem RF, Makhdoom HQ, Zumla AI, Memish ZA. 2013. Epidemiological, demographic, and clinical characteristics of 47 cases of Middle East respiratory syndrome coronavirus disease from Saudi Arabia: a descriptive study. *Lancet Infect Dis* 13:752–761. [http://dx.doi.org/10.1016/S1473-3099\(13\)70204-4](http://dx.doi.org/10.1016/S1473-3099(13)70204-4).
 64. Albarrak AM, Stephens GM, Hewson R, Memish ZA. 2012. Recovery from severe novel coronavirus infection. *Saudi Med J* 33:1265–1269.
 65. Memish ZA, Zumla AI, Assiri A. 2013. Middle East respiratory syndrome coronavirus infections in health care workers. *N Engl J Med* 369:884–886. <http://dx.doi.org/10.1056/NEJMc1308698>.
 66. Al-Abdallat MM, Payne DC, Alqasrawi S, Rha B, Tohme RA, Abedi GR, Al Nsour M, Iblan I, Jarour N, Farag NH, Haddadin A, Al-Sanouri T, Tamin A, Harcourt JL, Kuhar DT, Swerdlow DL, Erdman DD, Pallansch MA, Haynes LM, Gerber SI. 2014. Hospital-associated outbreak of middle East respiratory syndrome coronavirus: a serologic, epidemiologic, and clinical description. *Clin Infect Dis* 59:1225–1233. <http://dx.doi.org/10.1093/cid/ciu359>.
 67. Memish ZA, Zumla AI, Al-Hakeem RF, Al-Rabeeh AA, Stephens GM. 2013. Family cluster of Middle East respiratory syndrome coronavirus infections. *N Engl J Med* 368:2487–2494. <http://dx.doi.org/10.1056/NEJMoa1303729>.
 68. Mailles A, Blanckaert K, Chaud P, van der Werf S, Lina B, Caro V, Campese C, Guery B, Prouvost H, Lemaire X, Paty MC, Haeghebaert S, Antoine D, Ettahar N, Noel H, Behillil S, Hendrickx S, Manuguerra JC, Enouf V, La Ruche G, Semaille C, Coignard B, Levy-Bruhl D, Weber F, Saura C, Che D. 2013. First cases of Middle East respiratory syndrome coronavirus (MERS-CoV) infections in France, investigations and implications for the prevention of human-to-human transmission, France, May 2013. *Euro Surveill* 18(24):pii=20502. <http://www.eurosurveillance.org/ViewArticle.aspx?ArticleId=20502>.
 69. Guberina H, Witzke O, Timm J, Dittmer U, Muller MA, Drosten C, Bonin F. 2014. A patient with severe respiratory failure caused by novel human coronavirus. *Infection* 42:203–206. <http://dx.doi.org/10.1007/s15010-013-0509-9>.
 70. Omrani AS, Matin MA, Haddad Q, Al-Nakhli D, Memish ZA, Albarrak AM. 2013. A family cluster of Middle East respiratory syndrome coronavirus infections related to a likely unrecognized asymptomatic or mild case. *Int J Infect Dis* 17:e668–672. <http://dx.doi.org/10.1016/j.ijid.2013.07.001>.
 71. Guery B, Poissy J, el Mansouf L, Sejourne C, Ettahar N, Lemaire X, Vuotto F, Goffard A, Behillil S, Enouf V, Caro V, Mailles A, Che D, Manuguerra JC, Mathieu D, Fontanet A, van der Werf S. 2013. Clinical features and viral diagnosis of two cases of infection with Middle East respiratory syndrome coronavirus: a report of nosocomial transmission. *Lancet* 381:2265–2272. [http://dx.doi.org/10.1016/S0140-6736\(13\)60982-4](http://dx.doi.org/10.1016/S0140-6736(13)60982-4).
 72. Drosten C, Seilmaier M, Corman VM, Hartmann W, Scheible G, Sack S, Guggemos W, Kallies R, Muth D, Junglen S, Muller MA, Haas W, Guberina H, Rohnisch T, Schmid-Wendtner M, Aldabbagh S, Dittmer U, Gold H, Graf P, Bonin F, Rambaut A, Wendtner CM. 2013. Clinical features and virological analysis of a case of Middle East respiratory syndrome coronavirus infection. *Lancet Infect Dis* 13:745–751. [http://dx.doi.org/10.1016/S1473-3099\(13\)70154-3](http://dx.doi.org/10.1016/S1473-3099(13)70154-3).
 73. Health Protection Agency (HPA) UK Novel Coronavirus Investigation Team. 2013. Evidence of person-to-person transmission within a family cluster of novel coronavirus infections, United Kingdom, February 2013. *Euro Surveill* 18(11):pii=20427. <http://www.eurosurveillance.org/ViewArticle.aspx?ArticleId=20427>.
 74. Abroug F, Slim A, Ouane-Besbes L, Hadj Kacem MA, Dachraoui F, Ouane I, Lu X, Tao Y, Paden C, Caidi H, Miao C, Al-Hajri MM, Zorruga M, Ghaouar W, BenSalah A, Gerber SI, World Health Organization Global Outbreak Alert and Response Network Middle East Respiratory Syndrome Coronavirus International Investigation Team. 2014. Family cluster of Middle East respiratory syndrome coronavirus infections, Tunisia, 2013. *Emerg Infect Dis* 20:1527–1530. <http://dx.doi.org/10.3201/eid2009.140378>.
 75. Assiri A, McGeer A, Perl TM, Price CS, Al Rabeeh AA, Cummings DA, Alabdullatif ZN, Assad M, Almulhim A, Makhdoom H, Madani H, Alhakeem R, Al-Tawfiq JA, Cotten M, Watson SJ, Kellam P, Zumla AI, Memish ZA. 2013. Hospital outbreak of Middle East respiratory syndrome coronavirus. *N Engl J Med* 369:407–416. <http://dx.doi.org/10.1056/NEJMoa1306742>.
 76. Tsiodras S, Baka A, Mentis A, Iliopoulos D, Dedoukou X, Papamavrou G, Karadima S, Emmanouil M, Kossyvakis A, Spanakis N, Pavli A, Maltezou H, Karageorgou A, Spala G, Pitiriga V, Kosmas E, Tsiagklis S, Gkatzias S, Koulouris N, Koutsoukou A, Bakakos P, Markozanhs E, Dionellis G, Pontikis K, Rovina N, Kyriakopoulou M, Efstathiou P, Papadimitriou T, Kremastinou J, Tsakris A, Saroglou G. 2014. A case of imported Middle East respiratory syndrome coronavirus infection and public health response, Greece, April 2014. *Euro Surveill* 19(16):pii=20782. <http://www.eurosurveillance.org>.
 77. Bialek SR, Allen D, Alvarado-Ramy F, Arthur R, Balajee A, Bell D, Best S, Blackmore C, Breakwell L, Cannons A, Brown C, Cetron M, Chea N, Chommanard C, Cohen N, Conover C, Crespo A, Creviston J, Curns AT, Dahl R, Dearth S, DeMaria A, Echols F, Erdman DD, Feikin D, Frias M, Gerber SI, Gulati R, Hale C, Haynes LM, Heberlein-Larson L, Holton K, Ijaz K, Kapoor M, Kohl K, Kuhar DT, Kumar AM, Kundich M, Lippold S, Liu L, Lovchik JC, Madoff L, Martell S, Matthews S, Moore J, Murray LR, Onofrey S, Pallansch MA, Pesik N, Pham H, Pillai S, Pontones P, Pringle K, Pritchard S, Rasmussen S, Richards S, Sandoval M, Schneider E, Schuchat A, Sheedy K, Sherin K, Swerdlow DL, Tappero JW, Vernon MO, Watkins S, Watson J. 2014. First confirmed cases of Middle East respiratory syndrome coronavirus (MERS-CoV) infection in the United States, updated information on the epidemiology of MERS-CoV infection, and guidance for the public, clinicians, and public health authorities—May 2014. *MMWR Morb Mortal Wkly Rep* 63:431–436.
 78. Premila Devi J, Noraini W, Norhayati R, Chee Kheong C, Badrul AS, Zainah S, Fadzilah K, Hirman I, Lokman Hakim S, Noor Hisham A. 2014. Laboratory-confirmed case of Middle East respiratory syndrome coronavirus (MERS-CoV) infection in Malaysia: preparedness and response, April 2014. *Euro Surveill* 19(18):pii=20797. <http://www.eurosurveillance.org/ViewArticle.aspx?ArticleId=20797>.
 79. Kraaij-Dirkzwager M, Timen A, Dirksen K, Gelinck L, Leyten E, Groeneveld P, Jansen C, Jonges M, Raj S, Thurkow I, van Gageldonk-Lafeber R, van der Eijk A, Koopmans M. 2014. Middle East respiratory syndrome coronavirus (MERS-CoV) infections in two returning travellers in the Netherlands, May 2014. *Euro Surveill* 19(21):pii=20817. <http://www.eurosurveillance.org/ViewArticle.aspx?ArticleId=20817>.
 80. Al-Tawfiq JA, Hinedi K, Ghandour J, Khairalla H, Musleh S, Ujayli A, Memish ZA. 2014. Middle East respiratory syndrome coronavirus: a case-control study of hospitalized patients. *Clin Infect Dis* 59:160–165. <http://dx.doi.org/10.1093/cid/ciu226>.
 81. Kapoor M, Pringle K, Kumar A, Dearth S, Liu L, Lovchik J, Perez O, Pontones P, Richards S, Yeadon-Fagbohun J, Breakwell L, Chea N, Cohen NJ, Schneider E, Erdman D, Haynes L, Pallansch M, Tao Y, Tong S, Gerber S, Swerdlow D, Feikin DR. 2014. Clinical and laboratory findings of the first imported case of Middle East respiratory syndrome coronavirus to the United States. *Clin Infect Dis* 59:1511–1518. <http://dx.doi.org/10.1093/cid/ciu635>.
 82. Drosten C, Muth D, Corman V, Hussain R, Al Masri M, HajOmar W, Landt O, Assiri A, Eckerle I, Al Shangiti A, Al-Tawfiq JA, Albarrak A, Zumla A, Rambaut A, Memish Z. 16 October 2014. An observational, laboratory-based study of outbreaks of MERS-coronavirus in Jeddah and Riyadh, Kingdom of Saudi Arabia, 2014. *Clin Infect Dis* <http://dx.doi.org/10.1093/cid/ciu812>.
 83. Memish ZA, Cotten M, Watson SJ, Kellam P, Zumla A, Alhakeem RF, Assiri A, Rabeeh AA, Al-Tawfiq JA. 2014. Community case clusters of Middle East respiratory syndrome coronavirus in Hafr Al-Batin, Kingdom of Saudi Arabia: a descriptive genomic study. *Int J Infect Dis* 23:63–68. <http://dx.doi.org/10.1016/j.ijid.2014.03.1372>.
 84. Pebody RG, Chand MA, Thomas HL, Green HK, Boddington NL, Carvalho C, Brown CS, Anderson SR, Rooney C, Crawley-Boevey E, Irwin DJ, Arons E, Tong C, Newsholme W, Price N, Langrish C, Tucker D, Zhao H, Phin N, Crofts J, Birmingham A, Gilgunn-Jones E, Brown KE, Evans B, Catchpole M, Watson JM. 2012. The United Kingdom public health response to an imported laboratory confirmed case of a novel coronavirus in September 2012. *Euro Surveill* 17(40):pii=20292. <http://www.eurosurveillance.org/ViewArticle.aspx?ArticleId=20292>.
 85. Drosten C, Meyer B, Muller MA, Corman VM, Al-Masri M, Hossain

- R, Madani H, Sieberg A, Bosch BJ, Lattwein E, Alhakeem RF, Assiri AM, Hajomar W, Albarrak AM, Al-Tawfiq JA, Zumla AI, Memish ZA. 2014. Transmission of MERS-coronavirus in household contacts. *N Engl J Med* 371:828–835. <http://dx.doi.org/10.1056/NEJMoal405858>.
86. Penttinen PM, Kaasik-Aslask A, Friaux A, Donachie A, Sudre B, Amato-Gauci AJ, Memish ZA, Coulombier D. 2013. Taking stock of the first 133 MERS coronavirus cases globally—is the epidemic changing? *Euro Surveill* 18(39):pii=20596. <http://www.eurosurveillance.org/ViewArticle.aspx?ArticleId=20596>.
87. WHO MERS-CoV Research Group. 2013. State of knowledge and data gaps of Middle East respiratory syndrome coronavirus (MERS-CoV) in humans. *PLoS Curr* 5:recurrent.outbreaks.0bf719e352e7478f8ad85fa30127ddb8. <http://dx.doi.org/10.1371/currents.outbreaks.0bf719e352e7478f8ad85fa30127ddb8>.
88. Arabi YM, Arifi AA, Balkhy HH, Najm H, Aldawood AS, Ghabashi A, Hawa H, Alothman A, Khaldi A, Al Raiy B. 2014. Clinical course and outcomes of critically ill patients with Middle East respiratory syndrome coronavirus infection. *Ann Intern Med* 160:389–397. <http://dx.doi.org/10.7326/M13-2486>.
89. Alghamdi IG, Hussain II, Almalki SS, Alghamdi MS, Alghamdi MM, El-Sheemy MA. 2014. The pattern of Middle East respiratory syndrome coronavirus in Saudi Arabia: a descriptive epidemiological analysis of data from the Saudi Ministry of Health. *Int J Gen Med* 7:417–423. <http://dx.doi.org/10.2147/IJGM.S67061>.
90. Breban R, Riou J, Fontanet A. 2013. Interhuman transmissibility of Middle East respiratory syndrome coronavirus: estimation of pandemic risk. *Lancet* 382:694–699. [http://dx.doi.org/10.1016/S0140-6736\(13\)61492-0](http://dx.doi.org/10.1016/S0140-6736(13)61492-0).
91. Alqurashi KA, Aljabri KS, Bokhari SA. 2011. Prevalence of diabetes mellitus in a Saudi community. *Ann Saudi Med* 31:19–23. <http://dx.doi.org/10.4103/0256-4947.75773>.
92. Zumla AI, Memish ZA. 2014. Middle East respiratory syndrome coronavirus: epidemic potential or a storm in a teacup? *Eur Respir J* 43:1243–1248. <http://dx.doi.org/10.1183/09031936.00227213>.
93. Woo PC, Lau SK, Chu CM, Chan KH, Tsoi HW, Huang Y, Wong BH, Poon RW, Cai JJ, Luk WK, Poon LL, Wong SS, Guan Y, Peiris JS, Yuen KY. 2005. Characterization and complete genome sequence of a novel coronavirus, coronavirus HKU1, from patients with pneumonia. *J Virol* 79:884–895. <http://dx.doi.org/10.1128/JVI.79.2.884-895.2005>.
94. Woo PC, Lau SK, Tsoi HW, Huang Y, Poon RW, Chu CM, Lee RA, Luk WK, Wong GK, Wong BH, Cheng VC, Tang BS, Wu AK, Yung RW, Chen H, Guan Y, Chan KH, Yuen KY. 2005. Clinical and molecular epidemiological features of coronavirus HKU1-associated community-acquired pneumonia. *J Infect Dis* 192:1898–1907. <http://dx.doi.org/10.1086/497151>.
95. Lau SK, Woo PC, Yip CC, Tse H, Tsoi HW, Cheng VC, Lee P, Tang BS, Cheung CH, Lee RA, So LY, Lau YL, Chan KH, Yuen KY. 2006. Coronavirus HKU1 and other coronavirus infections in Hong Kong. *J Clin Microbiol* 44:2063–2071. <http://dx.doi.org/10.1128/JCM.02614-05>.
96. Chan CM, Tse H, Wong SS, Woo PC, Lau SK, Chen L, Zheng BJ, Huang JD, Yuen KY. 2009. Examination of seroprevalence of coronavirus HKU1 infection with S protein-based ELISA and neutralization assay against viral spike pseudotyped virus. *J Clin Virol* 45:54–60. <http://dx.doi.org/10.1016/j.jcv.2009.02.011>.
97. Gierer S, Hofmann-Winkler H, Albuoli WH, Bertram S, Al-Rubaish AM, Yousef AA, Al-Nafaie AN, Al-Ali AK, Obeid OE, Alkharsah KR, Pohlmann S. 2013. Lack of MERS coronavirus neutralizing antibodies in humans, eastern province, Saudi Arabia. *Emerg Infect Dis* 19:2034–2036. <http://dx.doi.org/10.3201/eid1912.130701>.
98. Aburizaiza AS, Mattes FM, Azhar EI, Hassan AM, Memish ZA, Muth D, Meyer B, Lattwein E, Muller MA, Drosten C. 2014. Investigation of anti-Middle East respiratory syndrome antibodies in blood donors and slaughterhouse workers in Jeddah and Makkah, Saudi Arabia, fall 2012. *J Infect Dis* 209:243–246. <http://dx.doi.org/10.1093/infdis/jit589>.
99. Lau SK, Li KS, Tsang AK, Lam CS, Ahmed S, Chen H, Chan KH, Woo PC, Yuen KY. 2013. Genetic characterization of Betacoronavirus lineage C viruses in bats reveals marked sequence divergence in the spike protein of pipistrellus bat coronavirus HKU5 in Japanese pipistrelle: implications for the origin of the novel Middle East respiratory syndrome coronavirus. *J Virol* 87:8638–8650. <http://dx.doi.org/10.1128/JVI.01055-13>.
100. Yang Y, Du L, Liu C, Wang L, Ma C, Tang J, Baric RS, Jiang S, Li F. 2014. Receptor usage and cell entry of bat coronavirus HKU4 provide insight into bat-to-human transmission of MERS coronavirus. *Proc Natl Acad Sci U S A* 111:12516–12521. <http://dx.doi.org/10.1073/pnas.1405889111>.
101. Wang Q, Qi J, Yuan Y, Xuan Y, Han P, Wan Y, Ji W, Li Y, Wu Y, Wang J, Iwamoto A, Woo PC, Yuen KY, Yan J, Lu G, Gao GF. 2014. Bat origins of MERS-CoV supported by bat coronavirus HKU4 usage of human receptor CD26. *Cell Host Microbe* 16:328–337. <http://dx.doi.org/10.1016/j.chom.2014.08.009>.
102. Lau SK, Woo PC, Li KS, Huang Y, Tsoi HW, Wong BH, Wong SS, Leung SY, Chan KH, Yuen KY. 2005. Severe acute respiratory syndrome coronavirus-like virus in Chinese horseshoe bats. *Proc Natl Acad Sci U S A* 102:14040–14045. <http://dx.doi.org/10.1073/pnas.0506735102>.
103. Woo PC, Lau SK, Lam CS, Lau CC, Tsang AK, Lau JH, Bai R, Teng JL, Tsang CC, Wang M, Zheng BJ, Chan KH, Yuen KY. 2012. Discovery of seven novel mammalian and avian coronaviruses in the genus deltacoronavirus supports bat coronaviruses as the gene source of alphacoronavirus and betacoronavirus and avian coronaviruses as the gene source of gammacoronavirus and deltacoronavirus. *J Virol* 86:3995–4008. <http://dx.doi.org/10.1128/JVI.06540-11>.
104. Lau SK, Woo PC, Li KS, Huang Y, Wang M, Lam CS, Xu H, Guo R, Chan KH, Zheng BJ, Yuen KY. 2007. Complete genome sequence of bat coronavirus HKU2 from Chinese horseshoe bats revealed a much smaller spike gene with a different evolutionary lineage from the rest of the genome. *Virology* 367:428–439. <http://dx.doi.org/10.1016/j.virol.2007.06.009>.
105. Lau SK, Li KS, Huang Y, Shek CT, Tse H, Wang M, Choi GK, Xu H, Lam CS, Guo R, Chan KH, Zheng BJ, Woo PC, Yuen KY. 2010. Ecoepidemiology and complete genome comparison of different strains of severe acute respiratory syndrome-related Rhinolophus bat coronavirus in China reveal bats as a reservoir for acute, self-limiting infection that allows recombination events. *J Virol* 84:2808–2819. <http://dx.doi.org/10.1128/JVI.02219-09>.
106. Lau SK, Poon RW, Wong BH, Wang M, Huang Y, Xu H, Guo R, Li KS, Gao K, Chan KH, Zheng BJ, Woo PC, Yuen KY. 2010. Coexistence of different genotypes in the same bat and serological characterization of Rousettus bat coronavirus HKU9 belonging to a novel Betacoronavirus subgroup. *J Virol* 84:11385–11394. <http://dx.doi.org/10.1128/JVI.01121-10>.
107. Lau SK, Li KS, Tsang AK, Shek CT, Wang M, Choi GK, Guo R, Wong BH, Poon RW, Lam CS, Wang SY, Fan RY, Chan KH, Zheng BJ, Woo PC, Yuen KY. 2012. Recent transmission of a novel alphacoronavirus, bat coronavirus HKU10, from Leschenault's rousettes to pomona leaf-nosed bats: first evidence of interspecies transmission of coronavirus between bats of different suborders. *J Virol* 86:11906–11918. <http://dx.doi.org/10.1128/JVI.01305-12>.
108. Cui J, Eden JS, Holmes EC, Wang LF. 2013. Adaptive evolution of bat dipeptidyl peptidase 4 (dpp4): implications for the origin and emergence of Middle East respiratory syndrome coronavirus. *Virol J* 10:304. <http://dx.doi.org/10.1186/1743-422X-10-304>.
109. Memish ZA, Mishra N, Olival KJ, Fagbo SF, Kapoor V, Epstein JH, Alhakeem R, Durosinioun A, Al Asmari M, Islam A, Kapoor A, Briese T, Daszak P, Al Rabeeah AA, Lipkin WI. 2013. Middle East respiratory syndrome coronavirus in bats, Saudi Arabia. *Emerg Infect Dis* 19:1819–1823.
110. Ithete NL, Stoffberg S, Corman VM, Cottontail VM, Richards LR, Schoeman MC, Drosten C, Drexler JF, Preiser W. 2013. Close relative of human Middle East respiratory syndrome coronavirus in bat, South Africa. *Emerg Infect Dis* 19:1697–1699. <http://dx.doi.org/10.3201/eid1910.130946>.
111. Corman VM, Ithete NL, Richards LR, Schoeman MC, Preiser W, Drosten C, Drexler JF. 2014. Rooting the phylogenetic tree of middle East respiratory syndrome coronavirus by characterization of a conspecific virus from an African bat. *J Virol* 88:11297–11303. <http://dx.doi.org/10.1128/JVI.01498-14>.
112. Cotten M, Watson SJ, Kellam P, Al-Rabeeah AA, Makhdoom HQ, Assiri A, Al-Tawfiq JA, Alhakeem RF, Madani H, AlRabiah FA, Al Hajjar S, Al-nassir WN, Albarrak A, Flemman H, Balkhy HH, Alsubaie S, Palser AL, Gall A, Bashford-Rogers R, Rambaut A, Zumla AI, Memish ZA. 2013. Transmission and evolution of the Middle East respiratory syndrome coronavirus in Saudi Arabia: a descriptive genomic study. *Lancet* 382:1993–2002. [http://dx.doi.org/10.1016/S0140-6736\(13\)61887-5](http://dx.doi.org/10.1016/S0140-6736(13)61887-5).
113. Corman VM, Kallies R, Philipps H, Gopner G, Muller MA, Eckerle I, Brunink S, Drosten C, Drexler JF. 2014. Characterization of a novel betacoronavirus related to middle East respiratory syndrome coronavirus in European hedgehogs. *J Virol* 88:717–724. <http://dx.doi.org/10.1128/JVI.01600-13>.
114. Guan Y, Zheng BJ, He YQ, Liu XL, Zhuang ZX, Cheung CL, Luo SW, Li PH, Zhang LJ, Guan YJ, Butt KM, Wong KL, Chan KW, Lim W, Shortridge KF, Yuen KY, Peiris JS, Poon LL. 2003. Isolation and

- characterization of viruses related to the SARS coronavirus from animals in southern China. *Science* 302:276–278. <http://dx.doi.org/10.1126/science.1087139>.
115. Wong S, Lau S, Woo P, Yuen KY. 2007. Bats as a continuing source of emerging infections in humans. *Rev Med Virol* 17:67–91. <http://dx.doi.org/10.1002/rmv.520>.
 116. Chan JF, Chan KH, Choi GK, To KK, Tse H, Cai JP, Yeung ML, Cheng VC, Chen H, Che XY, Lau SK, Woo PC, Yuen KY. 2013. Differential cell line susceptibility to the emerging novel human betacoronavirus 2c EMC/2012: implications for disease pathogenesis and clinical manifestation. *J Infect Dis* 207:1743–1752. <http://dx.doi.org/10.1093/infdis/jit123>.
 117. Muller MA, Raj VS, Muth D, Meyer B, Kallies S, Smits SL, Wollny R, Bestebroer TM, Specht S, Suliman T, Zimmermann K, Binger T, Eckerle I, Tschapka M, Zaki AM, Osterhaus AD, Fouchier RA, Haagmans BL, Drosten C. 2012. Human coronavirus EMC does not require the SARS-coronavirus receptor and maintains broad replicative capability in mammalian cell lines. *mBio* 3(6):e00515–12. <http://dx.doi.org/10.1128/mBio.00515-12>.
 118. Eckerle I, Corman VM, Muller MA, Lenk M, Ulrich RG, Drosten C. 2014. Replicative capacity of MERS coronavirus in livestock cell lines. *Emerg Infect Dis* 20:276–279. <http://dx.doi.org/10.3201/eid2002.131182>.
 119. Cockrell AS, Peck KM, Yount BL, Agnihothram SS, Scobey T, Curnes NR, Baric RS, Heise MT. 2014. Mouse dipeptidyl peptidase 4 is not a functional receptor for Middle East respiratory syndrome coronavirus infection. *J Virol* 88:5195–5199. <http://dx.doi.org/10.1128/JVI.03764-13>.
 120. Barlan A, Zhao J, Sarkar MK, Li K, McCray PB, Jr, Perlman S, Gallagher T. 2014. Receptor variation and susceptibility to Middle East respiratory syndrome coronavirus infection. *J Virol* 88:4953–4961. <http://dx.doi.org/10.1128/JVI.00161-14>.
 121. Reusken CB, Haagmans BL, Muller MA, Gutierrez C, Godeke GJ, Meyer B, Muth D, Raj VS, Smits-De Vries L, Corman VM, Drexler JF, Smits SL, El Tahir YE, De Sousa R, van Beek J, Nowotny N, van Maanen K, Hidalgo-Hermoso E, Bosch BJ, Rottier P, Osterhaus A, Gortazar-Schmidt C, Drosten C, Koopmans MP. 2013. Middle East respiratory syndrome coronavirus neutralising serum antibodies in dromedary camels: a comparative serological study. *Lancet Infect Dis* 13:859–866. [http://dx.doi.org/10.1016/S1473-3099\(13\)70164-6](http://dx.doi.org/10.1016/S1473-3099(13)70164-6).
 122. Perera RA, Wang P, Gomaa MR, El-Shesheny R, Kandeil A, Bagato O, Siu LY, Shehata MM, Kayed AS, Moatasim Y, Li M, Poon LL, Guan Y, Webby RJ, Ali MA, Peiris JS, Kayali G. 2013. Seroepidemiology for MERS coronavirus using microneutralisation and pseudoparticle virus neutralisation assays reveal a high prevalence of antibody in dromedary camels in Egypt, June 2013. *Euro Surveill* 18(36):pii=20574. <http://www.eurosurveillance.org/ViewArticle.aspx?ArticleId=20574>.
 123. Alagaili AN, Briese T, Mishra N, Kapoor V, Sameroff SC, Burbelo PD, de Wit E, Munster VJ, Hensley LE, Zalmout IS, Kapoor A, Epstein JH, Karesh WB, Daszak P, Mohammed OB, Lipkin WI. 2014. Middle East respiratory syndrome coronavirus infection in dromedary camels in Saudi Arabia. *mBio* 5(2):e00884–00884. <http://dx.doi.org/10.1128/mBio.00884-14>.
 124. Meyer B, Muller MA, Corman VM, Reusken CB, Ritz J, Godeke GJ, Lattwein E, Kallies S, Siemens A, van Beek J, Drexler JF, Muth D, Bosch BJ, Wernery U, Koopmans MP, Wernery R, Drosten C. 2014. Antibodies against MERS coronavirus in dromedary camels, United Arab Emirates, 2003 and 2013. *Emerg Infect Dis* 20:552–559. <http://dx.doi.org/10.3201/eid2004.131746>.
 125. Alexandersen S, Kobinger GP, Soule G, Wernery U. 2014. Middle East respiratory syndrome coronavirus antibody reactors among camels in Dubai, United Arab Emirates, in 2005. *Transbound Emerg Dis* 61:105–108. <http://dx.doi.org/10.1111/tbed.12212>.
 126. Reusken CB, Ababneh M, Raj VS, Meyer B, Eljarah A, Abutarbush S, Godeke GJ, Bestebroer TM, Zutt I, Muller MA, Bosch BJ, Rottier PJ, Osterhaus AD, Drosten C, Haagmans BL, Koopmans MP. 2013. Middle East respiratory syndrome coronavirus (MERS-CoV) serology in major livestock species in an affected region in Jordan, June to September 2013. *Euro Surveill* 18(50):pii=20662. <http://www.eurosurveillance.org/ViewArticle.aspx?ArticleId=20662>.
 127. Hemida MG, Perera RA, Wang P, Alhammadi MA, Siu LY, Li M, Poon LL, Saif L, Alnaeem A, Peiris M. 2013. Middle East respiratory syndrome (MERS) coronavirus seroprevalence in domestic livestock in Saudi Arabia, 2010 to 2013. *Euro Surveill* 18(50):pii=20659. <http://www.eurosurveillance.org/ViewArticle.aspx?ArticleId=20659>.
 128. Memish ZA, Cotten M, Meyer B, Watson SJ, Alsaifi AJ, Al Rabeeah AA, Corman VM, Sieberg A, Makhdoom HQ, Assiri A, Al Masri M, Aldabbagh S, Bosch BJ, Beer M, Muller MA, Kellam P, Drosten C. 2014. Human infection with MERS coronavirus after exposure to infected camels, Saudi Arabia, 2013. *Emerg Infect Dis* 20:1012–1015. <http://dx.doi.org/10.3201/eid2006.140402>.
 129. Hemida MG, Chu DK, Poon LL, Perera RA, Alhammadi MA, Ng HY, Siu LY, Guan Y, Alnaeem A, Peiris M. 2014. MERS coronavirus in dromedary camel herd, Saudi Arabia. *Emerg Infect Dis* 20:1231–1234. <http://dx.doi.org/10.3201/eid2007.140571>.
 130. Corman VM, Jores J, Meyer B, Younan M, Liljander A, Said MY, Gluecks I, Lattwein E, Bosch BJ, Drexler JF, Bornstein S, Drosten C, Muller MA. 2014. Antibodies against MERS coronavirus in dromedary camels, Kenya, 1992–2013. *Emerg Infect Dis* 20:1319–1322. <http://dx.doi.org/10.3201/eid2008.140596>.
 131. Raj VS, Farag EA, Reusken CB, Lamers MM, Pas SD, Voermans J, Smits SL, Osterhaus AD, Al-Mawlawi N, Al-Romaihi HE, Alhajri MM, El-Sayed AM, Mohran KA, Ghobashy H, Alhajri F, Al-Thani M, Al-Marri SA, El-Maghraby MM, Koopmans MP, Haagmans BL. 2014. Isolation of MERS coronavirus from a dromedary camel, Qatar, 2014. *Emerg Infect Dis* 20:1339–1342. <http://dx.doi.org/10.3201/eid2008.140663>.
 132. Müller MA, Corman VM, Jores J, Meyer B, Younan M, Liljander A, Bosch BJ, Lattwein E, Hilali M, Musa BE, Bornstein S, Drosten C. December 2014. MERS coronavirus neutralizing antibodies in camels, Eastern Africa, 1983–1997. *Emerg Infect Dis* <http://dx.doi.org/10.3201/eid2012.141026>.
 133. Haagmans BL, Al Dhahiry SH, Reusken CB, Raj VS, Galiano M, Myers R, Godeke GJ, Jonges M, Farag E, Diab A, Ghobashy H, Alhajri F, Al-Thani M, Al-Marri SA, Al Romaihi HE, Al Khal A, Birmingham A, Osterhaus AD, Alhajri MM, Koopmans MP. 2014. Middle East respiratory syndrome coronavirus in dromedary camels: an outbreak investigation. *Lancet Infect Dis* 14:140–145. [http://dx.doi.org/10.1016/S1473-3099\(13\)70690-X](http://dx.doi.org/10.1016/S1473-3099(13)70690-X).
 134. Chu DK, Poon LL, Gomaa MM, Shehata MM, Perera RA, Abu Zeid D, El Rifay AS, Siu LY, Guan Y, Webby RJ, Ali MA, Peiris M, Kayali G. 2014. MERS coronaviruses in dromedary camels, Egypt. *Emerg Infect Dis* 20:1049–1053. <http://dx.doi.org/10.3201/eid2006.140299>.
 135. Hemida M, Perera R, Al Jassim R, Kayali G, Siu L, Wang P, Chu K, Perlman S, Ali M, Alnaeem A, Guan Y, Poon L, Saif L, Peiris M. 2014. Seroepidemiology of Middle East respiratory syndrome (MERS) coronavirus in Saudi Arabia (1993) and Australia (2014) and characterisation of assay specificity. *Euro Surveill* 19(23):pii=20828. <http://www.eurosurveillance.org/ViewArticle.aspx?ArticleId=20828>.
 136. Memish ZA, Alsahly A, Masri MA, Heil GL, Anderson BD, Peiris M, Khan SU, Gray GC. 3 December 2014. Sparse evidence of MERS-CoV infection among animal workers living in Southern Saudi Arabia during 2012. *Influenza Other Respir Viruses* <http://dx.doi.org/10.1111/irv.12287>.
 137. Briese T, Mishra N, Jain K, Zalmout IS, Jabado OJ, Karesh WB, Daszak P, Mohammed OB, Alagaili AN, Lipkin WI. 2014. Middle East respiratory syndrome coronavirus quasiespecies that include homologues of human isolates revealed through whole-genome analysis and virus cultured from dromedary camels in Saudi Arabia. *mBio* 5(3):e01146–01146. <http://dx.doi.org/10.1128/mBio.01146-14>.
 138. Azhar EI, El-Kafrawy SA, Farraj SA, Hassan AM, Al-Saeed MS, Hashem AM, Madani TA. 2014. Evidence for camel-to-human transmission of MERS coronavirus. *N Engl J Med* 370:2499–2505. <http://dx.doi.org/10.1056/NEJMoa1401505>.
 139. Azhar EI, Hashem AM, El-Kafrawy SA, Sohrab SS, Aburizaiza AS, Farraj SA, Hassan AM, Al-Saeed MS, Jamjoom GA, Madani TA. 2014. Detection of the Middle East respiratory syndrome coronavirus genome in an air sample originating from a camel barn owned by an infected patient. *mBio* 5(4):e01450–01450. <http://dx.doi.org/10.1128/mBio.01450-14>.
 140. Woo PC, Lau SK, Wernery U, Wong EY, Tsang AK, Johnson B, Yip CC, Lau CC, Sivakumar S, Cai JP, Fan RY, Chan KH, Mareena R, Yuen KY. 2014. Novel betacoronavirus in dromedaries of the Middle East, 2013. *Emerg Infect Dis* 20:560–572. <http://dx.doi.org/10.3201/eid2004.131769>.
 141. Muylersmans S. 2001. Single domain camel antibodies: current status. *J Biotechnol* 74:277–302. [http://dx.doi.org/10.1016/S1389-0352\(01\)00021-6](http://dx.doi.org/10.1016/S1389-0352(01)00021-6).
 142. Fanoy EB, van der Sande MA, Kraaij-Dirkzwager M, Dirksen K, Jonges M, van der Hoek W, Koopmans MP, van der Werf D, Sonder G, van der Weijden C, van der Heuvel J, Gelinck L, Bouwhuis JW, van Gageldonk-Lafeber AB. 2014. Travel-related MERS-CoV cases: an assessment of exposures and risk factors in a group of Dutch travellers

- returning from the Kingdom of Saudi Arabia, May 2014. *Emerg Themes Epidemiol* 11:16. <http://dx.doi.org/10.1186/1742-7622-11-16>.
143. van Doremalen N, Bushmaker T, Karesh WB, Munster VJ. 2014. Stability of Middle East respiratory syndrome coronavirus in milk. *Emerg Infect Dis* 20:1263–1264. <http://dx.doi.org/10.3201/eid2007.140500>.
 144. Reusken CB, Farag EA, Jonges M, Godeke GJ, El-Sayed AM, Pas SD, Raj VS, Mohran KA, Moussa HA, Ghobashy H, Alhajri F, Ibrahim AK, Bosch BJ, Pasha SK, Al-Romaihi HE, Al-Thani M, Al-Marri SA, AlHajri MM, Haagmans BL, Koopmans MP. 2014. Middle East respiratory syndrome coronavirus (MERS-CoV) RNA and neutralising antibodies in milk collected according to local customs from dromedary camels, Qatar, April 2014. *Euro Surveill* 19(23):pii=20829. <http://www.eurosurveillance.org/ViewArticle.aspx?ArticleId=20829>.
 145. van Doremalen N, Bushmaker T, Munster VJ. 2013. Stability of Middle East respiratory syndrome coronavirus (MERS-CoV) under different environmental conditions. *Euro Surveill* 18(38):pii=20590. <http://www.eurosurveillance.org/ViewArticle.aspx?ArticleId=20590>.
 146. Cotten M, Watson SJ, Zumla AI, Makhdoom HQ, Palser AL, Ong SH, Al Rabeah AA, Alhakeem RF, Assiri A, Al-Tawfiq JA, Albarrak A, Barry M, Shibl A, Alrabiah FA, Hajjar S, Balkhy HH, Flemban H, Rambaut A, Kellam P, Memish ZA. 2014. Spread, circulation, and evolution of the Middle East respiratory syndrome coronavirus. *mBio* 5(1):e01062–13. <http://dx.doi.org/10.1128/mBio.01062-13>.
 147. Li W, Zhang C, Sui J, Kuhn JH, Moore MJ, Luo S, Wong SK, Huang IC, Xu K, Vasilieva N, Murakami A, He Y, Marasco WA, Guan Y, Choe H, Farzan M. 2005. Receptor and viral determinants of SARS-coronavirus adaptation to human ACE2. *EMBO J* 24:1634–1643. <http://dx.doi.org/10.1038/sj.emboj.7600640>.
 148. Sheahan T, Rockx B, Donaldson E, Sims A, Pickles R, Corti D, Baric R. 2008. Mechanisms of zoonotic severe acute respiratory syndrome coronavirus host range expansion in human airway epithelium. *J Virol* 82:2274–2285. <http://dx.doi.org/10.1128/JVI.02041-07>.
 149. McRoy WC, Baric RS. 2008. Amino acid substitutions in the S2 subunit of mouse hepatitis virus variant V51 encode determinants of host range expansion. *J Virol* 82:1414–1424. <http://dx.doi.org/10.1128/JVI.01674-07>.
 150. Poletto C, Pelat C, Levy-Bruhl D, Yazdanpanah Y, Boelle PY, Colizza V. 2014. Assessment of the Middle East respiratory syndrome coronavirus (MERS-CoV) epidemic in the Middle East and risk of international spread using a novel maximum likelihood analysis approach. *Euro Surveill* 19(23):pii=20824. <http://www.eurosurveillance.org/ViewArticle.aspx?ArticleId=20824>.
 151. Cauchemez S, Fraser C, Van Kerkhove MD, Donnelly CA, Riley S, Rambaut A, Enouf V, van der Werf S, Ferguson NM. 2014. Middle East respiratory syndrome coronavirus: quantification of the extent of the epidemic, surveillance biases, and transmissibility. *Lancet Infect Dis* 14:50–56. [http://dx.doi.org/10.1016/S1473-3099\(13\)70304-9](http://dx.doi.org/10.1016/S1473-3099(13)70304-9).
 152. Ajlan AM, Ahayd RA, Jamjoom LG, Alharthy A, Madani TA. 2014. Middle East respiratory syndrome coronavirus (MERS-CoV) infection: chest CT findings. *AJR Am J Roentgenol* 203:782–787. <http://dx.doi.org/10.2214/AJR.14.13021>.
 153. Cheng VC, To KK, Tse H, Hung IF, Yuen KY. 2012. Two years after pandemic influenza A/2009/H1N1: what have we learned? *Clin Microbiol Rev* 25:223–263. <http://dx.doi.org/10.1128/CMR.05012-11>.
 154. To KK, Chan JF, Yuen KY. 2014. Viral lung infections: epidemiology, virology, clinical features, and management of avian influenza A(H7N9). *Curr Opin Pulm Med* 20:225–232. <http://dx.doi.org/10.1097/MCP.000000000000047>.
 155. Yu L, Wang Z, Chen Y, Ding W, Jia H, Chan JF, To KK, Chen H, Yang Y, Liang W, Zheng S, Yao H, Yang S, Cao H, Dai X, Zhao H, Li J, Bao Q, Chen P, Hou X, Li L, Yuen KY. 2013. Clinical, virological, and histopathological manifestations of fatal human infections by avian influenza A(H7N9) virus. *Clin Infect Dis* 57:1449–1457. <http://dx.doi.org/10.1093/cid/cit541>.
 156. To KK, Hung IF, Li IW, Lee KL, Koo CK, Yan WW, Liu R, Ho KY, Chu KH, Watt CL, Luk WK, Lai KY, Chow FL, Mok T, Buckley T, Chan JF, Wong SS, Zheng B, Chen H, Lau CC, Tse H, Cheng VC, Chan KH, Yuen KY. 2010. Delayed clearance of viral load and marked cytokine activation in severe cases of pandemic H1N1 2009 influenza virus infection. *Clin Infect Dis* 50:850–859. <http://dx.doi.org/10.1086/650581>.
 157. Eckerle I, Muller MA, Kallies S, Gotthardt DN, Drosten C. 2013. In-vitro renal epithelial cell infection reveals a viral kidney tropism as a potential mechanism for acute renal failure during Middle East respiratory syndrome (MERS) coronavirus infection. *Virol J* 10:359. <http://dx.doi.org/10.1186/1743-422X-10-359>.
 158. Chu KH, Tsang WK, Tang CS, Lam MF, Lai FM, To KF, Fung KS, Tang HL, Yan WW, Chan HW, Lai TS, Tong KL, Lai KN. 2005. Acute renal impairment in coronavirus-associated severe acute respiratory syndrome. *Kidney Int* 67:698–705. <http://dx.doi.org/10.1111/j.1523-1755.2005.67130.x>.
 159. Fowler RA, Lapinsky SE, Hallett D, Detsky AS, Sibbald WJ, Slutsky AS, Stewart TE. 2003. Critically ill patients with severe acute respiratory syndrome. *JAMA* 290:367–373. <http://dx.doi.org/10.1001/jama.290.3.367>.
 160. Hung IF, Cheng VC, Wu AK, Tang BS, Chan KH, Chu CM, Wong MM, Hui WT, Poon LL, Tse DM, Chan KS, Woo PC, Lau SK, Peiris JS, Yuen KY. 2004. Viral loads in clinical specimens and SARS manifestations. *Emerg Infect Dis* 10:1550–1557. <http://dx.doi.org/10.3201/eid1009.040058>.
 161. Park SJ, Kim GY, Choy HE, Hong YJ, Saif LJ, Jeong JH, Park SI, Kim HH, Kim SK, Shin SS, Kang MI, Cho KO. 2007. Dual enteric and respiratory tropisms of winter dysentery bovine coronavirus in calves. *Arch Virol* 152:1885–1900. <http://dx.doi.org/10.1007/s00705-007-1005-2>.
 162. Peiris JS, Chu CM, Cheng VC, Chan KS, Hung IF, Poon LL, Law KI, Tang BS, Hon TY, Chan CS, Chan KH, Ng JS, Zheng BJ, Ng WL, Lai RW, Guan Y, Yuen KY. 2003. Clinical progression and viral load in a community outbreak of coronavirus-associated SARS pneumonia: a prospective study. *Lancet* 361:1767–1772. [http://dx.doi.org/10.1016/S0140-6736\(03\)13412-5](http://dx.doi.org/10.1016/S0140-6736(03)13412-5).
 163. Memish ZA, Al-Tawfiq JA, Assiri A, Alrabiah FA, Hajjar SA, Albarrak A, Flemban H, Alhakeem RF, Makhdoom HQ, Alsubaie S, Al-Rabeah AA. 2014. Middle East respiratory syndrome coronavirus disease in children. *Pediatr Infect Dis J* 33:904–906. <http://dx.doi.org/10.1097/INF.0000000000000325>.
 164. Munster VJ, de Wit E, Feldmann H. 2013. Pneumonia from human coronavirus in a macaque model. *N Engl J Med* 368:1560–1562. <http://dx.doi.org/10.1056/NEJMc1215691>.
 165. de Wit E, Rasmussen AL, Falzarano D, Bushmaker T, Feldmann F, Brining DL, Fischer ER, Martellaro C, Okumura A, Chang J, Scott D, Benecke AG, Katze MG, Feldmann H, Munster VJ. 2013. Middle East respiratory syndrome coronavirus (MERS-CoV) causes transient lower respiratory tract infection in rhesus macaques. *Proc Natl Acad Sci U S A* 110:16598–16603. <http://dx.doi.org/10.1073/pnas.1310744110>.
 166. Yao Y, Bao L, Deng W, Xu L, Li F, Lv Q, Yu P, Chen T, Xu Y, Zhu H, Yuan J, Gu S, Wei Q, Chen H, Yuen KY, Qin C. 2014. An animal model of MERS produced by infection of rhesus macaques with MERS coronavirus. *J Infect Dis* 209:236–242. <http://dx.doi.org/10.1093/infdis/jit590>.
 167. Falzarano D, de Wit E, Feldmann F, Rasmussen AL, Okumura A, Peng X, Thomas MJ, van Doremalen N, Haddock E, Nagy L, LaCasse R, Liu T, Zhu J, McLellan JS, Scott DP, Katze MG, Feldmann H, Munster VJ. 2014. Infection with MERS-CoV causes lethal pneumonia in the common marmoset. *PLoS Pathog* 10:e1004250. <http://dx.doi.org/10.1371/journal.ppat.1004250>.
 168. Prescott J, de Wit E, Falzarano D, Scott DP, Feldmann H, Munster VJ. 2014. Defining the effects of immunosuppression in the rhesus model of Middle East respiratory syndrome (MERS). *Final Progr 33rd Annu Meet Am Soc Virol*, Fort Collins, CO.
 169. Menachery VD, Eisfeld AJ, Schafer A, Josset L, Sims AC, Proll S, Fan S, Li C, Neumann G, Tilton SC, Chang J, Gralinski LE, Long C, Green R, Williams CM, Weiss J, Matzke MM, Webb-Robertson BJ, Schepmoes AA, Shukla AK, Metz TO, Smith RD, Waters KM, Katze MG, Kawaoka Y, Baric RS. 2014. Pathogenic influenza viruses and coronaviruses utilize similar and contrasting approaches to control interferon-stimulated gene responses. *mBio* 5(3):e01174–01114. <http://dx.doi.org/10.1128/mBio.01174-14>.
 170. Lau SK, Lau CC, Chan KH, Li CP, Chen H, Jin DY, Chan JF, Woo PC, Yuen KY. 2013. Delayed induction of proinflammatory cytokines and suppression of innate antiviral response by the novel Middle East respiratory syndrome coronavirus: implications for pathogenesis and treatment. *J Gen Virol* 94:2679–2690. <http://dx.doi.org/10.1099/vir.0.055533-0>.
 171. Mielech AM, Kilianski A, Baez-Santos YM, Mesecar AD, Baker SC. 2014. MERS-CoV papain-like protease has deISGylating and deubiquitinating activities. *Virology* 450–451:64–70. <http://dx.doi.org/10.1016/j.virol.2013.11.040>.
 172. Deng X, Agnihotram S, Mielech AM, Nichols DB, Wilson MW, StJohn SE, Larsen SD, Mesecar AD, Lenschow DJ, Baric RS, Baker SC. 2014. A chimeric virus-mouse model system for evaluating the function

- and inhibition of papain-like proteases of emerging coronaviruses. *J Virol* 88:11825–11833. <http://dx.doi.org/10.1128/JVI.01749-14>.
173. Zhao J, Li K, Wohlford-Lenane C, Agnihothram SS, Fett C, Gale MJ, Jr, Baric RS, Enjuanes L, Gallagher T, McCray PB, Jr, Perlman S. 2014. Rapid generation of a mouse model for Middle East respiratory syndrome. *Proc Natl Acad Sci U S A* 111:4970–4975. <http://dx.doi.org/10.1073/pnas.1323279111>.
 174. Falzarano D, de Wit E, Rasmussen AL, Feldmann F, Okumura A, Scott DP, Brining D, Bushmaker T, Martellaro C, Baseler L, Benecke AG, Katze MG, Munster VJ, Feldmann H. 2013. Treatment with interferon-alpha2b and ribavirin improves outcome in MERS-CoV-infected rhesus macaques. *Nat Med* 19:1313–1317. <http://dx.doi.org/10.1038/nm.3362>.
 175. Faure E, Poissy J, Goffard A, Fournier C, Kipnis E, Titecat M, Bortolotti P, Martinez L, Dubucquoi S, Dessein R, Gosset P, Mathieu D, Guery B. 2014. Distinct immune response in two MERS-CoV-infected patients: can we go from bench to bedside? *PLoS One* 9:e88716. <http://dx.doi.org/10.1371/journal.pone.0088716>.
 176. Josset L, Menachery VD, Gralinski LE, Agnihothram S, Sova P, Carter VS, Yount BL, Graham RL, Baric RS, Katze MG. 2013. Cell host response to infection with novel human coronavirus EMC predicts potential antiviral and important differences with SARS coronavirus. *mBio* 4(3):e00165–00113. <http://dx.doi.org/10.1128/mBio.00165-13>.
 177. Cameron MJ, Ran L, Xu L, Danesh A, Bermejo-Martin JF, Cameron CM, Muller MP, Gold WL, Richardson SE, Poutanen SM, Willey BM, DeVries ME, Fang Y, Seneviratne C, Bosinger SE, Persad D, Wilkinson P, Greller LD, Somogyi R, Humar A, Keshavjee S, Louie M, Loeb MB, Brunton J, McGeer AJ, Kelvin DJ. 2007. Interferon-mediated immunopathological events are associated with atypical innate and adaptive immune responses in patients with severe acute respiratory syndrome. *J Virol* 81:8692–8706. <http://dx.doi.org/10.1128/JVI.00527-07>.
 178. Perlman S, Netland J. 2009. Coronaviruses post-SARS: update on replication and pathogenesis. *Nat Rev Microbiol* 7:439–450. <http://dx.doi.org/10.1038/nrmicro2147>.
 179. Ryzhakov G, Lai CC, Blazek K, To KW, Hussell T, Udalova I. 2011. IL-17 boosts proinflammatory outcome of antiviral response in human cells. *J Immunol* 187:5357–5362. <http://dx.doi.org/10.4049/jimmunol.1100917>.
 180. Crowe CR, Chen K, Pociask DA, Alcorn JF, Krivich C, Enelow RI, Ross TM, Witztum JL, Kolls JK. 2009. Critical role of IL-17RA in immunopathology of influenza infection. *J Immunol* 183:5301–5310. <http://dx.doi.org/10.4049/jimmunol.0900995>.
 181. Poissy J, Goffard A, Parmentier-Decrucq E, Favory R, Kuv M, Kipnis E, Mathieu D, Guery B. 2014. Kinetics and pattern of viral excretion in biological specimens of two MERS-CoV cases. *J Clin Virol* 61:275–278. <http://dx.doi.org/10.1016/j.jcv.2014.07.002>.
 182. Buchholz U, Muller MA, Nitsche A, Sanewski A, Wevering N, Bauer-Balci T, Bonin F, Drosten C, Schweiger B, Wolff T, Muth D, Meyer B, Buda S, Krause G, Schaade L, Haas W. 2013. Contact investigation of a case of human novel coronavirus infection treated in a German hospital, October–November 2012. *Euro Surveill* 18(8):pii=20406. <http://www.eurosurveillance.org/ViewArticle.aspx?ArticleId=20406>.
 183. Spanakis N, Tsiodras S, Haagmans BL, Raj VS, Pontikis K, Koutsoukou A, Koulouris NG, Osterhaus AD, Koopmans MP, Tsakris A. 2014. Virological and serological analysis of a recent Middle East respiratory syndrome coronavirus infection case on a triple combination antiviral regimen. *Int J Antimicrob Agents* 44:528–532. <http://dx.doi.org/10.1016/j.ijantimicag.2014.07.026>.
 184. Tao X, Hill TE, Morimoto C, Peters CJ, Ksiazek TG, Tseng CT. 2013. Bilateral entry and release of Middle East respiratory syndrome coronavirus induces profound apoptosis of human bronchial epithelial cells. *J Virol* 87:9953–9958. <http://dx.doi.org/10.1128/JVI.01562-13>.
 185. Ziebeck F, Weber M, Eickmann M, Spiegelberg L, Zaki AM, Matrosovich M, Becker S, Weber F. 2013. Human cell tropism and innate immune system interactions of human respiratory coronavirus EMC compared to those of severe acute respiratory syndrome coronavirus. *J Virol* 87:5300–5304. <http://dx.doi.org/10.1128/JVI.03496-12>.
 186. Kindler E, Jonsdottir HR, Muth D, Hamming OJ, Hartmann R, Rodriguez R, Geffers R, Fouchier RA, Drosten C, Muller MA, Dijkman R, Thiel V. 2013. Efficient replication of the novel human betacoronavirus EMC on primary human epithelium highlights its zoonotic potential. *mBio* 4(1):e00611–00612. <http://dx.doi.org/10.1128/mBio.00611-12>.
 187. Scobey T, Yount BL, Sims AC, Donaldson EF, Agnihothram SS, Menachery VD, Graham RL, Swanstrom J, Bove PF, Kim JD, Grego S, Randell SH, Baric RS. 2013. Reverse genetics with a full-length infectious cDNA of the Middle East respiratory syndrome coronavirus. *Proc Natl Acad Sci U S A* 110:16157–16162. <http://dx.doi.org/10.1073/pnas.1311542110>.
 188. Hocke AC, Becher A, Knepper J, Peter A, Holland G, Tonnie M, Bauer TT, Schneider P, Neudecker J, Muth D, Wendtner CM, Ruckert JC, Drosten C, Gruber AD, Laue M, Suttrop N, Hippenstiel S, Wolff T. 2013. Emerging human middle East respiratory syndrome coronavirus causes widespread infection and alveolar damage in human lungs. *Am J Respir Crit Care Med* 188:882–886. <http://dx.doi.org/10.1164/rccm.201305-0954LE>.
 189. Chan RW, Chan MC, Agnihothram S, Chan LL, Kuok DI, Fong JH, Guan Y, Poon LL, Baric RS, Nicholls JM, Peiris JS. 2013. Tropism of and innate immune responses to the novel human betacoronavirus lineage C virus in human ex vivo respiratory organ cultures. *J Virol* 87:6604–6614. <http://dx.doi.org/10.1128/JVI.00009-13>.
 190. Zhou J, Chu H, Li C, Wong BH, Cheng ZS, Poon VK, Sun T, Lau CC, Wong KK, Chan JY, Chan JF, To KK, Chan KH, Zheng BJ, Yuen KY. 2014. Active replication of Middle East respiratory syndrome coronavirus and aberrant induction of inflammatory cytokines and chemokines in human macrophages: implications for pathogenesis. *J Infect Dis* 209:1331–1342. <http://dx.doi.org/10.1093/infdis/jit504>.
 191. Ziegler AF, Ladman BS, Dunn PA, Schneider A, Davison S, Miller PG, Lu H, Weinstock D, Salem M, Eckroade RJ, Gelb J, Jr. 2002. Nephropathogenic infectious bronchitis in Pennsylvania chickens 1997–2000. *Avian Dis* 46:847–858. [http://dx.doi.org/10.1637/0005-2086\(2002\)0460847:NIBIPC2.0.CO;2](http://dx.doi.org/10.1637/0005-2086(2002)0460847:NIBIPC2.0.CO;2).
 192. Chu H, Zhou J, Wong BH, Li C, Cheng ZS, Lin X, Poon VK, Sun T, Lau CC, Chan JF, To KK, Chan KH, Lu L, Zheng BJ, Yuen KY. 2014. Productive replication of Middle East respiratory syndrome coronavirus in monocyte-derived dendritic cells modulates innate immune response. *Virology* 454:455:197–205. <http://dx.doi.org/10.1016/j.virol.2014.02.018>.
 193. Memish ZA, Al-Tawfiq JA, Makhdoom HQ, Assiri A, Alhakeem RF, Albarak A, Alsabaie S, Al-Rabieah AA, Hajomar WH, Hussain R, Kheyami AM, Almutairi A, Azhar EI, Drosten C, Watson SJ, Kellam P, Cotten M, Zumla A. 2014. Respiratory tract samples, viral load and genome fraction yield in patients with Middle East respiratory syndrome. *J Infect Dis* 210:1590–1594. <http://dx.doi.org/10.1093/infdis/jiu292>.
 194. de Sousa R, Reusken C, Koopmans M. 2014. MERS coronavirus: data gaps for laboratory preparedness. *J Clin Virol* 59:4–11. <http://dx.doi.org/10.1016/j.jcv.2013.10.030>.
 195. Cheng VC, Hung IF, Tang BS, Chu CM, Wong MM, Chan KH, Wu AK, Tse DM, Chan KS, Zheng BJ, Peiris JS, Sung JJ, Yuen KY. 2004. Viral replication in the nasopharynx is associated with diarrhea in patients with severe acute respiratory syndrome. *Clin Infect Dis* 38:467–475. <http://dx.doi.org/10.1086/382681>.
 196. Chan KH, Poon LL, Cheng VC, Guan Y, Hung IF, Kong J, Yam LY, Seto WH, Yuen KY, Peiris JS. 2004. Detection of SARS coronavirus in patients with suspected SARS. *Emerg Infect Dis* 10:294–299. <http://dx.doi.org/10.3201/eid1002.030610>.
 197. Memish ZA, Assiri AM, Al-Tawfiq JA. 2014. Middle East respiratory syndrome coronavirus (MERS-CoV) viral shedding in the respiratory tract: an observational analysis with infection control implications. *Int J Infect Dis* 29:307–308. <http://dx.doi.org/10.1016/j.ijid.2014.10.002>.
 198. Palm D, Pereyaslov D, Vaz J, Broberg E, Zeller H, Gross D, Brown CS, Struelens MJ. 2012. Laboratory capability for molecular detection and confirmation of novel coronavirus in Europe, November 2012. *Euro Surveill* 17(49):pii=20335. <http://www.eurosurveillance.org/ViewArticle.aspx?ArticleId=20335>.
 199. Abd El Wahed A, Patel P, Heidenreich D, Hufert FT, Weidmann M. 2013. Reverse transcription recombinase polymerase amplification assay for the detection of middle East respiratory syndrome coronavirus. *PLoS Curr* 5:recurrent.outbreaks.62df1c7c75ffc96cd59034531e2e8364. <http://dx.doi.org/10.1371/currents.outbreaks.62df1c7c75ffc96cd59034531e2e8364>.
 200. Shirato K, Yano T, Senba S, Akachi S, Kobayashi T, Nishinaka T, Notomi T, Matsuyama S. 2014. Detection of Middle East respiratory syndrome coronavirus using reverse transcription loop-mediated isothermal amplification (RT-LAMP). *Virol J* 11:139. <http://dx.doi.org/10.1186/1743-422X-11-139>.
 201. Agnihothram S, Gopal R, Yount BL, Jr, Donaldson EF, Menachery VD, Graham RL, Scobey TD, Gralinski LE, Denison MR, Zambon M, Baric RS. 2014. Evaluation of serologic and antigenic relationships between middle eastern respiratory syndrome coronavirus and other coro-

- naviruses to develop vaccine platforms for the rapid response to emerging coronaviruses. *J Infect Dis* 209:995–1006. <http://dx.doi.org/10.1093/infdis/jit609>.
202. Chan KH, Chan JF, Tse H, Chen H, Lau CC, Cai JP, Tsang AK, Xiao X, To KK, Lau SK, Woo PC, Zheng BJ, Wang M, Yuen KY. 2013. Cross-reactive antibodies in convalescent SARS patients' sera against the emerging novel human coronavirus EMC (2012) by both immunofluorescent and neutralizing antibody tests. *J Infect* 67:130–140. <http://dx.doi.org/10.1016/j.jinf.2013.03.015>.
 203. Cheng VC, Tang BS, Wu AK, Chu CM, Yuen KY. 2004. Medical treatment of viral pneumonia including SARS in immunocompetent adult. *J Infect* 49:262–273. <http://dx.doi.org/10.1016/j.jinf.2004.07.010>.
 204. Wong SS, Yuen KY. 2008. The management of coronavirus infections with particular reference to SARS. *J Antimicrob Chemother* 62:437–441. <http://dx.doi.org/10.1093/jac/dkn243>.
 205. Ho PL, Sin WC, Chan JF, Cheng VC, Chan KH. 2014. Severe influenza A H7N9 pneumonia with rapid virological response to intravenous zanamivir. *Eur Respir J* 44:535–537. <http://dx.doi.org/10.1183/09031936.00006414>.
 206. Omrani AS, Saad MM, Baig K, Bahloul A, Abdul-Matin M, Alaidaroos AY, Almakhlaifi GA, Albarrak MM, Memish ZA, Albarrak AM. 2014. Ribavirin and interferon alfa-2a for severe Middle East respiratory syndrome coronavirus infection: a retrospective cohort study. *Lancet Infect Dis* 14:1090–1095. [http://dx.doi.org/10.1016/S1473-3099\(14\)70920-X](http://dx.doi.org/10.1016/S1473-3099(14)70920-X).
 207. Frausto SD, Lee E, Tang H. 2013. Cyclophilins as modulators of viral replication. *Viruses* 5:1684–1701. <http://dx.doi.org/10.3390/v5071684>.
 208. Falzarano D, de Wit E, Martellaro C, Callison J, Munster VJ, Feldmann H. 2013. Inhibition of novel beta coronavirus replication by a combination of interferon- α 2b and ribavirin. *Sci Rep* 3:1686. <http://dx.doi.org/10.1038/srep01686>.
 209. Chan JF, Chan KH, Kao RY, To KK, Zheng BJ, Li CP, Li PT, Dai J, Mok FK, Chen H, Hayden FG, Yuen KY. 2013. Broad-spectrum antivirals for the emerging Middle East respiratory syndrome coronavirus. *J Infect* 67:606–616. <http://dx.doi.org/10.1016/j.jinf.2013.09.029>.
 210. Khalid M, Al Rabiah F, Khan B, Al Mobeireek A, Butt TS, Al Mutairy E. 15 May 2014. Ribavirin and interferon (IFN)- α -2b as primary and preventive treatment for Middle East respiratory syndrome coronavirus (MERS-CoV): a preliminary report of two cases. *Antivir Ther* <http://dx.doi.org/10.3851/IMP2792>.
 211. Dyall J, Coleman CM, Hart BJ, Venkataraman T, Holbrook MR, Kindrachuk J, Johnson RF, Olinger GG, Jr, Jahrling PB, Laidlaw M, Johansen LM, Lear-Rooney CM, Glass PJ, Hensley LE, Frieman MB. 2014. Repurposing of clinically developed drugs for treatment of Middle East respiratory syndrome coronavirus infection. *Antimicrob Agents Chemother* 58:4885–4893. <http://dx.doi.org/10.1128/AAC.03036-14>.
 212. de Wilde AH, Jochmans D, Posthumus CC, Zevenhoven-Dobbe JC, van Nieuwkoop S, Bestebroer TM, van den Hoogen BG, Neyts J, Snijder EJ. 2014. Screening of an FDA-approved compound library identifies four small-molecule inhibitors of Middle East respiratory syndrome coronavirus replication in cell culture. *Antimicrob Agents Chemother* 58:4875–4884. <http://dx.doi.org/10.1128/AAC.03011-14>.
 213. Liu Q, Xia S, Sun Z, Wang Q, Du L, Lu L, Jiang S. 20 October 2014. Testing of MERS-CoV replication inhibitors for their ability to block viral entry. *Antimicrob Agents Chemother* <http://dx.doi.org/10.1128/AAC.03977-14>.
 214. Kindrachuk J, Ork B, Hart BJ, Mazur S, Holbrook MR, Frieman MB, Traynor D, Johnson RF, Dyall J, Kuhn JH, Olinger GG, Hensley LE, Jahrling PB. 8 December 2014. The antiviral potential of ERK/MAPK and PI3K/AKT/mTOR signaling modulation for MERS-CoV infection as identified by temporal kinome analysis. *Antimicrob Agents Chemother* <http://dx.doi.org/10.1128/AAC.03659-14>.
 215. Chu CM, Cheng VC, Hung IF, Wong MM, Chan KH, Chan KS, Kao RY, Poon LL, Wong CL, Guan Y, Peiris JS, Yuen KY. 2004. Role of lopinavir/ritonavir in the treatment of SARS: initial virological and clinical findings. *Thorax* 59:252–256. <http://dx.doi.org/10.1136/thorax.2003.012658>.
 216. Vincent MJ, Bergeron E, Benjannet S, Erickson BR, Rollin PE, Ksiazek TG, Seidah NG, Nichol ST. 2005. Chloroquine is a potent inhibitor of SARS coronavirus infection and spread. *Virol J* 2:69. <http://dx.doi.org/10.1186/1743-422X-2-69>.
 217. Barnard DL, Day CW, Bailey K, Heiner M, Montgomery R, Lauridsen I, Chan PK, Sidwell RW. 2006. Evaluation of immunomodulators, interferons and known in vitro SARS-CoV inhibitors for inhibition of SARS-CoV replication in BALB/c mice. *Antivir Chem Chemother* 17:275–284.
 218. Barnard DL, Kumaki Y. 2011. Recent developments in anti-severe acute respiratory syndrome coronavirus chemotherapy. *Future Virol* 6:615–631. <http://dx.doi.org/10.2217/fvl.11.33>.
 219. Kilianski A, Baker SC. 2014. Cell-based antiviral screening against coronaviruses: developing virus-specific and broad-spectrum inhibitors. *Antiviral Res* 101:105–112. <http://dx.doi.org/10.1016/j.antiviral.2013.11.004>.
 220. Yang ZY, Werner HC, Kong WP, Leung K, Traggiai E, Lanzavecchia A, Nabel GJ. 2005. Evasion of antibody neutralization in emerging severe acute respiratory syndrome coronaviruses. *Proc Natl Acad Sci U S A* 102:797–801. <http://dx.doi.org/10.1073/pnas.0409065102>.
 221. Weingartl H, Czub M, Czub S, Neufeld J, Marszal P, Gren J, Smith G, Jones S, Proulx R, Deschambault Y, Grudeski E, Andonov A, He R, Li Y, Copps J, Grolla A, Dick D, Berry J, Ganske S, Manning L, Cao J. 2004. Immunization with modified vaccinia virus Ankara-based recombinant vaccine against severe acute respiratory syndrome is associated with enhanced hepatitis in ferrets. *J Virol* 78:12672–12676. <http://dx.doi.org/10.1128/JVI.78.22.12672-12676.2004>.
 222. Ren Z, Yan L, Zhang N, Guo Y, Yang C, Lou Z, Rao Z. 2013. The newly emerged SARS-like coronavirus HCoV-EMC also has an “Achilles’ heel”: current effective inhibitor targeting a 3C-like protease. *Protein Cell* 4:248–250. <http://dx.doi.org/10.1007/s13238-013-2841-3>.
 223. Kilianski A, Mielech AM, Deng X, Baker SC. 2013. Assessing activity and inhibition of Middle East respiratory syndrome coronavirus papain-like and 3C-like proteases using luciferase-based biosensors. *J Virol* 87:11955–11962. <http://dx.doi.org/10.1128/JVI.02105-13>.
 224. Agnihothram S, Yount BL, Jr, Donaldson EF, Huynh J, Menachery VD, Gralinski LE, Graham RL, Becker MM, Tomar S, Scobey TD, Osswald HL, Whitmore A, Gopal R, Ghosh AK, Mesecar A, Zambon M, Heise M, Denison MR, Baric RS. 2014. A mouse model for Beta-coronavirus subgroup 2c using a bat coronavirus strain HKU5 variant. *mBio* 5(2):e00047–00014. <http://dx.doi.org/10.1128/mBio.00047-14>.
 225. Adedeji AO, Singh K, Kassim A, Coleman CM, Elliott R, Weiss SR, Frieman MB, Sarafianos SG. 2014. Evaluation of SSYA10-001 as a replication inhibitor of SARS, MHV and MERS coronaviruses. *Antimicrob Agents Chemother* 58:4894–4898. <http://dx.doi.org/10.1128/AAC.02994-14>.
 226. Bosch BJ, Smits SL, Haagmans BL. 2014. Membrane ectopeptidases targeted by human coronaviruses. *Curr Opin Virol* 6:55–60. <http://dx.doi.org/10.1016/j.coviro.2014.03.011>.
 227. Reinhold D, Bank U, Tager M, Ansorge S, Wrenger S, Thielitz A, Lendeckel U, Faust J, Neubert K, Brocke S. 2008. DP IV/CD26, APN/CD13 and related enzymes as regulators of T cell immunity: implications for experimental encephalomyelitis and multiple sclerosis. *Front Biosci* 13:2356–2363. <http://dx.doi.org/10.2741/2849>.
 228. Reinhold D, Brocke S. 2014. DPP4-directed therapeutic strategies for MERS-CoV. *Lancet Infect Dis* 14:100–101. [http://dx.doi.org/10.1016/S1473-3099\(13\)70696-0](http://dx.doi.org/10.1016/S1473-3099(13)70696-0).
 229. Chandran K, Sullivan NJ, Felbor U, Whelan SP, Cunningham JM. 2005. Endosomal proteolysis of the Ebola virus glycoprotein is necessary for infection. *Science* 308:1643–1645. <http://dx.doi.org/10.1126/science.1110656>.
 230. Marzi A, Reinheckel T, Feldmann H. 2012. Cathepsin B & L are not required for ebola virus replication. *PLoS Negl Trop Dis* 6:e1923. <http://dx.doi.org/10.1371/journal.pntd.0001923>.
 231. Chen Y, Liang W, Yang S, Wu N, Gao H, Sheng J, Yao H, Wo J, Fang Q, Cui D, Li Y, Yao X, Zhang Y, Wu H, Zheng S, Diao H, Xia S, Chan KH, Tsoi HW, Teng JL, Song W, Wang P, Lau SY, Zheng M, Chan JF, To KK, Chen H, Li L, Yuen KY. 2013. Human infections with the emerging avian influenza A H7N9 virus from wet market poultry: clinical analysis and characterisation of viral genome. *Lancet* 381:1916–1925. [http://dx.doi.org/10.1016/S0140-6736\(13\)60903-4](http://dx.doi.org/10.1016/S0140-6736(13)60903-4).
 232. To KK, Tsang AK, Chan JF, Cheng VC, Chen H, Yuen KY. 2014. Emergence in China of human disease due to avian influenza A(H10N8)—cause for concern? *J Infect* 68:205–215. <http://dx.doi.org/10.1016/j.jinf.2013.12.014>.
 233. Cheng VC, Chan JF, To KK, Yuen KY. 2013. Clinical management and infection control of SARS: lessons learned. *Antiviral Res* 100:407–419. <http://dx.doi.org/10.1016/j.antiviral.2013.08.016>.
 234. Memish ZA, Al-Tawfiq JA, Assiri A. 2013. Hospital-associated Middle East respiratory syndrome coronavirus infections. *N Engl J Med* 369:1761–1762. <http://dx.doi.org/10.1056/NEJMc1311004>.
 235. Coburn BJ, Blower S. 2014. Predicting the potential for within-flight

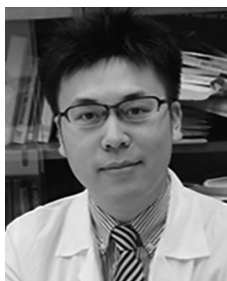
- transmission and global dissemination of MERS. *Lancet Infect Dis* 14:99. [http://dx.doi.org/10.1016/S1473-3099\(13\)70358-X](http://dx.doi.org/10.1016/S1473-3099(13)70358-X).
236. Thomas HL, Zhao H, Green HK, Boddington NL, Carvalho CF, Osman HK, Sadler C, Zambon M, Bermingham A, Pebody RG. 2014. Enhanced MERS coronavirus surveillance of travelers from the Middle East to England. *Emerg Infect Dis* 20:1562–1564. <http://dx.doi.org/10.3201/eid2009.140817>.
 237. Leclercq I, Batejat C, Burguiere AM, Manuguerra JC. 2014. Heat inactivation of the Middle East respiratory syndrome coronavirus. *Influenza Other Respir Viruses* 8:585–586. <http://dx.doi.org/10.1111/irv.12261>.
 238. Gautret P, Charrel R, Belhouchat K, Drali T, Benkouiten S, Nougaiere A, Zandotti C, Memish ZA, al Masri M, Gaillard C, Brouqui P, Parola P. 2013. Lack of nasal carriage of novel corona virus (HCoV-EMC) in French Hajj pilgrims returning from the Hajj 2012, despite a high rate of respiratory symptoms. *Clin Microbiol Infect* 19:E315–E317. <http://dx.doi.org/10.1111/1469-0691.12174>.
 239. Gautret P, Charrel R, Benkouiten S, Belhouchat K, Nougaiere A, Drali T, Salez N, Memish ZA, Al Masri M, Lagier JC, Million M, Raoult D, Brouqui P, Parola P. 2014. Lack of MERS coronavirus but prevalence of influenza virus in French pilgrims after 2013 Hajj. *Emerg Infect Dis* 20:728–730. <http://dx.doi.org/10.3201/eid2004.131708>.
 240. Memish ZA, Almasri M, Turkestani A, Al-Shangiti AM, Yezli S. 2014. Etiology of severe community-acquired pneumonia during the 2013 Hajj—part of the MERS-CoV surveillance program. *Int J Infect Dis* 25:186–190. <http://dx.doi.org/10.1016/j.ijid.2014.06.003>.
 241. Memish ZA, Al-Rabeiah AA. 2013. Health conditions of travellers to Saudi Arabia for the pilgrimage to Mecca (Hajj and Umra) for 1434 (2013). *J Epidemiol Glob Health* 3:59–61. <http://dx.doi.org/10.1016/j.jegh.2013.03.001>.
 242. Al-Tawfiq JA, Memish ZA. 2014. Mass gathering medicine: 2014 Hajj and Umra preparation as a leading example. *Int J Infect Dis* 27:26–31. <http://dx.doi.org/10.1016/j.ijid.2014.07.001>.
 243. Chung SJ, Ling ML, Seto WH, Ang BS, Tambyah PA. 2014. Debate on MERS-CoV respiratory precautions: surgical mask or N95 respirators? *Singapore Med J* 55:294–297. <http://dx.doi.org/10.11622/smedj.2014076>.
 244. Cheng VC, Tai JW, Wong LM, Chan JF, Li IW, To KK, Hung IF, Chan KH, Ho PL, Yuen KY. 2010. Prevention of nosocomial transmission of swine-origin pandemic influenza virus A/H1N1 by infection control bundle. *J Hosp Infect* 74:271–277. <http://dx.doi.org/10.1016/j.jhin.2009.09.009>.
 245. Al-Gethamy M, Corman VM, Hussain R, Al-Tawfiq JA, Drosten C, Memish ZA. 16 December 2014. A case of long-term excretion and subclinical infection with MERS-Coronavirus in a health care worker. *Clin Infect Dis* <http://dx.doi.org/10.1093/cid/ciu1135>.
 246. Madani TA. 2014. Case definition and management of patients with MERS coronavirus in Saudi Arabia. *Lancet Infect Dis* 14:911–913. [http://dx.doi.org/10.1016/S1473-3099\(14\)70918-1](http://dx.doi.org/10.1016/S1473-3099(14)70918-1).
 247. Song F, Fux R, Provacia LB, Volz A, Eickmann M, Becker S, Osterhaus AD, Haagmans BL, Sutter G. 2013. Middle East respiratory syndrome coronavirus spike protein delivered by modified vaccinia virus Ankara efficiently induces virus-neutralizing antibodies. *J Virol* 87:11950–11954. <http://dx.doi.org/10.1128/JVI.01672-13>.
 248. Coleman CM, Liu YV, Mu H, Taylor JK, Massare M, Flyer DC, Glenn GM, Smith GE, Frieman MB. 2014. Purified coronavirus spike protein nanoparticles induce coronavirus neutralizing antibodies in mice. *Vaccine* 32:3169–3174. <http://dx.doi.org/10.1016/j.vaccine.2014.04.016>.
 249. He Y, Zhou Y, Wu H, Luo B, Chen J, Li W, Jiang S. 2004. Identification of immunodominant sites on the spike protein of severe acute respiratory syndrome (SARS) coronavirus: implication for developing SARS diagnostics and vaccines. *J Immunol* 173:4050–4057. <http://dx.doi.org/10.4049/jimmunol.173.6.4050>.
 250. Lan J, Deng Y, Chen H, Lu G, Wang W, Guo X, Lu Z, Gao GF, Tan W. 2014. Tailoring subunit vaccine immunity with adjuvant combinations and delivery routes using the Middle East respiratory coronavirus (MERS-CoV) receptor-binding domain as an antigen. *PLoS One* 9:e112602. <http://dx.doi.org/10.1371/journal.pone.0112602>.
 251. Zhang N, Jiang S, Du L. 2014. Current advancements and potential strategies in the development of MERS-CoV vaccines. *Expert Rev Vaccines* 13:761–774. <http://dx.doi.org/10.1586/14760584.2014.912134>.
 252. Cheng Y, Wong R, Soo YO, Wong WS, Lee CK, Ng MH, Chan P, Wong KC, Leung CB, Cheng G. 2005. Use of convalescent plasma therapy in SARS patients in Hong Kong. *Eur J Clin Microbiol Infect Dis* 24:44–46. <http://dx.doi.org/10.1007/s10096-004-1271-9>.
 253. Yeh KM, Chiueh TS, Siu LK, Lin JC, Chan PK, Peng MY, Wan HL, Chen JH, Hu BS, Perng CL, Lu JJ, Chang FY. 2005. Experience of using convalescent plasma for severe acute respiratory syndrome among healthcare workers in a Taiwan hospital. *J Antimicrob Chemother* 56:919–922. <http://dx.doi.org/10.1093/jac/dki346>.
 254. Hung IF, To KK, Lee CK, Lee KL, Yan WW, Chan K, Chan WM, Ngai CW, Law KI, Chow FL, Liu R, Lai KY, Lau CC, Liu SH, Chan KH, Lin CK, Yuen KY. 2013. Hyperimmune IV immunoglobulin treatment: a multicenter double-blind randomized controlled trial for patients with severe 2009 influenza A(H1N1) infection. *Chest* 144:464–473. <http://dx.doi.org/10.1378/chest.12-2907>.
 255. Hung IF, To KK, Lee CK, Lee KL, Chan K, Yan WW, Liu R, Watt CL, Chan WM, Lai KY, Koo CK, Buckley T, Chow FL, Wong KK, Chan HS, Ching CK, Tang BS, Lau CC, Li IW, Liu SH, Chan KH, Lin CK, Yuen KY. 2011. Convalescent plasma treatment reduced mortality in patients with severe pandemic influenza A (H1N1) 2009 virus infection. *Clin Infect Dis* 52:447–456. <http://dx.doi.org/10.1093/cid/ciq106>.
 256. van Doremalen N, de Wit E, Falzarano D, Scott DP, Schountz T, Bowen D, McLellan JS, Zhu J, Munster VJ. 2014. Modeling the host ecology of Middle East respiratory syndrome coronavirus (MERS-CoV): from host reservoir to disease. *Final Progr 33rd Annu Meet Am Soc Virol*, Fort Collins, CO.
 257. Adney DR, Brown VR, Dominguez SR, Bielefeldt-Ohmann H, Bowen RA. 2014. Experimental infection of goats and insectivorous bats with MERS-CoV. *Final Progr 33rd Annu Meet Am Soc Virol*, Fort Collins, CO.
 258. Adney DR, van Doremalen N, Brown VR, Bushmaker T, Scott D, de Wit E, Bowen RA, Munster VJ. 2014. Replication and shedding of MERS-CoV in upper respiratory tract of inoculated dromedary camels. *Emerg Infect Dis* 20:1999–2005. <http://dx.doi.org/10.3201/eid2012.141280>.
 259. Poon LL, Chu DK, Chan KH, Wong OK, Ellis TM, Leung YH, Lau SK, Woo PC, Suen KY, Yuen KY, Guan Y, Peiris JS. 2005. Identification of a novel coronavirus in bats. *J Virol* 79:2001–2009. <http://dx.doi.org/10.1128/JVI.79.4.2001-2009.2005>.
 260. Woo PC, Lau SK, Huang Y, Tsoi HW, Chan KH, Yuen KY. 2005. Phylogenetic and recombination analysis of coronavirus HKU1, a novel coronavirus from patients with pneumonia. *Arch Virol* 150:2299–2311. <http://dx.doi.org/10.1007/s00705-005-0573-2>.
 261. Woo PC, Huang Y, Lau SK, Tsoi HW, Yuen KY. 2005. In silico analysis of ORF1ab in coronavirus HKU1 genome reveals a unique putative cleavage site of coronavirus HKU1 3C-like protease. *Microbiol Immunol* 49:899–908. <http://dx.doi.org/10.1111/j.1348-0421.2005.tb03681.x>.
 262. Woo PC, Lau SK, Yip CC, Huang Y, Tsoi HW, Chan KH, Yuen KY. 2006. Comparative analysis of 22 coronavirus HKU1 genomes reveals a novel genotype and evidence of natural recombination in coronavirus HKU1. *J Virol* 80:7136–7145. <http://dx.doi.org/10.1128/JVI.00509-06>.
 263. Huang Y, Lau SK, Woo PC, Yuen KY. 2008. CoVDB: a comprehensive database for comparative analysis of coronavirus genes and genomes. *Nucleic Acids Res* 36:D504–D511. <http://dx.doi.org/10.1093/nar/gkm754>.
 264. Woo PC, Lau SK, Lam CS, Lai KK, Huang Y, Lee P, Luk GS, Dyrting KC, Chan KH, Yuen KY. 2009. Comparative analysis of complete genome sequences of three avian coronaviruses reveals a novel group 3c coronavirus. *J Virol* 83:908–917. <http://dx.doi.org/10.1128/JVI.01977-08>.
 265. Woo PC, Lau SK, Yip CC, Huang Y, Yuen KY. 2009. More and more coronaviruses: human coronavirus HKU1. *Viruses* 1:57–71. <http://dx.doi.org/10.3390/v1010057>.
 266. Woo PC, Huang Y, Lau SK, Yuen KY. 2010. Coronavirus genomics and bioinformatics analysis. *Viruses* 2:1804–1820. <http://dx.doi.org/10.3390/v2081803>.
 267. Lau SK, Lee P, Tsang AK, Yip CC, Tse H, Lee RA, So LY, Lau YL, Chan KH, Woo PC, Yuen KY. 2011. Molecular epidemiology of human coronavirus OC43 reveals evolution of different genotypes over time and recent emergence of a novel genotype due to natural recombination. *J Virol* 85:11325–11337. <http://dx.doi.org/10.1128/JVI.05512-11>.
 268. Lau SK, Woo PC, Yip CC, Fan RY, Huang Y, Wang M, Guo R, Lam CS, Tsang AK, Lai KK, Chan KH, Che XY, Zheng BJ, Yuen KY. 2012. Isolation and characterization of a novel Betacoronavirus subgroup A coronavirus, rabbit coronavirus HKU14, from domestic rabbits. *J Virol* 86:5481–5496. <http://dx.doi.org/10.1128/JVI.06927-11>.
 269. Woo PC, Lau SK, Lam CS, Tsang AK, Hui SW, Fan RY, Martelli P, Yuen KY. 2014. Discovery of a novel bottlenose dolphin coronavirus reveals a distinct species of marine mammal coronavirus in Gammacoronavirus. *J Virol* 88:1318–1331. <http://dx.doi.org/10.1128/JVI.02351-13>.
 270. Pereyaslov D, Rosin P, Palm D, Zeller H, Gross D, Brown C, Struelens M.

2014. Laboratory capability and surveillance testing for Middle East respiratory syndrome coronavirus infection in the WHO European Region, June 2013. *Euro Surveill* 19(40):pii=20923. <http://www.eurosurveillance.org/ViewArticle.aspx?ArticleId=20923>.
271. Woo PC, Lau SK, Teng JL, Tsang AK, Joseph M, Wong EY, Tang Y, Sivakumar S, Xie J, Bai R, Wernery R, Wernery U, Yuen KY. 2014. New hepatitis E virus genotype in camels, the Middle East. *Emerg Infect Dis* 20:1044–1048. <http://dx.doi.org/10.3201/eid2006.140140>.
272. Woo PC, Lau SK, Teng JL, Tsang AK, Joseph M, Wong EY, Tang Y, Sivakumar S, Bai R, Wernery R, Wernery U, Yuen KY. 2014. Metagenomic analysis of viromes of dromedary camel fecal samples reveals large number and high diversity of circoviruses and picobirnaviruses. *Virology* 471-473C:117–125. <http://dx.doi.org/10.1016/j.virol.2014.09.020>.
273. Li W, Shi Z, Yu M, Ren W, Smith C, Epstein JH, Wang H, Crameri G, Hu Z, Zhang H, Zhang J, McEachern J, Field H, Daszak P, Eaton BT, Zhang S, Wang LF. 2005. Bats are natural reservoirs of SARS-like coronaviruses. *Science* 310:676–679. <http://dx.doi.org/10.1126/science.1118391>.
274. Ge XY, Li JL, Yang XL, Chmura AA, Zhu G, Epstein JH, Mazet JK, Hu B, Zhang W, Peng C, Zhang YJ, Luo CM, Tan B, Wang N, Zhu Y, Crameri G, Zhang SY, Wang LF, Daszak P, Shi ZL. 2013. Isolation and characterization of a bat SARS-like coronavirus that uses the ACE2 receptor. *Nature* 503:535–538. <http://dx.doi.org/10.1038/nature12711>.
275. Chu CM, Cheng VC, Hung IF, Chan KS, Tang BS, Tsang TH, Chan KH, Yuen KY. 2005. Viral load distribution in SARS outbreak. *Emerg Infect Dis* 11:1882–1886. <http://dx.doi.org/10.3201/eid1112.040949>.
276. Lim PL, Kurup A, Gopalakrishna G, Chan KP, Wong CW, Ng LC, Se-Thoe SY, Oon L, Bai X, Stanton LW, Ruan Y, Miller LD, Vega VB, James L, Ooi PL, Kai CS, Olsen SJ, Ang B, Leo YS. 2004. Laboratory-acquired severe acute respiratory syndrome. *N Engl J Med* 350:1740–1745. <http://dx.doi.org/10.1056/NEJMoa032565>.
277. Olsen SJ, Chang HL, Cheung TY, Tang AF, Fisk TL, Ooi SP, Kuo HW, Jiang DD, Chen KT, Lando J, Hsu KH, Chen TJ, Dowell SF. 2003. Transmission of the severe acute respiratory syndrome on aircraft. *N Engl J Med* 349:2416–2422. <http://dx.doi.org/10.1056/NEJMoa031349>.
278. Anderson RM, Fraser C, Ghani AC, Donnelly CA, Riley S, Ferguson NM, Leung GM, Lam TH, Hedley AJ. 2004. Epidemiology, transmission dynamics and control of SARS: the 2002–2003 epidemic. *Philos Trans R Soc Lond B Biol Sci* 359:1091–1105. <http://dx.doi.org/10.1098/rstb.2004.1490>.
279. Wallinga J, Teunis P. 2004. Different epidemic curves for severe acute respiratory syndrome reveal similar impacts of control measures. *Am J Epidemiol* 160:509–516. <http://dx.doi.org/10.1093/aje/kwh255>.
280. Nishiura H, Kuratsuki T, Quy T, Phi NC, Van Ban V, Ha LE, Long HT, Yanai H, Keicho N, Kirikae T, Sasazuki T, Anderson RM. 2005. Rapid awareness and transmission of severe acute respiratory syndrome in Hanoi French Hospital, Vietnam. *Am J Trop Med Hyg* 73:17–25.
281. Fouchier RA, Kuiken T, Schutten M, van Amerongen G, van Doornum GJ, van den Hoogen BG, Peiris M, Lim W, Stohr K, Osterhaus AD. 2003. Aetiology: Koch's postulates fulfilled for SARS virus. *Nature* 423:240. <http://dx.doi.org/10.1038/423240a>.
282. Li W, Moore MJ, Vasilieva N, Sui J, Wong SK, Berne MA, Somasundaran M, Sullivan JL, Luzuriaga K, Greenough TC, Choe H, Farzan M. 2003. Angiotensin-converting enzyme 2 is a functional receptor for the SARS coronavirus. *Nature* 426:450–454. <http://dx.doi.org/10.1038/nature02145>.
283. Simmons G, Gosalia DN, Rennekamp AJ, Reeves JD, Diamond SL, Bates P. 2005. Inhibitors of cathepsin L prevent severe acute respiratory syndrome coronavirus entry. *Proc Natl Acad Sci U S A* 102:11876–11881. <http://dx.doi.org/10.1073/pnas.0505577102>.
284. Glowacka I, Bertram S, Muller MA, Allen P, Soilleux E, Pfefferle S, Steffen I, Tsegaye TS, He Y, Gnirss K, Niemeyer D, Schneider H, Drosten C, Pohlmann S. 2011. Evidence that TMPRSS2 activates the severe acute respiratory syndrome coronavirus spike protein for membrane fusion and reduces viral control by the humoral immune response. *J Virol* 85:4122–4134. <http://dx.doi.org/10.1128/JVI.02232-10>.
285. Matsuyama S, Nagata N, Shirato K, Kawase M, Takeda M, Taguchi F. 2010. Efficient activation of the severe acute respiratory syndrome coronavirus spike protein by the transmembrane protease TMPRSS2. *J Virol* 84:12658–12664. <http://dx.doi.org/10.1128/JVI.01542-10>.
286. Heurich A, Hofmann-Winkler H, Gierer S, Liepold T, Jahn O, Pohlmann S. 2014. TMPRSS2 and ADAM17 cleave ACE2 differentially and only proteolysis by TMPRSS2 augments entry driven by the severe acute respiratory syndrome coronavirus spike protein. *J Virol* 88:1293–1307. <http://dx.doi.org/10.1128/JVI.02202-13>.
287. Huang IC, Bosch BJ, Li F, Li W, Lee KH, Ghiran S, Vasilieva N, Dermody TS, Harrison SC, Dormitzer PR, Farzan M, Rottier PJ, Choe H. 2006. SARS coronavirus, but not human coronavirus NL63, utilizes cathepsin L to infect ACE2-expressing cells. *J Biol Chem* 281:3198–3203. <http://dx.doi.org/10.1074/jbc.M508381200>.
288. Siu KL, Kok KH, Ng MH, Poon VK, Yuen KY, Zheng BJ, Jin DY. 2009. Severe acute respiratory syndrome coronavirus M protein inhibits type I interferon production by impeding the formation of TRAF3-TANK-TBK1/IKKepsilon complex. *J Biol Chem* 284:16202–16209. <http://dx.doi.org/10.1074/jbc.M109.008227>.
289. Kopecky-Bromberg SA, Martinez-Sobrido L, Frieman M, Baric RA, Palese P. 2007. Severe acute respiratory syndrome coronavirus open reading frame (ORF) 3b, ORF 6, and nucleocapsid proteins function as interferon antagonists. *J Virol* 81:548–557. <http://dx.doi.org/10.1128/JVI.01782-06>.
290. Narayanan K, Huang C, Lokugamage K, Kamitani W, Ikegami T, Tseng CT, Makino S. 2008. Severe acute respiratory syndrome coronavirus nsp1 suppresses host gene expression, including that of type I interferon, in infected cells. *J Virol* 82:4471–4479. <http://dx.doi.org/10.1128/JVI.02472-07>.
291. Devaraj SG, Wang N, Chen Z, Tseng M, Barretto N, Lin R, Peters CJ, Tseng CT, Baker SC, Li K. 2007. Regulation of IRF-3-dependent innate immunity by the papain-like protease domain of the severe acute respiratory syndrome coronavirus. *J Biol Chem* 282:32208–32211. <http://dx.doi.org/10.1074/jbc.M704870200>.
292. Snijder EJ, Bredenbeek PJ, Dobbe JC, Thiel V, Ziebuhr J, Poon LL, Guan Y, Rozanov M, Spaan WJ, Gorbalenya AE. 2003. Unique and conserved features of genome and proteome of SARS-coronavirus, an early split-off from the coronavirus group 2 lineage. *J Mol Biol* 331:991–1004. [http://dx.doi.org/10.1016/S0022-2836\(03\)00865-9](http://dx.doi.org/10.1016/S0022-2836(03)00865-9).
293. Woo PC, Lau SK, Tsoi HW, Chan KH, Wong BH, Che XY, Tam VK, Tam SC, Cheng VC, Hung IF, Wong SS, Zheng BJ, Guan Y, Yuen KY. 2004. Relative rates of non-pneumonic SARS coronavirus infection and SARS coronavirus pneumonia. *Lancet* 363:841–845. [http://dx.doi.org/10.1016/S0140-6736\(04\)15729-2](http://dx.doi.org/10.1016/S0140-6736(04)15729-2).
294. Nie Y, Wang G, Shi X, Zhang H, Qiu Y, He Z, Wang W, Lian G, Yin X, Du L, Ren L, Wang J, He X, Li T, Deng H, Ding M. 2004. Neutralizing antibodies in patients with severe acute respiratory syndrome-associated coronavirus infection. *J Infect Dis* 190:1119–1126. <http://dx.doi.org/10.1086/423286>.
295. Graham RL, Donaldson EF, Baric RS. 2013. A decade after SARS: strategies for controlling emerging coronaviruses. *Nat Rev Microbiol* 11:836–848. <http://dx.doi.org/10.1038/nrmicro3143>.
296. Mair-Jenkins J, Saavedra-Campos M, Baillie JK, Cleary P, Khaw FM, Lim WS, Makki S, Rooney KD, Nguyen-Van-Tam JS, Beck CR. 2015. The effectiveness of convalescent plasma and hyperimmune immunoglobulin for the treatment of severe acute respiratory infections of viral etiology: a systematic review and exploratory meta-analysis. *J Infect Dis* 211:80–90. <http://dx.doi.org/10.1093/infdis/jiu396>.
297. Pfefferle S, Schopf J, Kogl M, Friedel CC, Muller MA, Carbajo-Lozoya J, Stellberger T, von Dall'Armi E, Herzog P, Kallies S, Niemeyer D, Ditt V, Kuri T, Züst R, Pumpor K, Hilgenfeld R, Schwarz F, Zimmer R, Steffen I, Weber F, Thiel V, Herrler G, Thiel HJ, Schwegmann-Wessels C, Pohlmann S, Haas J, Drosten C, von Brunn A. 2011. The SARS-coronavirus-host interactome: identification of cyclophilins as target for pan-coronavirus inhibitors. *PLoS Pathog* 7:e1002331. <http://dx.doi.org/10.1371/journal.ppat.1002331>.
298. Huang C, Lokugamage KG, Rozovics JM, Narayanan K, Semler BL, Makino S. 2011. SARS coronavirus nsp1 protein induces template-dependent endonucleolytic cleavage of mRNAs: viral mRNAs are resistant to nsp1-induced RNA cleavage. *PLoS Pathog* 7:e1002433. <http://dx.doi.org/10.1371/journal.ppat.1002433>.
299. Cornillez-Ty CT, Liao L, Yates JR 3rd, Kuhn P, Buchmeier MJ. 2009. Severe acute respiratory syndrome coronavirus nonstructural protein 2 interacts with a host protein complex involved in mitochondrial biogenesis and intracellular signaling. *J Virol* 83:10314–10318. <http://dx.doi.org/10.1128/JVI.00842-09>.
300. Lin MH, Chuang SJ, Chen CC, Cheng SC, Cheng KW, Lin CH, Sun CY, Chou CY. 2014. Structural and functional characterization of MERS coronavirus papain-like protease. *J Biomed Sci* 21:54. <http://dx.doi.org/10.1186/1423-0127-21-54>.

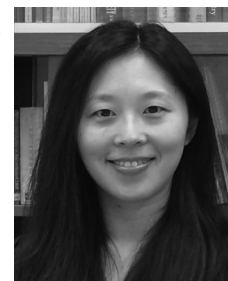
301. Baez-Santos YM, Mielech AM, Deng X, Baker S, Mesecar AD. 2014. Catalytic function and substrate specificity of the papain-like protease domain of nsp3 from the Middle East respiratory syndrome coronavirus. *J Virol* 88:12511–12527. <http://dx.doi.org/10.1128/JVI.01294-14>.
302. Lei J, Mesters JR, Drosten C, Anemuller S, Ma Q, Hilgenfeld R. 2014. Crystal structure of the papain-like protease of MERS coronavirus reveals unusual, potentially druggable active-site features. *Antiviral Res* 109:72–82. <http://dx.doi.org/10.1016/j.antiviral.2014.06.011>.
303. Bailey-Elkin BA, Knaap RC, Johnson GG, Dalebout TJ, Ninaber DK, van Kasteren PB, Bredenbeek PJ, Snijder EJ, Kikkert M, Mark BL. 15 October 2014. Crystal structure of the MERS coronavirus papain-like protease bound to ubiquitin facilitates targeted disruption of deubiquitinating activity to demonstrate its role in innate immune suppression. *J Biol Chem* <http://dx.doi.org/10.1074/jbc.M114.609644>.
304. Lundin A, Dijkman R, Bergstrom T, Kann N, Adamiak B, Hannoun C, Kindler E, Jonsdottir HR, Muth D, Kint J, Forlenza M, Muller MA, Drosten C, Thiel V, Trybala E. 2014. Targeting membrane-bound viral RNA synthesis reveals potent inhibition of diverse coronaviruses including the middle East respiratory syndrome virus. *PLoS Pathog* 10:e1004166. <http://dx.doi.org/10.1371/journal.ppat.1004166>.
305. te Velthuis AJ, van den Worm SH, Snijder EJ. 2012. The SARS-coronavirus nsp7+nsp8 complex is a unique multimeric RNA polymerase capable of both de novo initiation and primer extension. *Nucleic Acids Res* 40:1737–1747. <http://dx.doi.org/10.1093/nar/gkr893>.
306. Miknis ZJ, Donaldson EF, Umland TC, Rimmer RA, Baric RS, Schultz LW. 2009. Severe acute respiratory syndrome coronavirus nsp9 dimerization is essential for efficient viral growth. *J Virol* 83:3007–3018. <http://dx.doi.org/10.1128/JVI.01505-08>.
307. Chen Y, Su C, Ke M, Jin X, Xu L, Zhang Z, Wu A, Sun Y, Yang Z, Tien P, Ahola T, Liang Y, Liu X, Guo D. 2011. Biochemical and structural insights into the mechanisms of SARS coronavirus RNA ribose 2'-O-methylation by nsp16/nsp10 protein complex. *PLoS Pathog* 7:e1002294. <http://dx.doi.org/10.1371/journal.ppat.1002294>.
308. Menachery VD, Debbink K, Baric RS. 2014. Coronavirus non-structural protein 16: evasion, attenuation, and possible treatments. *Virus Res* 194C:191–199. <http://dx.doi.org/10.1016/j.virusres.2014.09.009>.
309. Almazan F, DeDiego ML, Sola I, Zuniga S, Nieto-Torres JL, Marquez-Jurado S, Andres G, Enjuanes L. 2013. Engineering a replication-competent, propagation-defective Middle East respiratory syndrome coronavirus as a vaccine candidate. *mBio* 4(5):e00650–00613. <http://dx.doi.org/10.1128/mBio.00650-13>.
310. Corman VM, Eckerle I, Bleicker T, Zaki A, Landt O, Eschbach-Bludau M, van Boheemen S, Gopal R, Ballhause M, Bestebroer TM, Muth D, Muller MA, Drexler JF, Zambon M, Osterhaus AD, Fouchier RM, Drosten C. 2012. Detection of a novel human coronavirus by real-time reverse-transcription polymerase chain reaction. *Euro Surveill* 17(39):pii=20285. <http://www.eurosurveillance.org/ViewArticle.aspx?ArticleId=20285>.
311. Saad M, Omrani AS, Baig K, Bahloul A, Elzein F, Matin MA, Selim MA, Mutairi MA, Nakhli DA, Aidaroos AY, Sherbeeni NA, Al-Khashan HI, Memish ZA, Albarrak AM. 7 October 2014. Clinical aspects and outcomes of 70 patients with Middle East respiratory syndrome coronavirus infection: a single-center experience in Saudi Arabia. *Int J Infect Dis* <http://dx.doi.org/10.1016/j.ijid.2014.09.003>.
312. Yang L, Wu Z, Ren X, Yang F, Zhang J, He G, Dong J, Sun L, Zhu Y, Zhang S, Jin Q. 2014. MERS-related betacoronavirus in *Vespertilio superans* bats, China. *Emerg Infect Dis* 20:1260–1262. <http://dx.doi.org/10.3201/eid2007.140318>.
313. Annan A, Baldwin HJ, Corman VM, Klose SM, Owusu M, Nkrumah EE, Badu EK, Anti P, Agbenyega O, Meyer B, Oppong S, Sarkodie YA, Kalko EK, Lina PH, Godlevska EV, Reusken C, Seebens A, Gloza-Rausch F, Vallo P, Tschapka M, Drosten C, Drexler JF. 2013. Human betacoronavirus 2c EMC/2012-related viruses in bats, Ghana and Europe. *Emerg Infect Dis* 19:456–459. <http://dx.doi.org/10.3201/eid1903.121503>.
314. Lelli D, Papetti A, Sabelli C, Rosti E, Moreno A, Boniotti MB. 2013. Detection of coronaviruses in bats of various species in Italy. *Viruses* 5:2679–2689. <http://dx.doi.org/10.3390/v5112679>.
315. Anthony SJ, Ojeda-Flores R, Rico-Chavez O, Navarrete-Macias I, Zambrana-Torrel CM, Rostal MK, Epstein JH, Tipps T, Liang E, Sanchez-Leon M, Sotomayor-Bonilla J, Aguirre AA, Avila-Flores R, Medellin RA, Goldstein T, Suzan G, Daszak P, Lipkin WI. 2013. Coronaviruses in bats from Mexico. *J Gen Virol* 94:1028–1038. <http://dx.doi.org/10.1099/vir.0.049759-0>.
316. Goes LG, Ruvalcaba SG, Campos AA, Queiroz LH, de Carvalho C, Jerez JA, Durigon EL, Davalos LI, Dominguez SR. 2013. Novel bat coronaviruses, Brazil and Mexico. *Emerg Infect Dis* 19:1711–1713. <http://dx.doi.org/10.3201/eid1910.130525>.
317. Nowotny N, Kolodziejek J. 2014. Middle East respiratory syndrome coronavirus (MERS-CoV) in dromedary camels, Oman, 2013. *Euro Surveill* 19(16):pii=20781. <http://www.eurosurveillance.org/ViewArticle.aspx?ArticleId=20781>.
318. Reusken CB, Messadi L, Feyisa A, Ullaramu H, Godeke GJ, Danmarwa A, Dawo F, Jemli M, Melaku S, Shamaki D, Woma Y, Wungak Y, Gebremedhin EZ, Zutt I, Bosch BJ, Haagmans BL, Koopmans MP. 2014. Geographic distribution of MERS coronavirus among dromedary camels, Africa. *Emerg Infect Dis* 20:1370–1374. <http://dx.doi.org/10.3201/eid2008.140590>.
319. Cai Y, Yu SQ, Postnikova EN, Mazur S, Bernbaum JG, Burk R, Zhāng T, Radoshitzky SR, Müller MA, Jordan I, Bollinger L, Hensley LE, Jahrling PB, Kuhn JH. 2014. CD26/DPP4 cell-surface expression in bat cells correlates with bat cell susceptibility to Middle East respiratory syndrome coronavirus (MERS-CoV) infection and evolution of persistent infection. *PLoS One* 9:e112060. <http://dx.doi.org/10.1371/journal.pone.0112060>.
320. Payne DC, Iblan I, Alqasrawi S, Al Nsour M, Rha B, Tohme RA, Abedi GR, Farag NH, Haddadin A, Al Sanhoury T, Jarour N, Swerdlow DL, Jamieson DJ, Pallsch MA, Haynes LM, Gerber SI, Al Abdallat MM. 2014. Stillbirth during infection with Middle East respiratory syndrome coronavirus. *J Infect Dis* 209:1870–1872. <http://dx.doi.org/10.1093/infdis/jiu068>.
321. Corman VM, Olschlager S, Wendtner CM, Drexler JF, Hess M, Drosten C. 2014. Performance and clinical validation of the RealStar MERS-CoV kit for detection of Middle East respiratory syndrome coronavirus RNA. *J Clin Virol* 60:168–171. <http://dx.doi.org/10.1016/j.jcv.2014.03.012>.
322. Lu X, Whitaker B, Sakthivel SK, Kamili S, Rose LE, Lowe L, Mohareb E, Ellassal EM, Al-sanouri, Haddadin TA, Erdman DD. 2014. Real-time reverse transcription-PCR assay panel for Middle East respiratory syndrome coronavirus. *J Clin Microbiol* 52:67–75. <http://dx.doi.org/10.1128/JCM.02533-13>.
323. Reusken C, Mou H, Godeke GJ, van der Hoek L, Meyer B, Muller MA, Haagmans B, de Sousa R, Schuurman N, Dittmer U, Rottier P, Osterhaus A, Drosten C, Bosch BJ, Koopmans M. 2013. Specific serology for emerging human coronaviruses by protein microarray. *Euro Surveill* 18(14):pii=20441. <http://www.eurosurveillance.org/ViewArticle.aspx?ArticleId=20441>.
324. Hart BJ, Dyall J, Postnikova E, Zhou H, Kindrachuk J, Johnson RF, Olinger GG, Jr, Frieman MB, Holbrook MR, Jahrling PB, Hensley L. 2014. Interferon-beta and mycophenolic acid are potent inhibitors of Middle East respiratory syndrome coronavirus in cell-based assays. *J Gen Virol* 95:571–577. <http://dx.doi.org/10.1099/vir.0.061911-0>.
325. Tao X, Mei F, Agrawal A, Peters CJ, Ksiazek TG, Cheng X, Tseng CT. 2014. Blocking of exchange proteins directly activated by cAMP leads to reduced replication of Middle East respiratory syndrome coronavirus. *J Virol* 88:3902–3910. <http://dx.doi.org/10.1128/JVI.03001-13>.
326. Al-Tawfiq JA, Momattin H, Dib J, Memish ZA. 2014. Ribavirin and interferon therapy in patients infected with the Middle East respiratory syndrome coronavirus: an observational study. *Int J Infect Dis* 20:42–46. <http://dx.doi.org/10.1016/j.ijid.2013.12.003>.
327. de Wit E, Prescott J, Baseler L, Bushmaker T, Thomas T, Lackemeyer MG, Martellaro C, Milne-Price S, Haddock E, Haagmans BL, Feldmann H, Munster VJ. 2013. The Middle East respiratory syndrome coronavirus (MERS-CoV) does not replicate in Syrian hamsters. *PLoS One* 8:e69127. <http://dx.doi.org/10.1371/journal.pone.0069127>.
328. Coleman CM, Matthews KL, Goicochea L, Frieman MB. 2014. Wild-type and innate immune-deficient mice are not susceptible to the Middle East respiratory syndrome coronavirus. *J Gen Virol* 95:408–412. <http://dx.doi.org/10.1099/vir.0.060640-0>.
329. Chan JF, To KK, Chen H, Yuen KY. 2015. Cross-species transmission and emergence of novel viruses from birds. *Curr Opin Virol* 10C:63–69. <http://dx.doi.org/10.1016/j.coviro.2015.01.006>.
330. Loon SC, Teoh SC, Oon LL, Se-Thoe SY, Ling AE, Leo YS, Leong HN. 2004. The severe acute respiratory syndrome coronavirus in tears. *Br J Ophthalmol* 88:861–863.
331. Wang WK, Chen SY, Liu JJ, Chen YC, Chen HL, Yang CF, Chen PJ, Yeh SH, Kao CL, Huang LM, Hsueh PR, Wang JT, Sheng WH, Fang CT, Hung CC, Hsieh SM, Su CP, Chiang WC, Yang JY, Lin JH, Hsieh SC, Hu HP, Chiang YP, Wang JT, Yang PC, Chang SC; SARS Research Group of the National Taiwan University/National Taiwan University

- Hospital. 2004. Detection of SARS-associated coronavirus in throat wash and saliva in early diagnosis. *Emerg Infect Dis* 10:1213–1219.
332. Ding Y, He L, Zhang Q, Huang Z, Che X, Hou J, Wang H, Shen H, Qiu L, Li Z, Geng J, Cai J, Han H, Li X, Kang W, Weng D, Liang P, Jiang S. 2004. Organ distribution of severe acute respiratory syndrome (SARS) associated coronavirus (SARS-CoV) in SARS patients: implications for pathogenesis and virus transmission pathways. *J Pathol* 203:622–630.
 333. Agrawal AS, Garron T, Tao X, Peng BH, Wakamiya M, Chan TS, Couch RB, Tseng CT. 14 January 2015. Generation of transgenic mouse model of Middle East respiratory syndrome-coronavirus infection and disease. *J Virol* <http://dx.doi.org/10.1128/JVI.03427-14>.
 334. Shalhoub S, AlZahrani A, Simhairi R, Mushtaq A. 2015. Successful recovery of MERS CoV pneumonia in a patient with acquired immunodeficiency syndrome: a case report. *J Clin Virol* 62:69–71. <http://dx.doi.org/10.1016/j.jcv.2014.11.030>.
 335. AlGhamdi M, Mushtaq F, Awn N, Shalhoub S. 25 February 2015. MERS CoV infection in two renal transplant recipients: case report. *Am J Transplant* <http://dx.doi.org/10.1111/ajt.13085>.
 336. Meyer B, García-Bocanegra I, Wernery U, Wernery R, Sieberg A, Müller MA, Drexler JF, Drosten C, Eckerle I. 2015. Serologic assessment of possibility for MERS-CoV infection in equids. *Emerg Infect Dis* 21:181–182. <http://dx.doi.org/10.3201/eid2101.141342>.
 337. Gossner C, Danielson N, Gervelmeyer A, Berthe F, Faye B, Kaasik Aaslav K, Adlhoeh C, Zeller H, Penttinen P, Coulombier D. 27 December 2014. Human-dromedary camel interactions and the risk of acquiring zoonotic Middle East respiratory syndrome coronavirus infection. *Zoonoses Public Health* <http://dx.doi.org/10.1111/zph.12171>.
 338. Chan RW, Hemida MG, Kayali G, Chu DK, Poon LL, Alnaeem A, Ali MA, Tao KP, Ng HY, Chan MC, Guan Y, Nicholls JM, Peiris JS. 2014. Tropism and replication of Middle East respiratory syndrome coronavirus from dromedary camels in the human respiratory tract: an in-vitro and ex-vivo study. *Lancet Respir Med* 2:813–822. [http://dx.doi.org/10.1016/S2213-2600\(14\)70158-4](http://dx.doi.org/10.1016/S2213-2600(14)70158-4).
 339. Majumder MS, Rivers C, Lofgren E, Fisman D. 18 December 2014. Estimation of MERS-coronavirus reproductive number and case fatality rate for the spring 2014 Saudi Arabia outbreak: insights from publicly available data. *PLoS Curr* 6. <http://dx.doi.org/10.1371/currents.outbreaks.98d2f8f3382d84f390736cd5f5fe133c>.
 340. Song D, Ha G, Serhan W, Eltahir Y, Yusuf M, Hashem F, Elsayed E, Marzoug B, Abdelazim A, Al Muhairi S. 2015. Development and validation of a rapid immunochromatographic assay for the detection of Middle East respiratory syndrome coronavirus antigen in dromedary camels. *J Clin Microbiol* 53:1178–1182. <http://dx.doi.org/10.1128/JCM.03096-14>.
 341. Cheng KW, Cheng SC, Chen WY, Lin MH, Chuang SJ, Cheng IH, Sun CY, Chou CY. 2015. Thiopurine analogs and mycophenolic acid synergistically inhibit the papain-like protease of Middle East respiratory syndrome coronavirus. *Antiviral Res* 115:9–16. <http://dx.doi.org/10.1016/j.antiviral.2014.12.011>.
 342. Maltezou HC, Tsiodras S. 2014. Middle East respiratory syndrome coronavirus: implications for health care facilities. *Am J Infect Control* 42:1261–1265. <http://dx.doi.org/10.1016/j.ajic.2014.06.019>.
 343. Cheng VC, Tai JW, Lee WM, Chan WM, Wong SC, Chen JH, Poon RW, To KK, Chan JF, Ho PL, Chan KH, Yuen KY. 2015. Infection control preparedness for human infection with influenza A H7N9 in Hong Kong. *Infect Control Hosp Epidemiol* 36:87–92. <http://dx.doi.org/10.1017/ice.2014.2>.
 344. Zhang N, Channappanavar R, Ma C, Wang L, Tang J, Garron T, Tao X, Tasneem S, Lu L, Tseng CT, Zhou Y, Perlman S, Jiang S, Du L. 2 February 2015. Identification of an ideal adjuvant for receptor-binding domain-based subunit vaccines against Middle East respiratory syndrome coronavirus. *Cell Mol Immunol* <http://dx.doi.org/10.1038/cmi.2015.03>.
 345. Yavarian J, Rezaei F, Shadab A, Soroush M, Gooya MM, Azad TM. 2015. Cluster of Middle East respiratory syndrome coronavirus infections in Iran, 2014. *Emerg Infect Dis* 21:362–364. <http://dx.doi.org/10.3201/eid2102.141405>.

Jasper F. W. Chan is a Clinical Assistant Professor at the Department of Microbiology, The University of Hong Kong (HKU). He received his M.B.B.S. from HKU in 2005 and completed postgraduate specialist training at the Department of Medicine and Department of Microbiology at Queen Mary Hospital, Hong Kong, to become Fellow of the Royal College of Physicians of Edinburgh, the Royal College of Pathologists of the United Kingdom, the Hong Kong College of Pathologists, and the Hong Kong Academy of Medicine. He joined the Department of Microbiology at his alma mater as an Honorary Assistant Professor in 2008 and a Clinical Assistant Professor in 2013. His research focuses on emerging respiratory viral infections and opportunistic infections in immunocompromised hosts. He has published more than 100 peer-reviewed research and review articles. He is an Associate Editor of *BMC Infectious Diseases*.



Susanna K. P. Lau is a Clinical Professor at the Department of Microbiology, The University of Hong Kong (HKU). She received her M.B.B.S. with the CP Fong Gold Medal in Medicine and her M.D. with the Sir Patrick Manson Gold Medal from HKU in 1998 and 2007, respectively. Her research focuses on emerging infectious diseases, including the discovery and genomic characterization of novel pathogens and their evolutionary origin and interspecies transmission. She is particularly interested in the discovery, evolution, and interspecies transmission of emerging coronaviruses such as SARS coronavirus and MERS coronavirus. Her team's discoveries include the following: SARS coronavirus-like virus in Chinese horseshoe bats, the origin of SARS coronavirus; the prototype lineage C betacoronaviruses *Tylonycteris* bat CoV HKU4 and *Pipistrellus* bat CoV HKU5, which are closely related to and precede the discovery of MERS-CoV; and interspecies transmission of bat coronavirus HKU10 between bats of different suborders. She has published over 260 peer-reviewed articles and is an Associate Editor of *Virology Journal*.



Continued next page

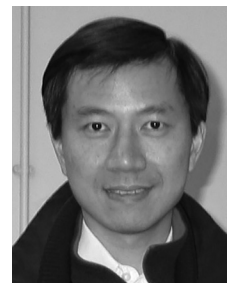
Kelvin K. W. To is a Clinical Assistant Professor at the Department of Microbiology, The University of Hong Kong (HKU). He received his B.Sc. from The University of British Columbia in 1998 and his M.B.B.S. from HKU in 2003. He then pursued specialist training in clinical microbiology and infectious diseases at Queen Mary Hospital, Hong Kong, to obtain Fellowships from the Royal College of Pathologists of the United Kingdom, the Hong Kong College of Pathologists, and the Royal College of Physicians of Edinburgh. He has published over 100 peer-reviewed articles. His research focuses on severe respiratory tract infections, including those caused by influenza viruses, coronaviruses, *Mycoplasma pneumoniae*, and *Pneumocystis jirovecii*. He is an Associate Editor of *BMC Infect Diseases*.



Vincent C. C. Cheng is a Consultant Microbiologist and Infection Control Officer at Queen Mary Hospital, Hong Kong, and an Honorary Associate Professor at the Department of Microbiology, The University of Hong Kong (HKU). He obtained his M.B.B.S. from HKU with distinction in medicine and trained in the field of internal medicine at Queen Mary Hospital to obtain membership from the Royal Colleges of Physicians of the United Kingdom. He then pursued training in clinical microbiology and infectious diseases at Queen Mary Hospital to obtain a Fellowship from The Royal College of Pathologists of the United Kingdom. He also received training in clinical infectious diseases and HIV medicine under the tutelage of Davidson Hamer, David Snyderman, and Sherwood Gorbach at Tufts Medical Center, Boston, MA, USA, in 2001. He was conferred Doctor of Medicine by HKU and was awarded the Sir Patrick Manson Gold Medal for the best M.D. thesis in 2012. He has published over 170 peer-reviewed articles in the areas of clinical infectious diseases, diagnostic microbiology, proactive infection control measures, and hospital outbreak investigations.



Patrick C. Y. Woo received his M.B.B.S from The University of Hong Kong (HKU) in 1991. He joined the Department of Microbiology at The University of Hong Kong as a Clinical Assistant Professor in 1997 and became Clinical Professor of Microbiology in 2006 and Head of Department in 2011. He has established himself as one of the leaders in the fields of emerging infectious diseases, novel microbe discovery, and microbial genomics, with over 360 peer-reviewed articles in these areas. Notable examples of novel coronaviruses discovered in his laboratory include human coronavirus HKU1, bat SARS coronavirus, dromedary camel coronavirus UAE-HKU23, and 20 other bat and avian coronaviruses. He is currently a member of the Coronavirus Taxonomy Study Group of the International Committee on Taxonomy of Viruses.



Kwok-Yung Yuen works on emerging infections and microbial discovery at the Department of Microbiology of The University of Hong Kong (HKU). Besides his work on avian and pandemic influenza viruses, he and his team have discovered and characterized over 40 novel viruses in human and animals, including human coronavirus HKU1 and the bat and human SARS coronaviruses. He has published over 740 peer-reviewed articles, including those in the *Nature* series, *Proceedings of the National Academy of Sciences of the United States of America*, *Journal of Virology*, and others, with over 10,000 citations. He is presently the Henry Fok Professor in Infectious Diseases and Chair of Microbiology at HKU. He also serves as the Director of the Clinical Diagnostic Microbiology Service at Queen Mary Hospital and the Co-Director of the State Key Laboratory of Emerging Infectious Diseases of China in the Hong Kong Special Administrative Region of the People's Republic of China. He was also the founding Co-Director of the HKU-Pasteur Research Centre. He is an elected Academician of the Chinese Academy of Engineering (Basic Medicine and Health) and a Fellow of the Royal College of Physicians (London, Edinburgh, and Ireland), Surgeons (Glasgow), and Pathologists (United Kingdom).

